Heavy-Ion Physics

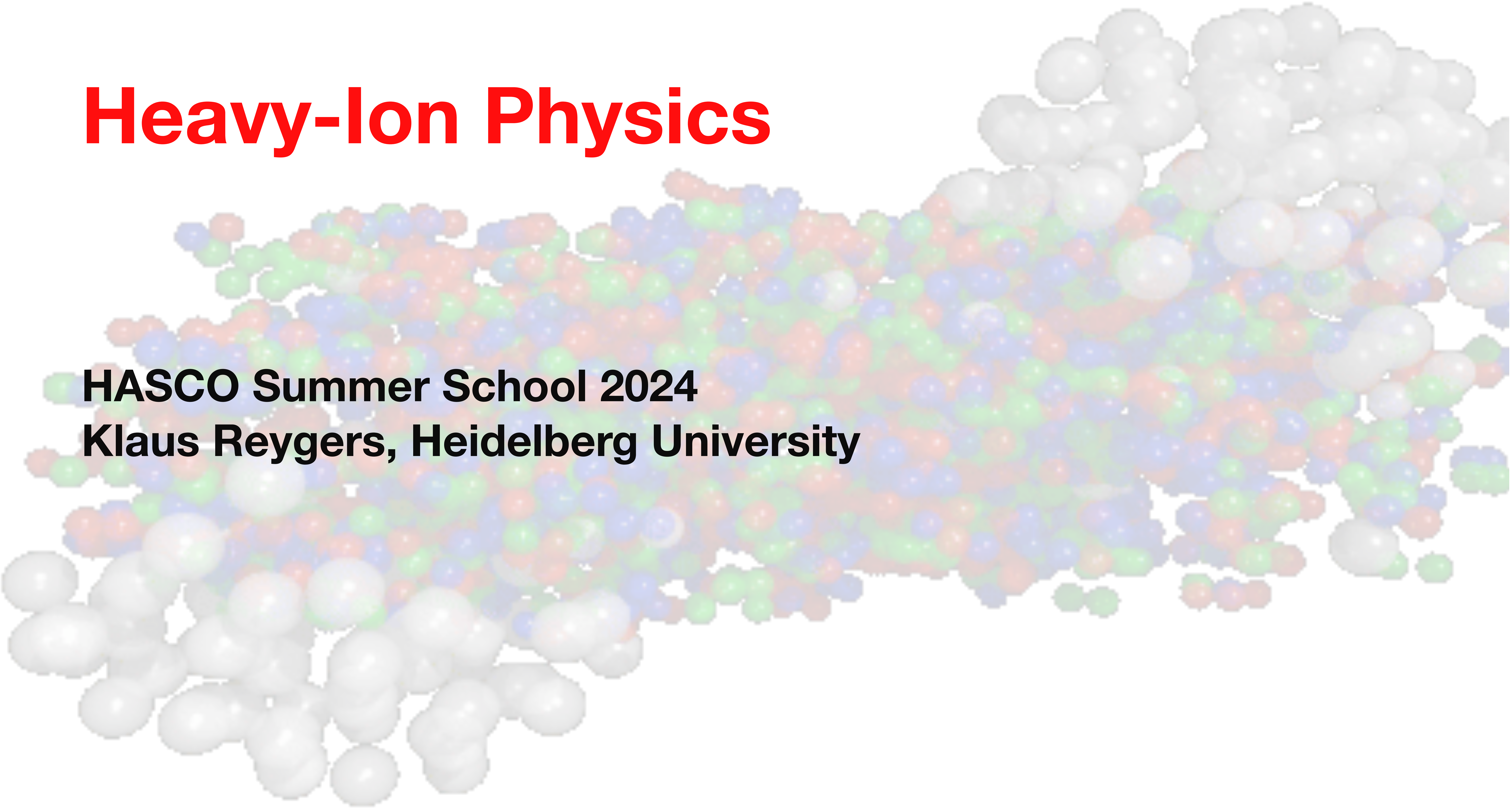

HASCO Summer School 2024
Klaus Reygers, Heidelberg University

Introduction

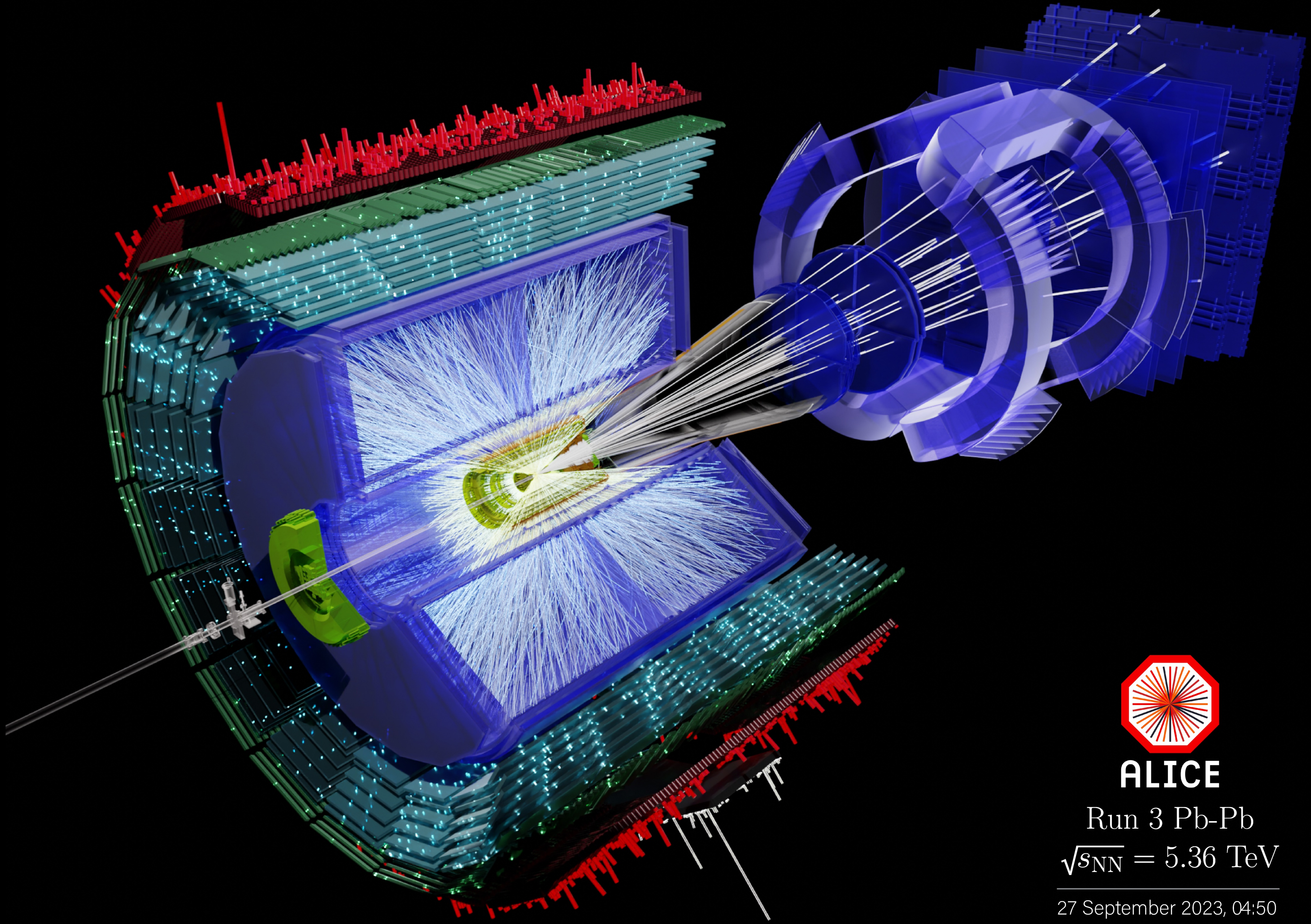

3000 tracks of charged particles in ALICE TPC in a single Pb–Pb collision

this lecture:
physics of these collisions – what to learn from this picture

What is the question?

Do we unterstand matter at extreme temperatures and/or densities?

Expectation: we'll get a deconfined soup of quarks and gluons – the quark-gluon plasma

heating

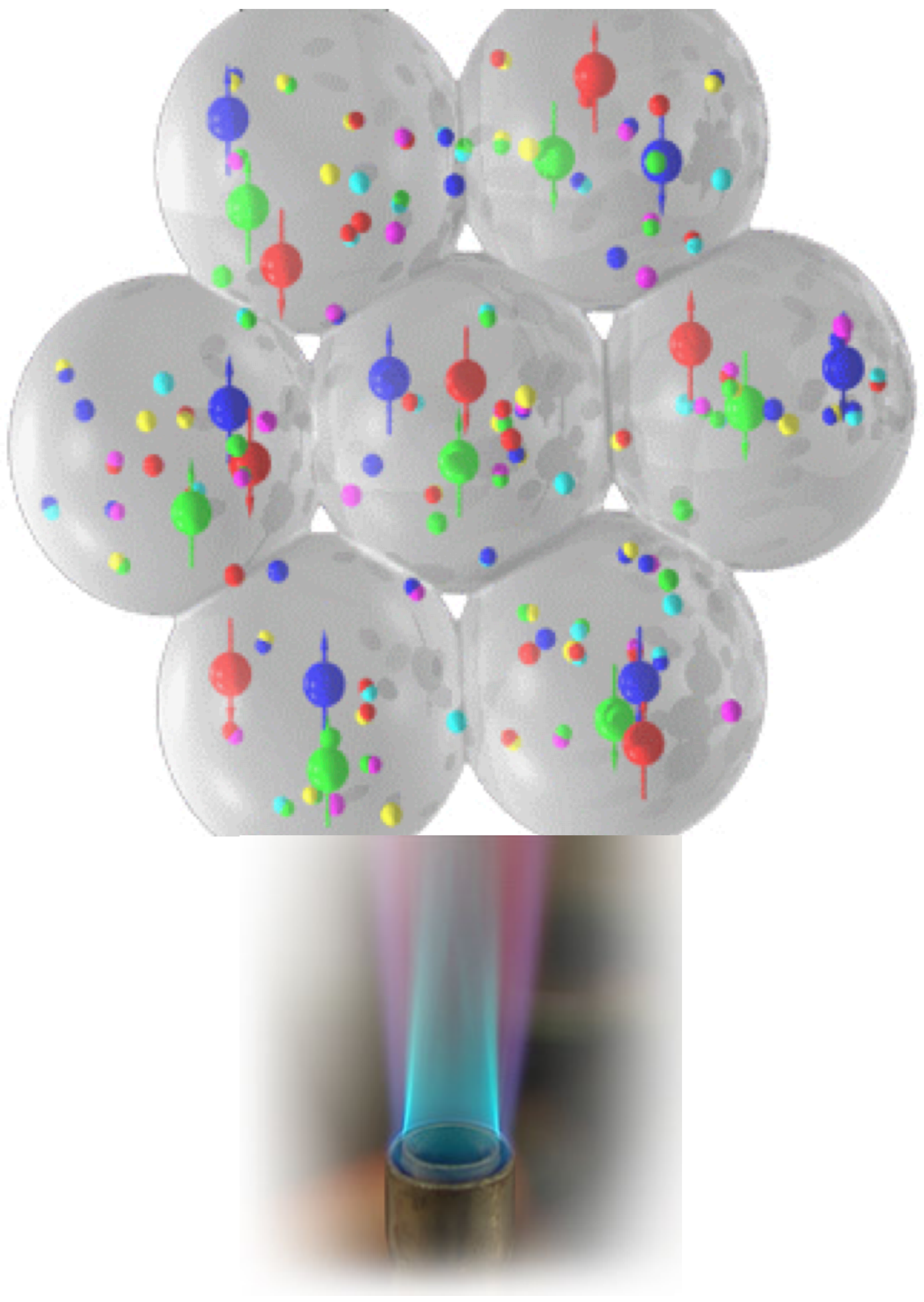

compression

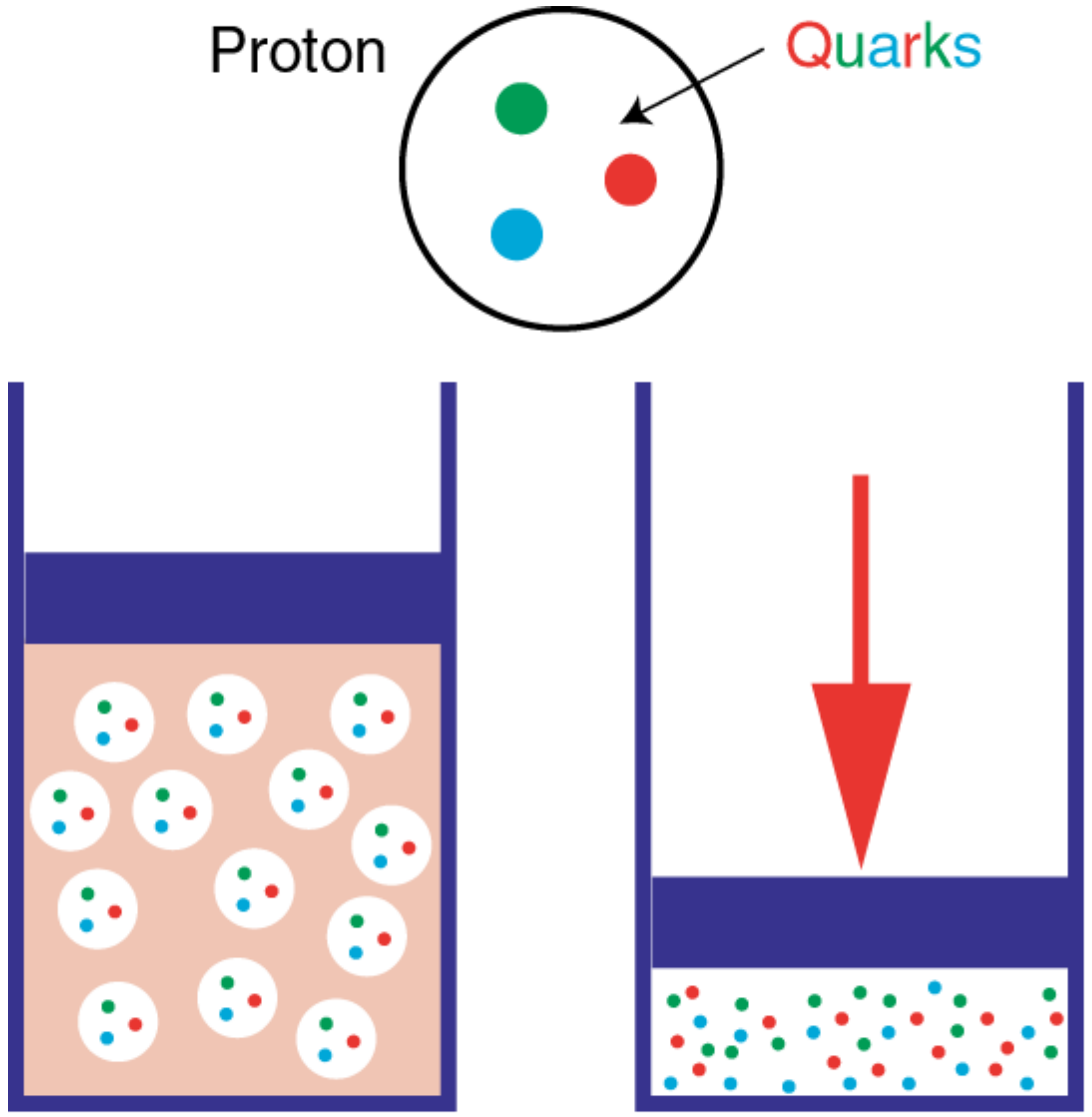

The goal: determine “material properties" of the QGP

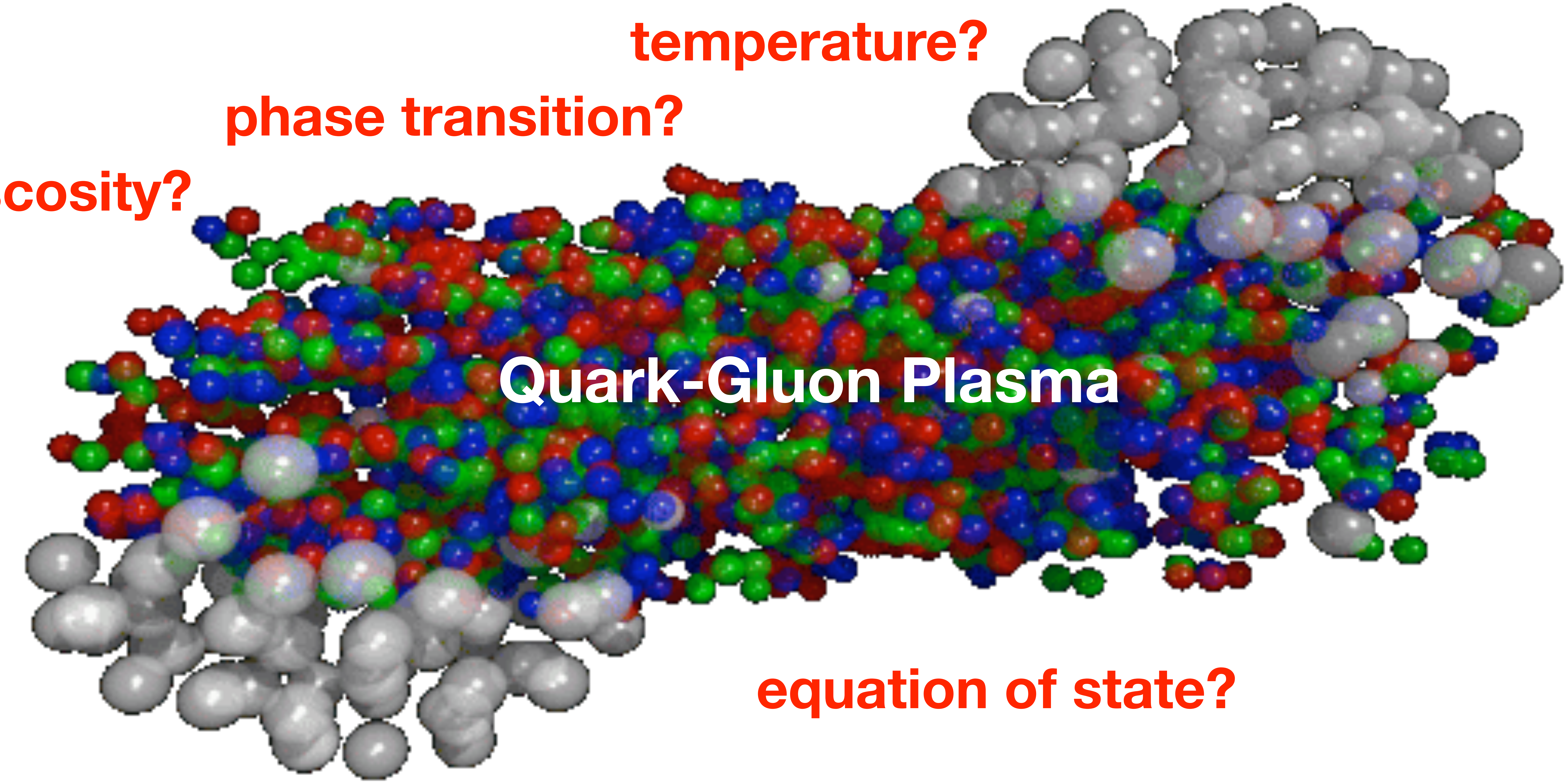

Quelle: urqmd.org

Heavy-ion physics: QCD thermodynamics

A brief history of the quark-gluon plasma

1973 — Birth of QCD:

All ideas in place: Yang-Mills theory, SU(3) color symmetry, asymptotic freedom, confinement in color-neutral objects

1975 — Idea of quark deconfinement at high temperature and/or density:

Initial idea: at high temperature, asymptomatic freedom gives rise to dedonfinement [Collins, Perry, PRL 34 (1975) 1353]

Exponential hadron spectrum does not give rise to an ultimate limited temperature (T_{Hagedorn}) of matter.
Rather: Different phase in which quarks are not confined
[Cabibbo, Parisi, PLB, 59 (1975) 67]

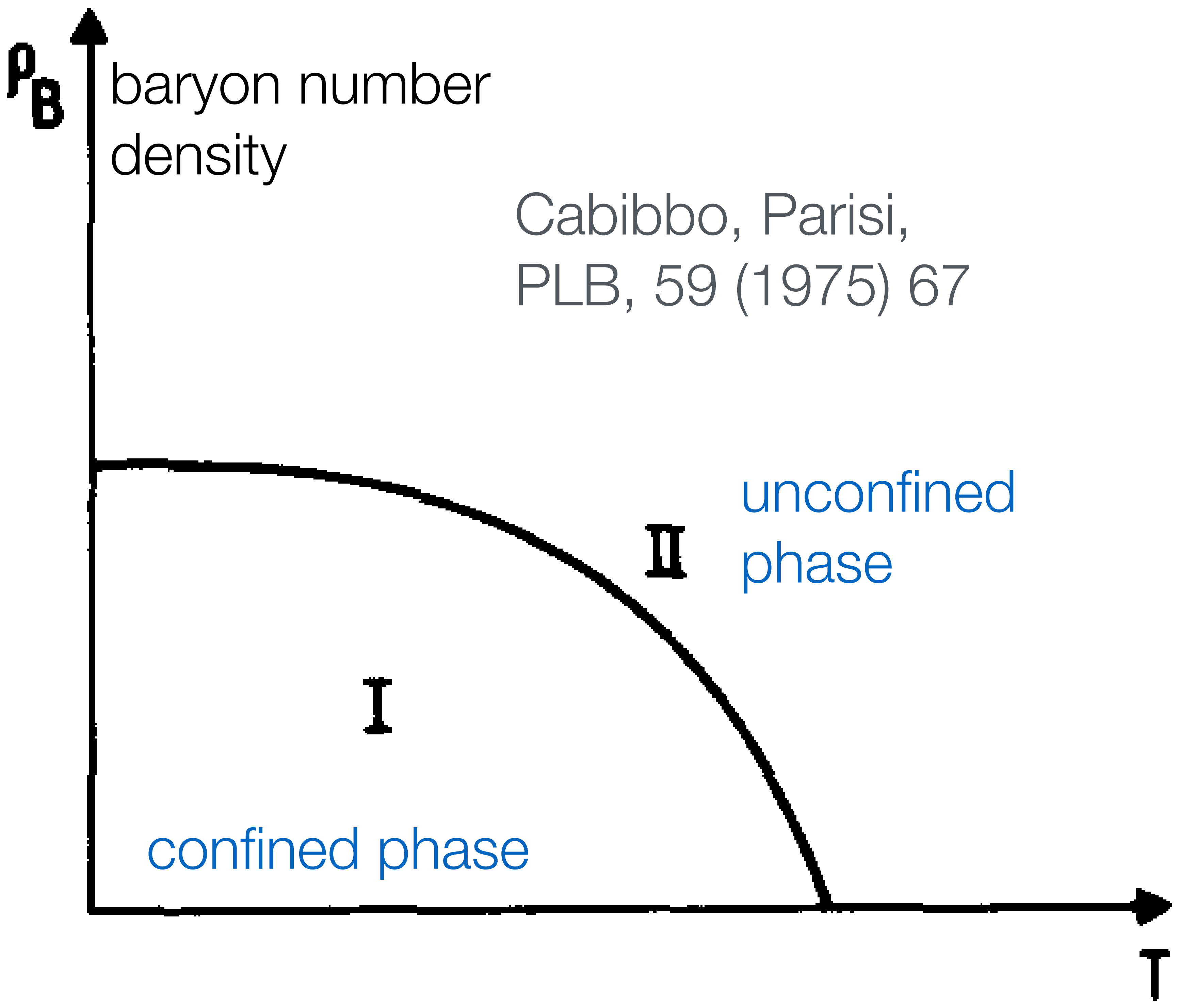

It was soon realized that this new state could be created and studied in heavy-ion collisions

Critical temperature at vanishing net baryon number

Consider an ideal gas of u, d quarks and antiquarks, and gluons. Calculate temperature at which energy density equals that within a proton:

Energy density in a proton:

$$\varepsilon_{\text{proton}} = \frac{m}{V} = \frac{0.94\,\text{GeV}}{4/3\pi(0.8\,\text{fm})^3} \approx 0.44\,\text{GeV}/\text{fm}^3$$

Temperature of an ideal gas of quark, antiquarks and gluons at that energy density:

$$\varepsilon_{\text{id.gas}} = 37\frac{\pi^2}{30}T^4 = 0.44\,\text{GeV}/\text{fm}^3 \to T \approx 130\,\text{MeV} \qquad (k_B = 1)$$

$$= 1.5 \times 10^{12}\,\text{K}$$

Note, however, that the α_s around T = 200 MeV is not small (ideal gas assumption not fully justified)

Critical density at vanishing temperature

Baryon density of nuclear matter ($R = r_0 A^{1/3}$, $r_0 \approx 1.15$ fm):

$$\rho_0 = \frac{A}{4\pi/3R^3} = \frac{1}{4\pi/3r_0^3} \approx 0.16\,\mathrm{fm}^{-3}$$

Nucleons start to overlap at a critical density ρ_C if nuclear matter is compressed ($r_N \approx 0.8$ fm):

$$\rho_c = \frac{1}{4\pi/3r_n^3} \approx 0.47/\mathrm{fm}^3 = 3\rho_0$$

A refined calculation in fact gives a somewhat higher critical density

Figure: CERN

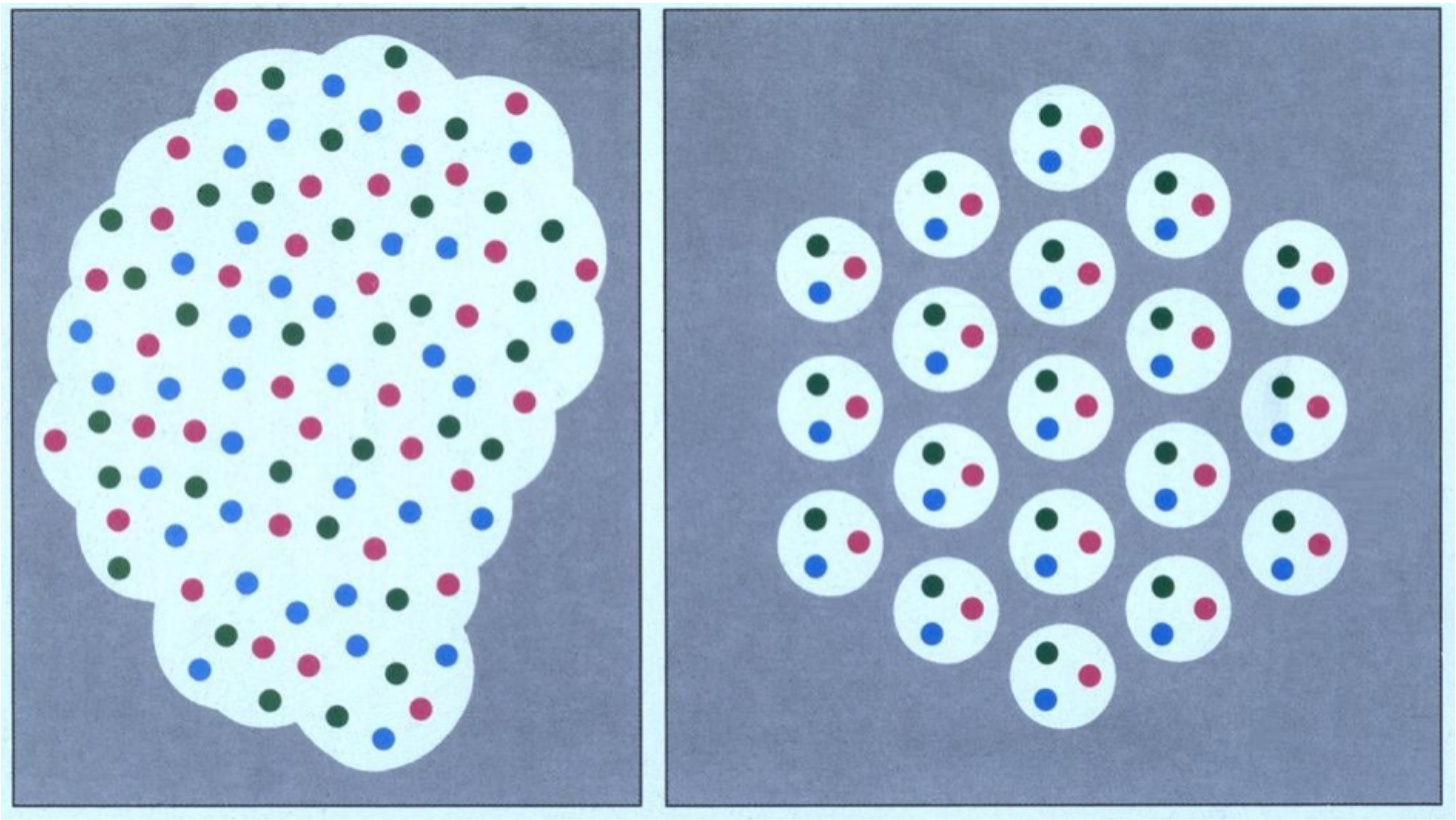

A more recent version of the (conjectured) QCD phase diagram

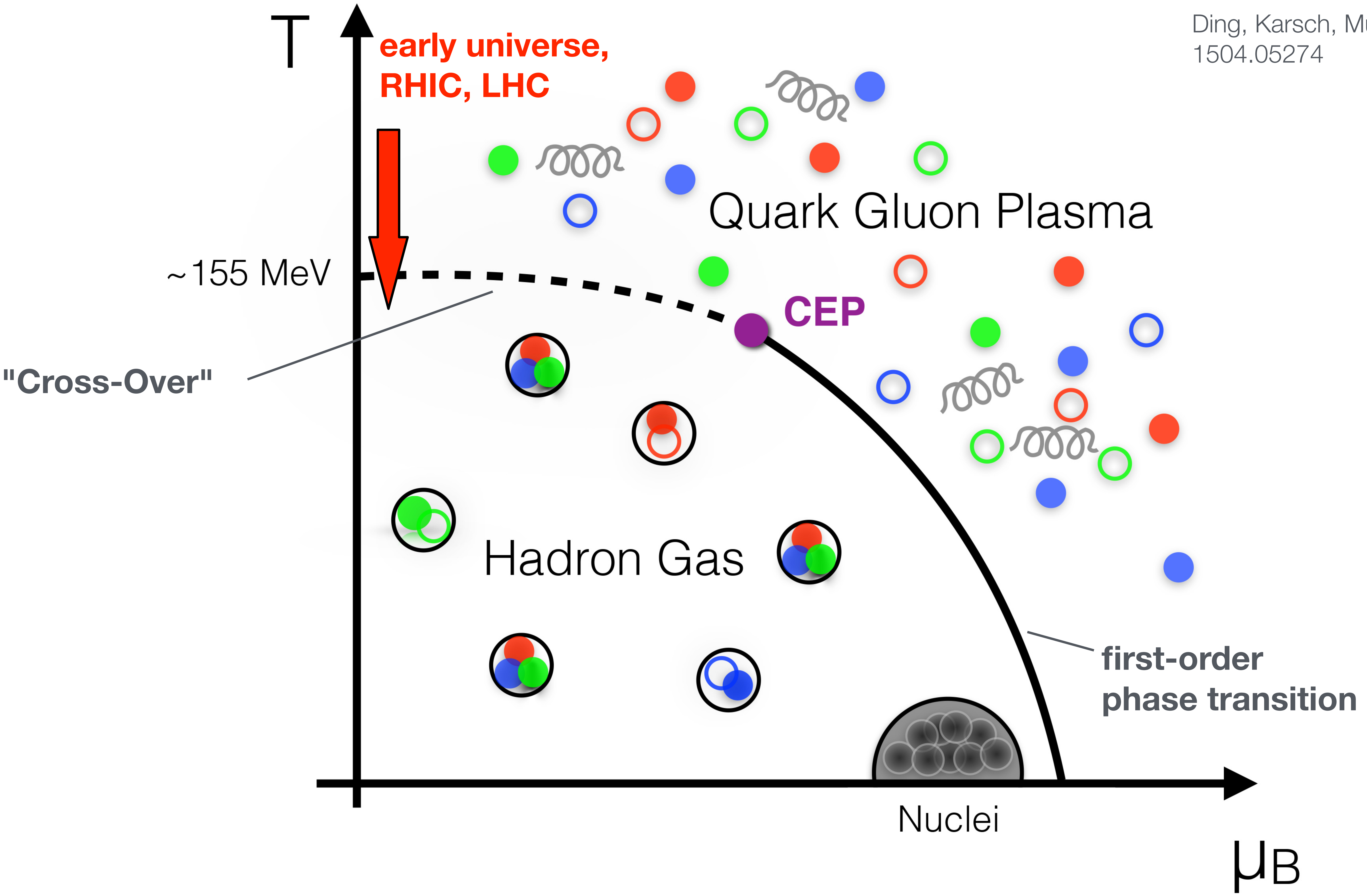

Ding, Karsch, Mukherjee
1504.05274

Results from lattice QCD

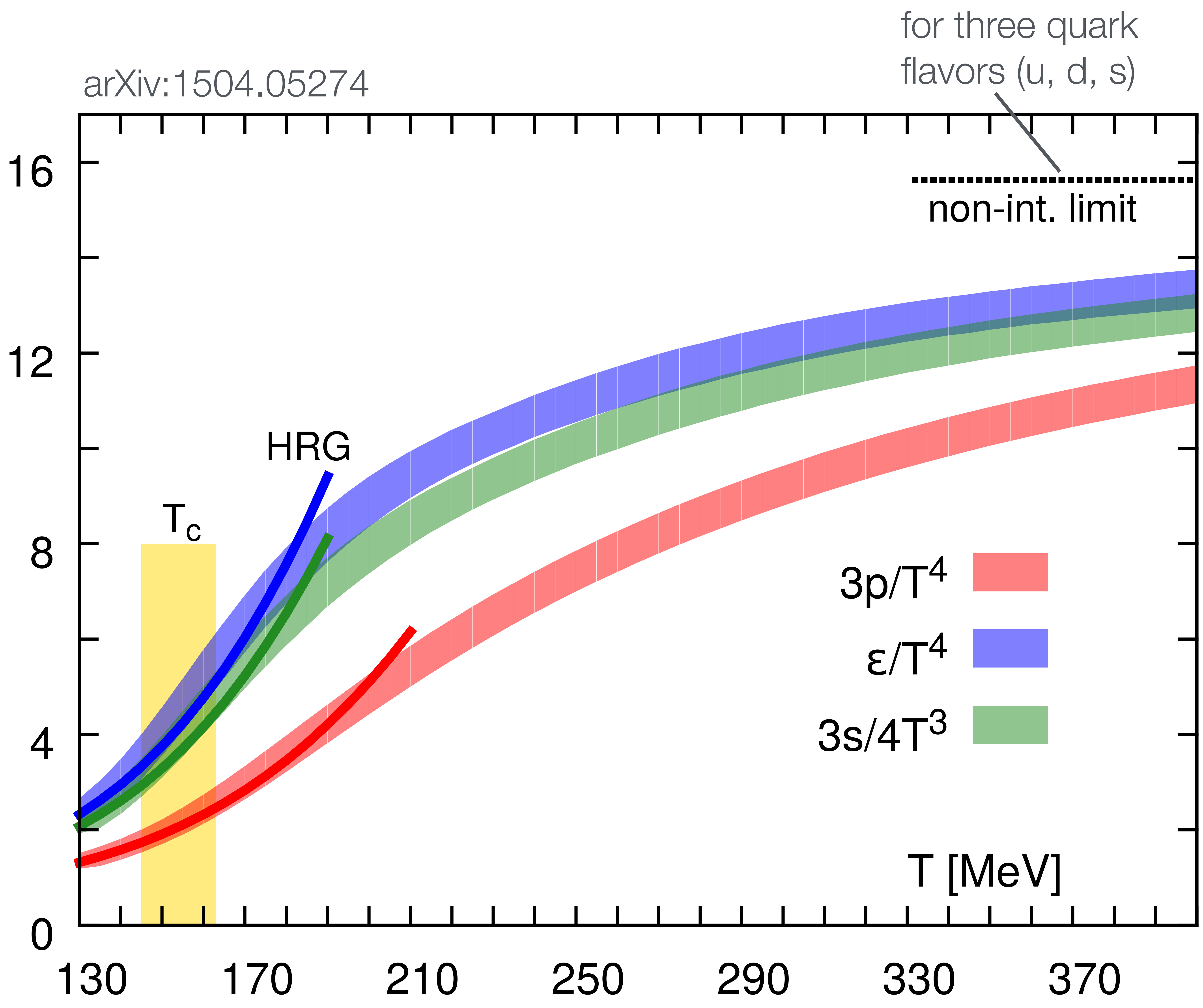

(2+1) flavor QCD:
two light (u,d) + one heavier quark (s)

Pseudo-critical temperature for chiral cross-over transition:

$T_{pc} = (156.5 \pm 1.5)$ MeV

$\varepsilon_{pc} = (0.42 \pm 0.06)$ GeV/fm^3

[Hot QCD coll., PLB 795 (2019) 15

Hadron resonance gas (HRG) agrees with lattice results for $T < T_{pc}$

Lattice QCD:

for massless u,d quarks:
second order chiral transition at $T_c = 132^{+3}_{-6}\,\mathrm{MeV}$

realistic u, d, s masses:
cross over: pseudo-critical temperature T_{pc}

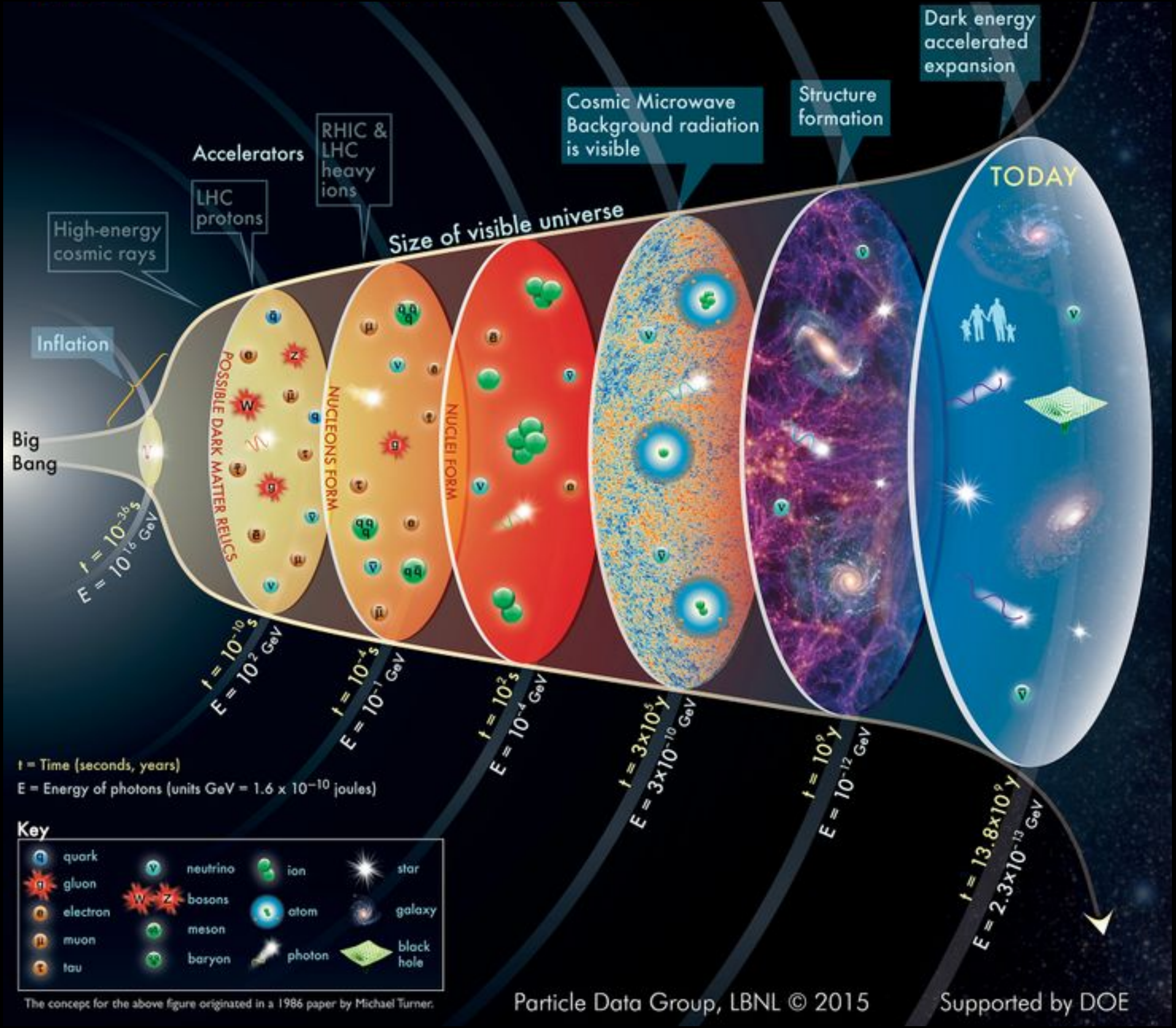

Transitions in the early universe:

electroweak transition:

T ~ 100 GeV, t ~ 10^{-12} s

QCD transition:

T ~150 MeV, t ~ 10^{-5} s

Boyanovsky, D., Schwarz, D.J., de Vega, H.J., Phase transitions in the early and the present universe, Ann.Rev.Nucl.Part.Sci., 56, 441-500 (2006)

RHIC:
Relativistic Heavy Ion Collider
Brookhaven National Laboratory

circumference 3.83 km, 2 independent rings, superconducting,
max. energy *Z/A* x 500 GeV = 200 GeV per nucleon pair in Au


LHCb
ATLAS
CERN Meyrin
PS 628 m
CERN Prévessin
SPS 7 km
SUISSE
FRANCE
ALICE
CMS
LHC 27 km
LHC lead beam 2023:
2.68 TeV/nucleon Pb beams → $\sqrt{s_{NN}}$ = 5.36 TeV

Stages of a heavy-ion collision

Dariusz Miśkowiec, Heavy-ion collision basics, arXiv:2211.04384

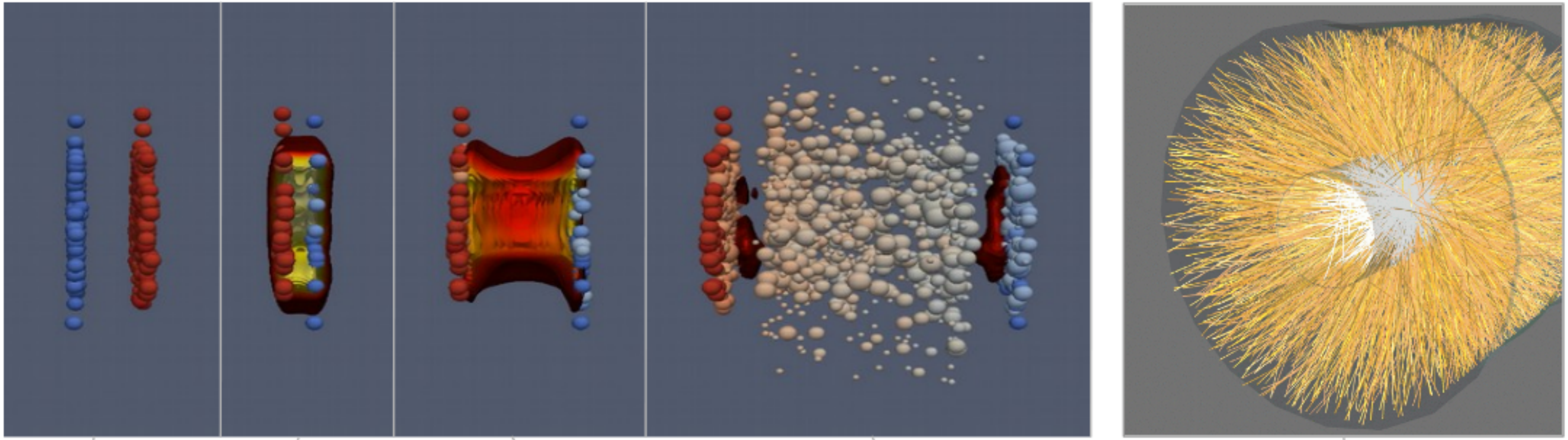

initial conditions	parton scattering	quark-gluon plasma	hadron scattering	particles interact with detectors

$\tau \sim 1$ fm/c

$\tau \sim 10$ fm/c

Space-time evolution

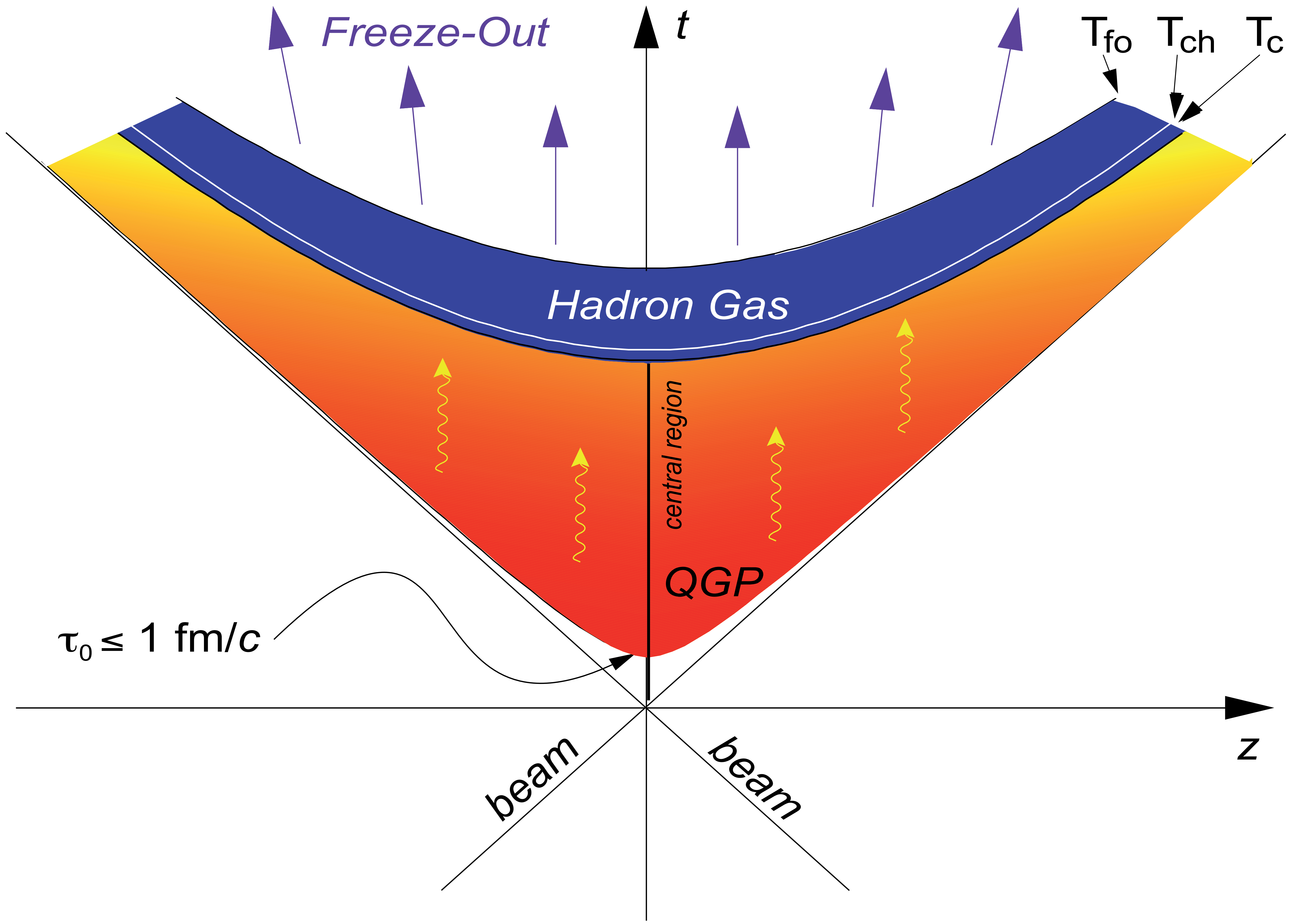

arxiv:0807.1610

Lines of constant proper time: $\tau = \sqrt{t^2 - z^2}$

Strong color-electric glue fields between nuclei

Rapid thermalization:
QGP created at τ ~ 1–2 fm/c

Expected initial temperatures of 500 MeV or higher

Expansion and cooling: $T \sim \tau^{-1/3}$

Transition QGP to hadrons at T_{pc} = 150–160 MeV

Chemical freeze-out at $T_{ch} \approx T_{pc}$
(hadron yields are frozen in)

Expansion of the hadron gas

Kinetic freeze-out at $T = T_{fo}$ at about 10 fm/*c*: momentum distributions are frozen in (T_{fo})

Material

Papers

John W. Harris, Berndt Müller, "*QGP Signatures*" *Revisited*, arXiv:2308.05743v3

ALICE coll., *The ALICE experiment -- A journey through QCD*, arXiv:2211.04384v1

50 Years of Quantum Chromodynamics, arXiv:2212.11107

Books

Yagi, Hatsuda, Miake, Quark-Gluon Plasma, Cambridge University Press, 2005

Sarkar, Satz, Sinha, The Physics of the Quark-Gluon Plasma, Springer, 2010

Satz, Extreme States of Matter in Strong Interaction Physics, Springer, 2012

Lectures

Quark-Gluon Plasma Physics, Uni Heidelberg (2023, 2019, 2017, …)

F. Bellini, Heavy Ion – CERN summer students lectures 2024 (part 1 , 2 , 3)

Basics

Quantifying the centrality of a heavy-on collision

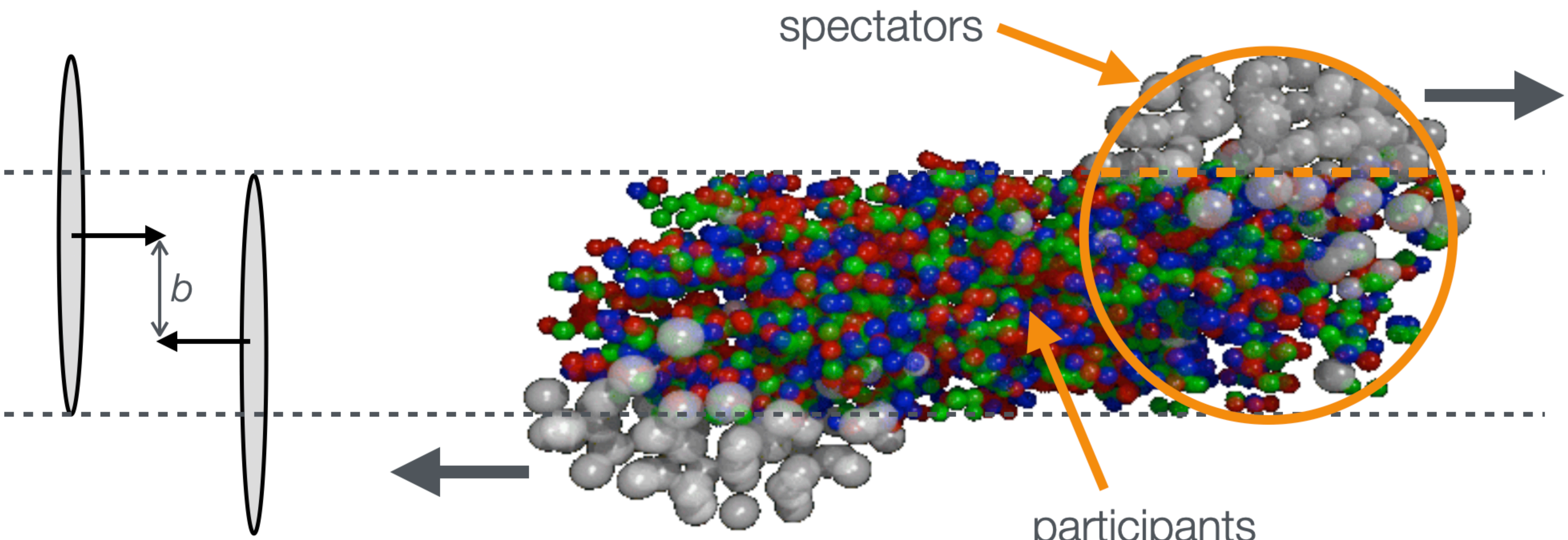

N_{coll}: number of inelastic nucleon-nucleon collisions

N_{part}: number of nucleons which underwent at least one inelastic nucleon-nucleon collisions

Smaller impact parameter *b* corresponds to higher centrality. Centrality often quantified by N_{part} and/or N_{coll} calculated in a simple geometric model which treats a A-A collision as simple superposition of nucleon-nucleon collisions (“Glauber model”)

Centrality determination

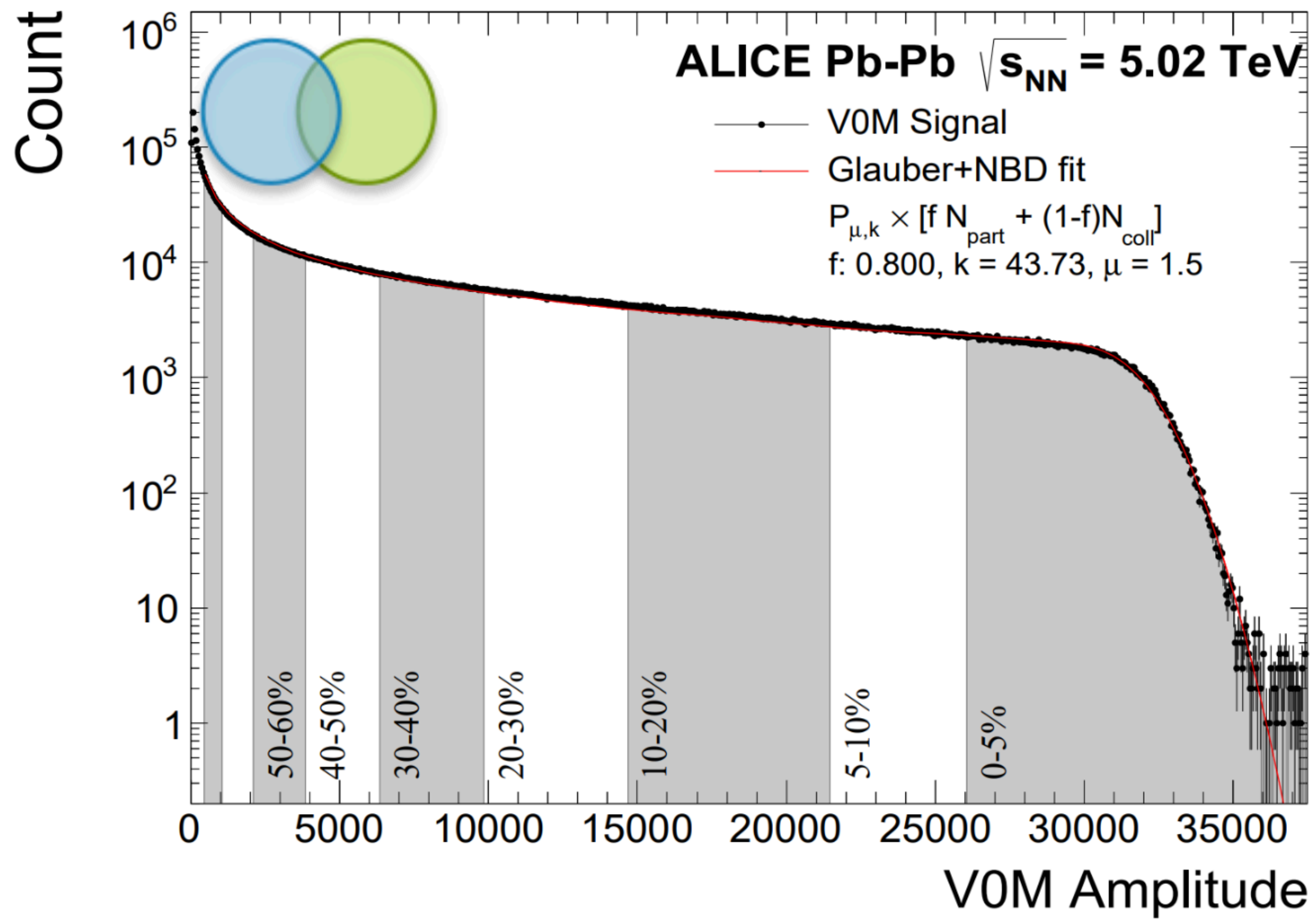

ALICE, PRL 106 (2011) 032301, PRC 91 (2015) 064905

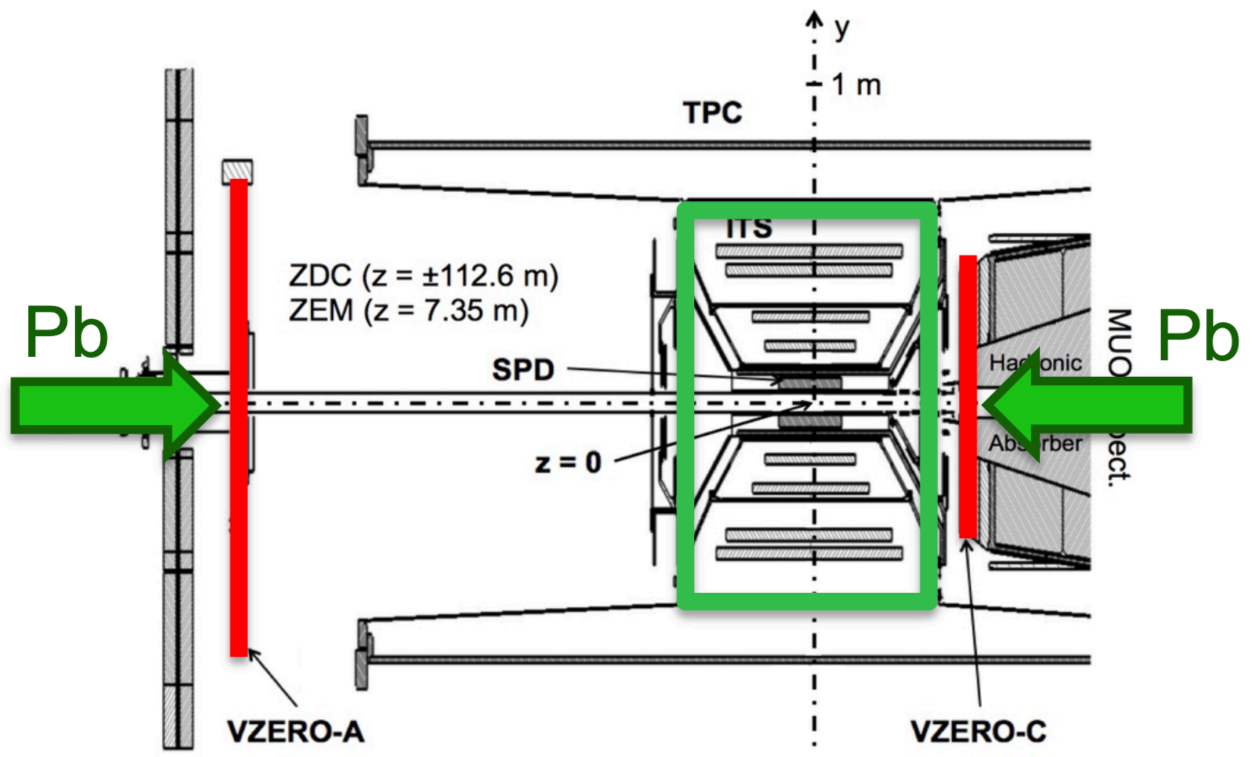

ALICE: centrality determination based on charges-particle multiplicity

Measured multiplicity distribution nicely reproduced by Glauber model
→ N_{part} and N_{coll}

Glauber Monte Carlo event:
Ann.Rev.Nucl.Part.Sci. 57 (2007) 205-243

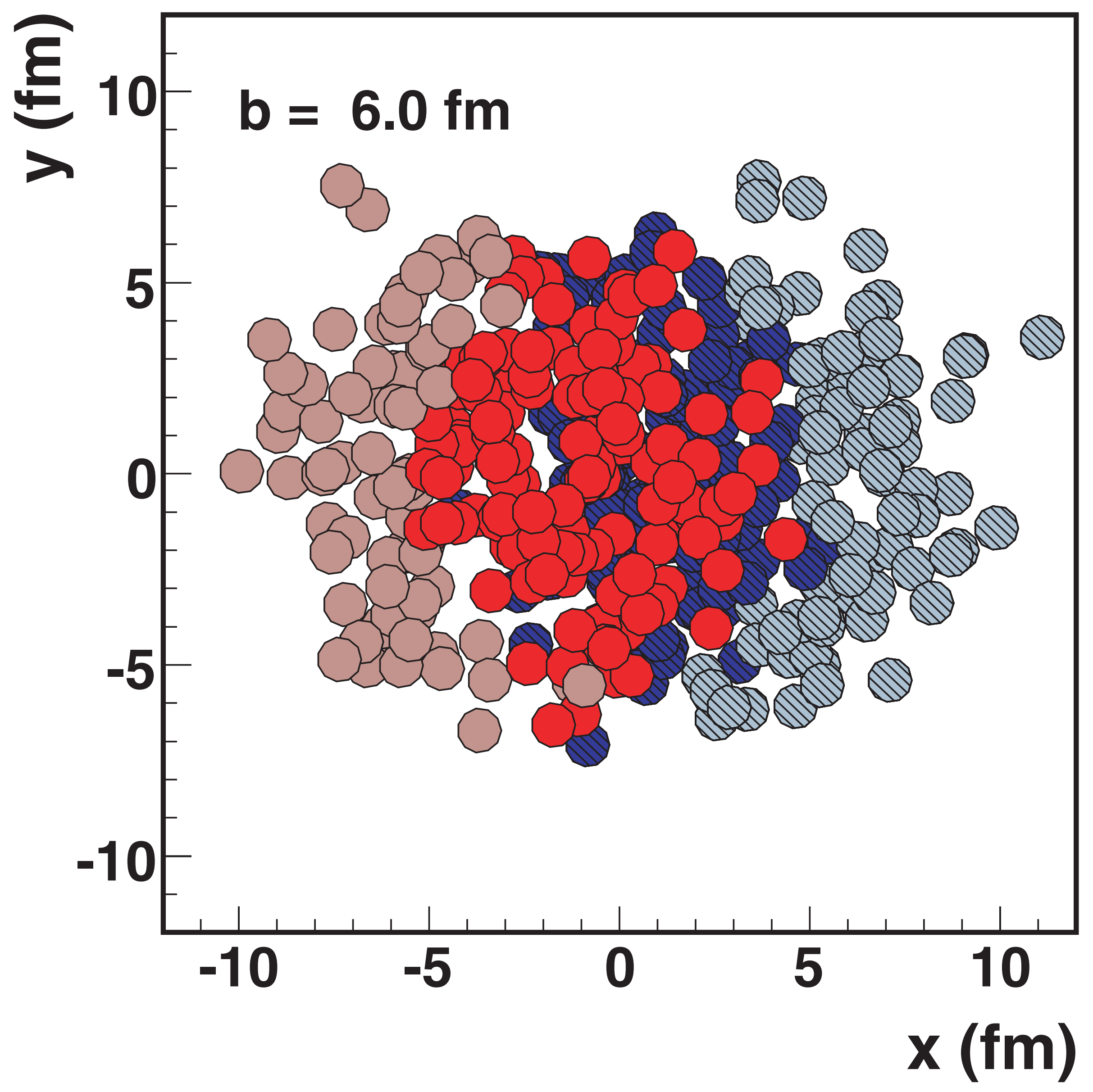

Forward and transverse energy in a fixed-target experiment

Example: Pb–Pb, $\sqrt{s_{NN}}$ = 17.3 GeV, fixed-target experiment (WA98, CERN SPS)

Forward energy measured in the Zero Degree Calorimeter (ZDC)

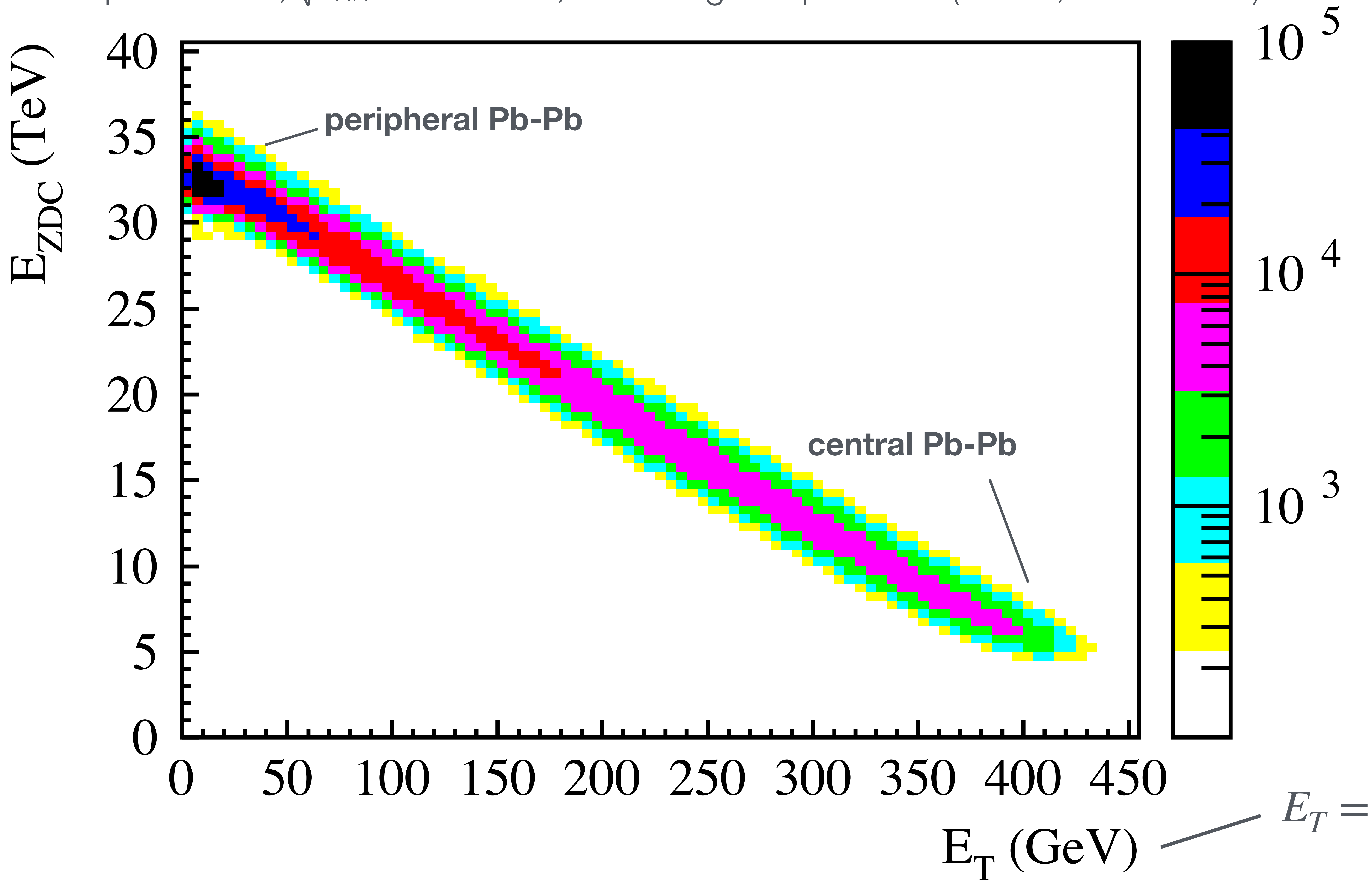

$$E_T = \sum_i E_i \sin\theta_i$$

Both E_T and E_{ZDC} can be used to define centrality classes

Kinematic variables

Transverse momentum and transverse mass:

$$p_T = p \sin\theta \qquad p = \sqrt{p_T^2 + p_L^2} \qquad m_T = \sqrt{m^2 + p_T^2}$$

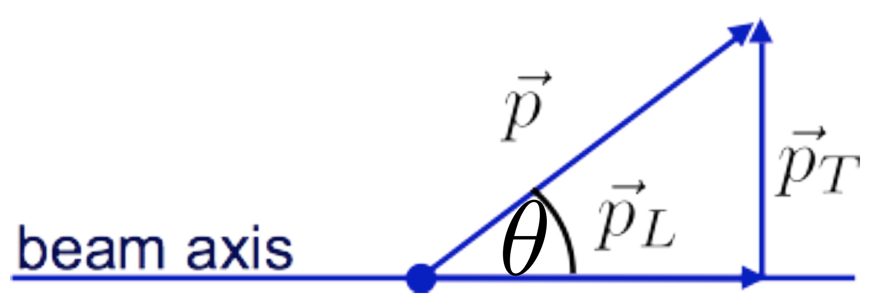

The rapidity y is a generalization of the (longitudinal) velocity $\beta_L = p_L/E$:

$$y := \operatorname{arctanh} \beta_L = \frac{1}{2} \ln \frac{1+\beta_L}{1-\beta_L} = \frac{1}{2} \ln \frac{E+p_L}{E-p_L} \qquad y \approx \beta_L \ \text{ for } \ \beta_L \ll 1$$

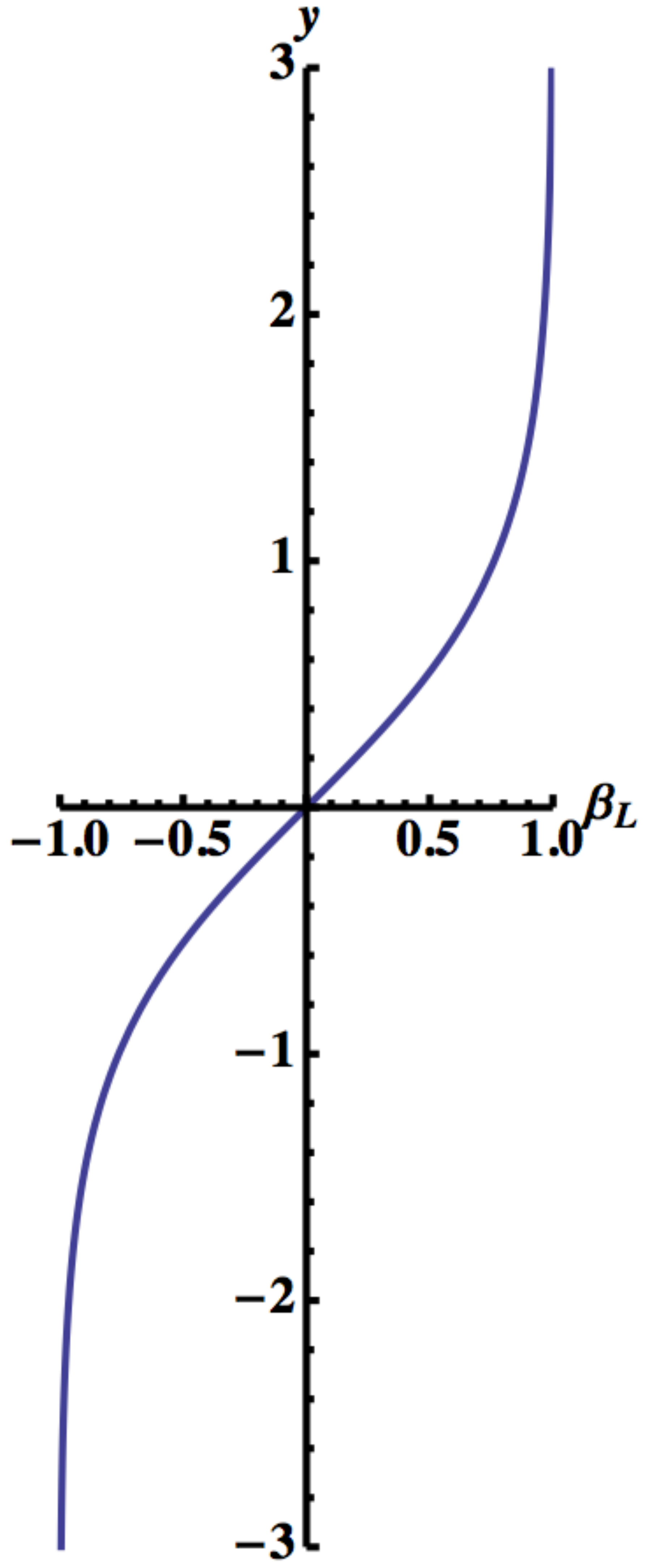

Pseudorapidity:

$$\cos(2\alpha) = 2\cos^2\alpha - 1 = 1 - 2\sin^2\alpha$$

$$y = \frac{1}{2} \ln \frac{E + p\cos\vartheta}{E - p\cos\vartheta} \overset{p \gg m}{\approx} \frac{1}{2} \ln \frac{1+\cos\vartheta}{1-\cos\vartheta} = \frac{1}{2} \ln \frac{2\cos^2\frac{\vartheta}{2}}{2\sin^2\frac{\vartheta}{2}} = -\ln\left[\tan\frac{\vartheta}{2}\right] =: \eta$$

$$y = \eta \quad \text{for} \quad m = 0$$

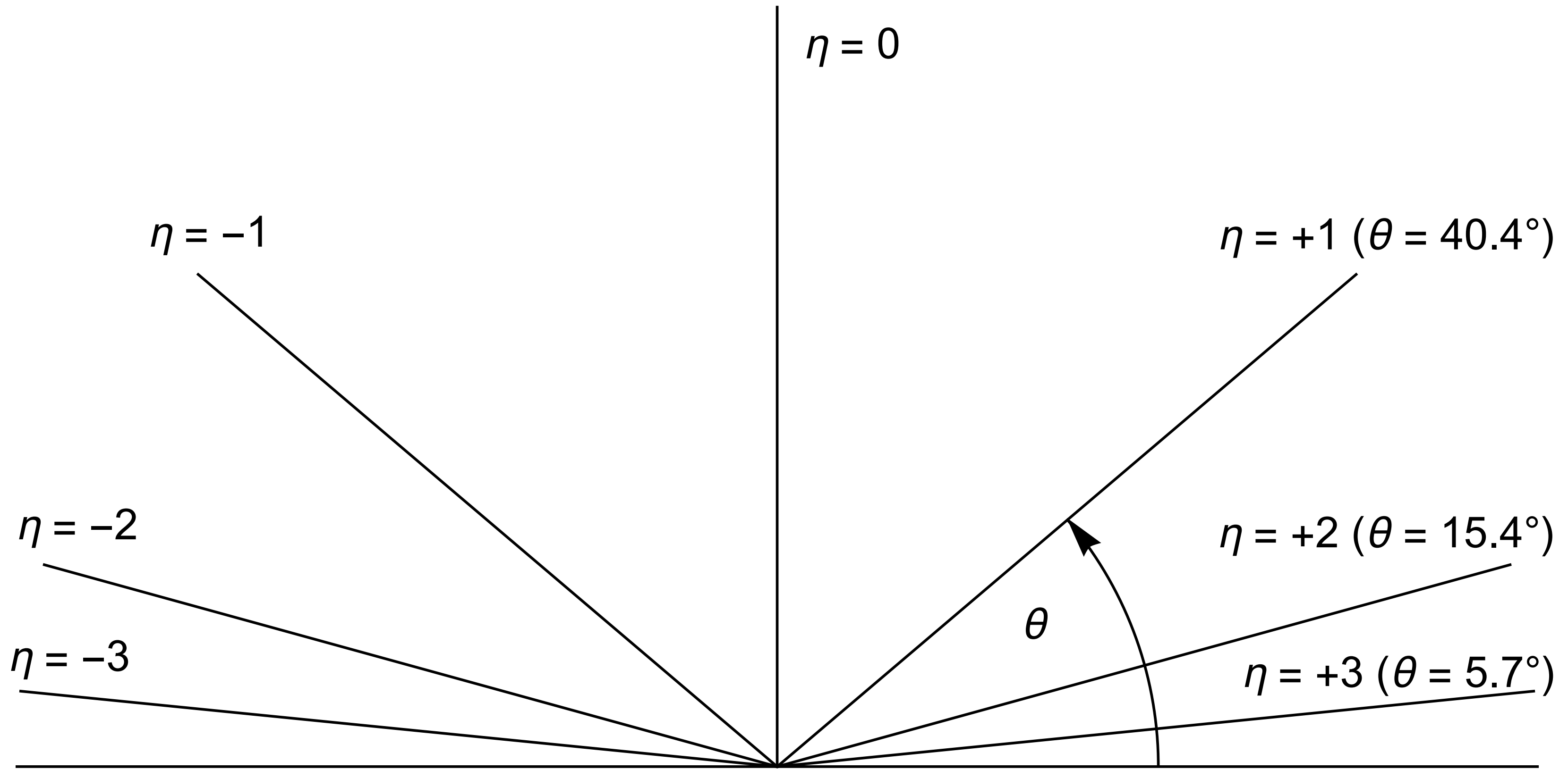

Useful relations:

$$E = m_T \cosh y, \qquad p_L = m_T \sinh y$$

$$p = p_T \cosh \eta, \qquad p_L = p_T \sinh \eta$$

Nuclear stopping

Brahms, PRL 93:102301, 2004

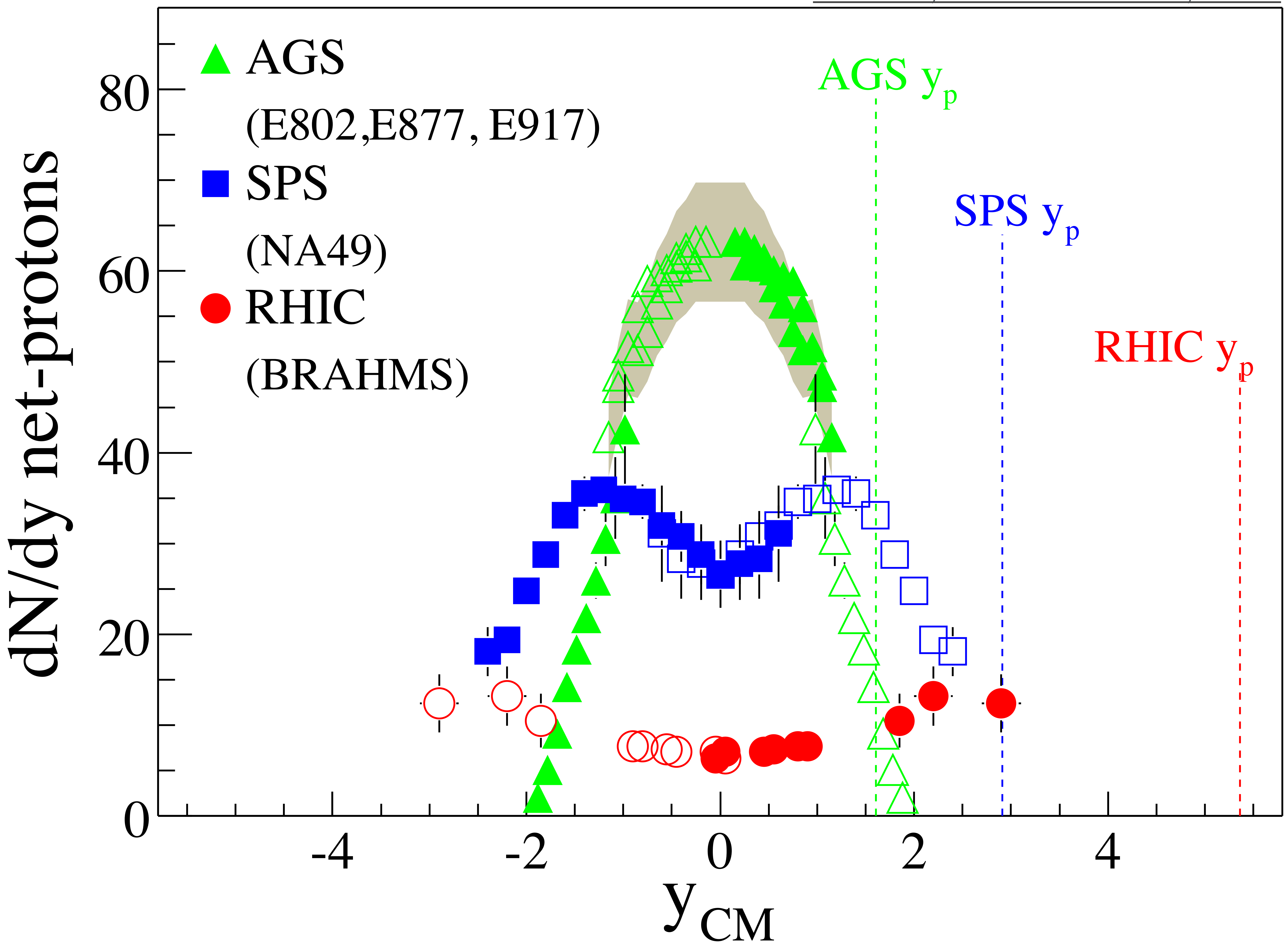

Participating nucleons lose on average about 2 units of rapidity:

$$\langle \Delta y \rangle = y_p - \langle y \rangle \approx 2$$

beam rapidity

At RHIC and the LHC, the nuclei pass through each other and produce a fireball at midrapidity with very small net baryon number

Particle production in heavy-ion collisions

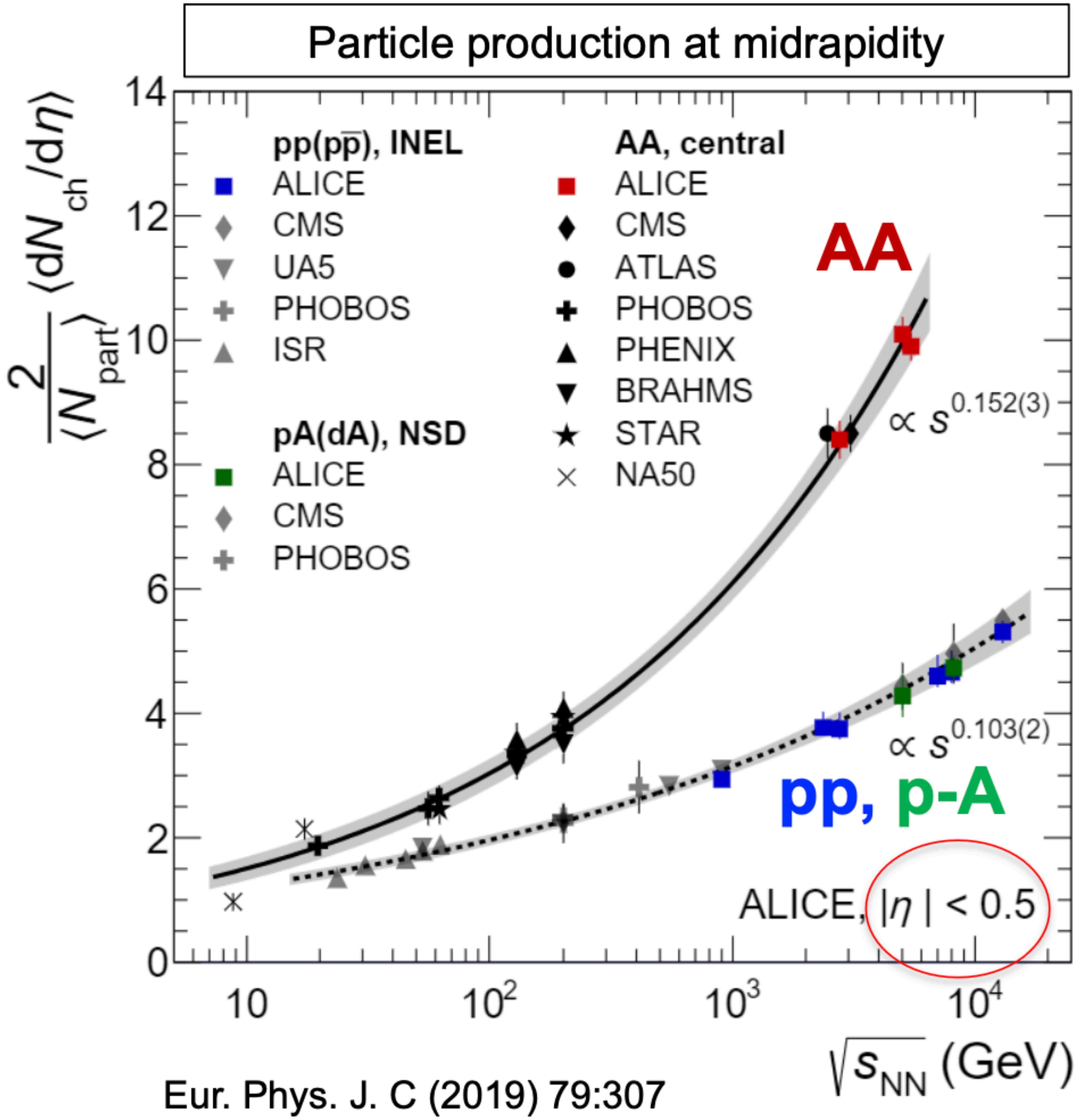

Eur. Phys. J. C (2019) 79:307

Higher yield per participant in A-A collisions than in pp and p-A

A-A collisions more efficient in transforming the initial energy into particles

More than factor 2 increase from RHIC to LHC

Total number of produced charged particles in central collisions Pb–Pb at the LHC: **~ 20.000**

ALICE, Phys.Lett. B 772 (2017) 567-577

Average transverse momentum

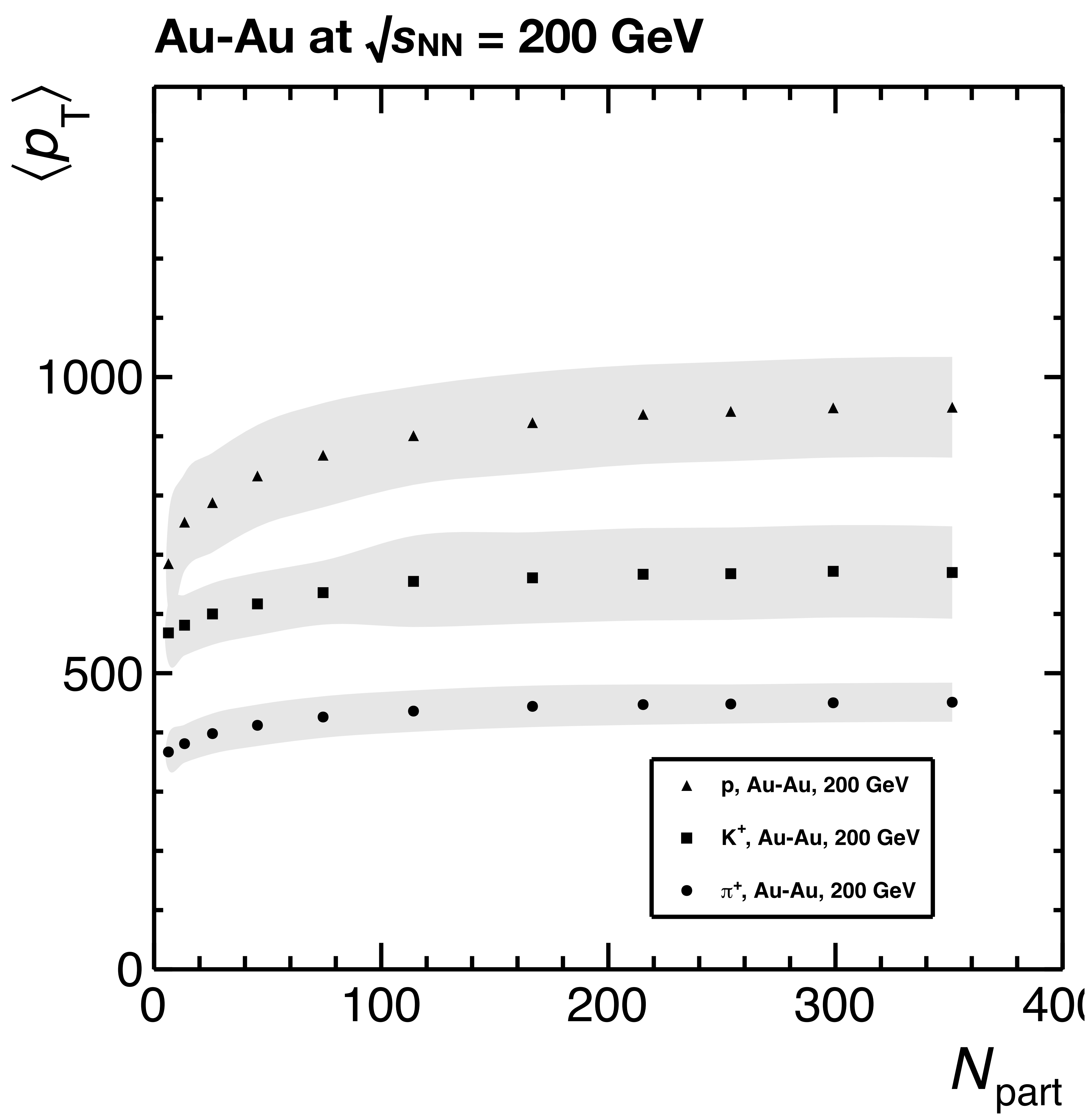

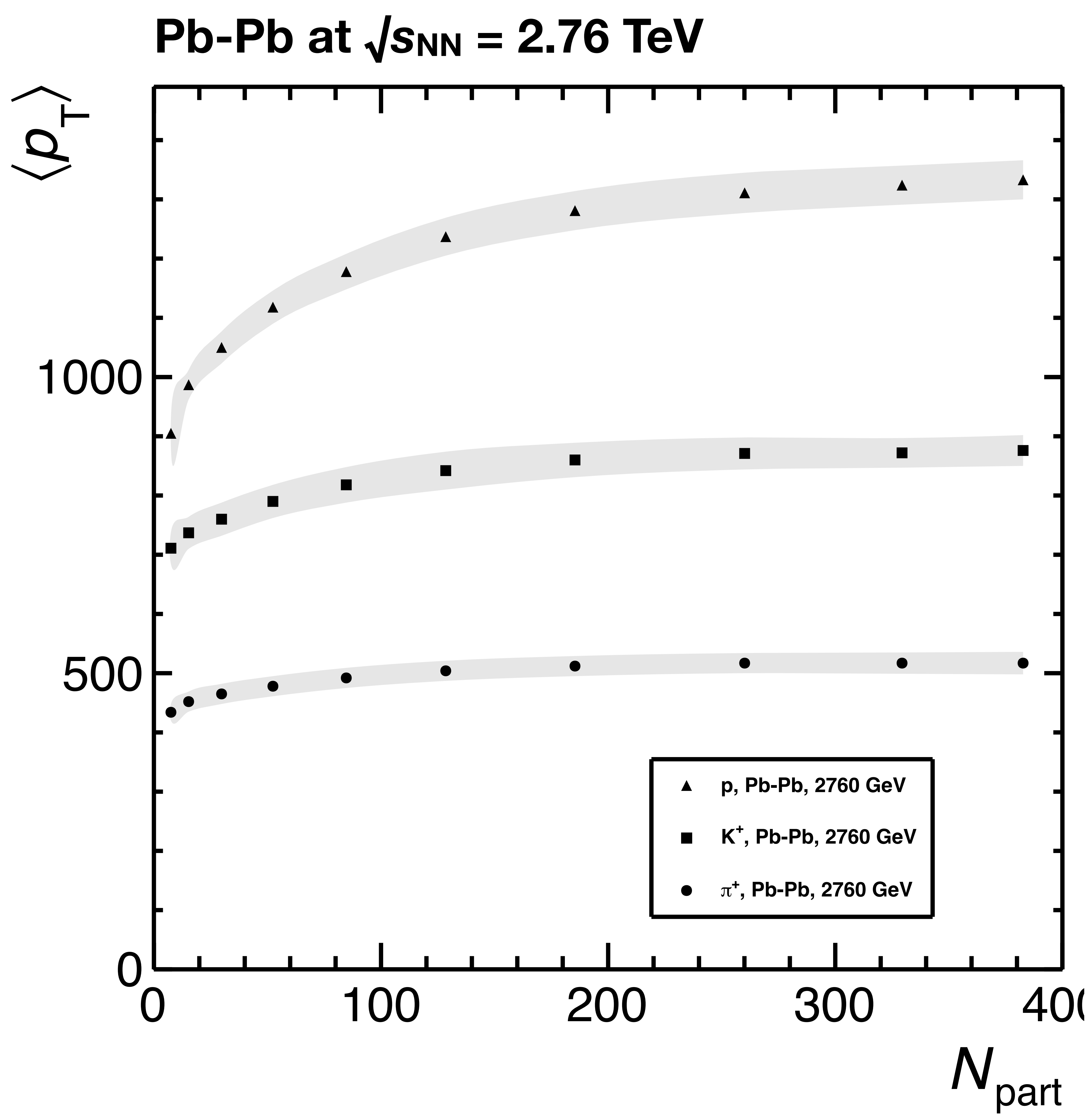

Stronger increase in $\langle p_T \rangle$ for heavier particles

Estimate of the initial energy density

Bjorken formula:

$$\varepsilon = \frac{1}{A \cdot \tau_0} \frac{\mathrm{d}E_\mathrm{T}}{\mathrm{d}y}\bigg|_{y=0}, \qquad \tau_0 \approx 1\,\mathrm{fm}/c$$

transverse area of the overlap zone

J.D. Bjorken, Phys.Rev. D27 (1983) 140-151,
3664 citations on inspirehep.net on July 30, 2024

PHENIX, arXiv:1509.06727

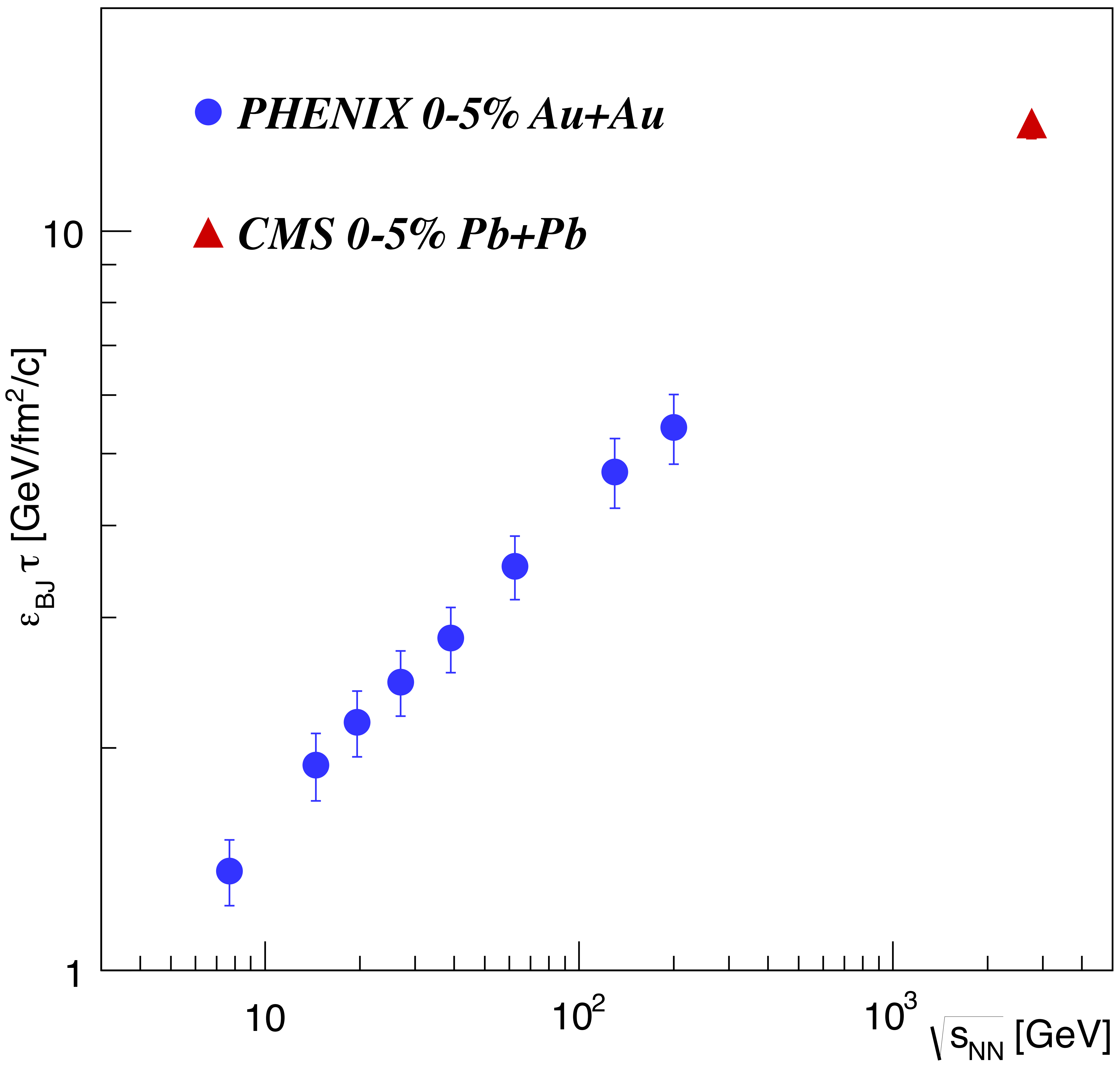

Even at $\sqrt{s_{NN}}$ = 7.7 GeV the estimated initial energy density is above $\varepsilon_{pc} \approx 0.4$ GeV/fm^3

Statistical Model and Strangeness

Hadronization of the nuclear fireball

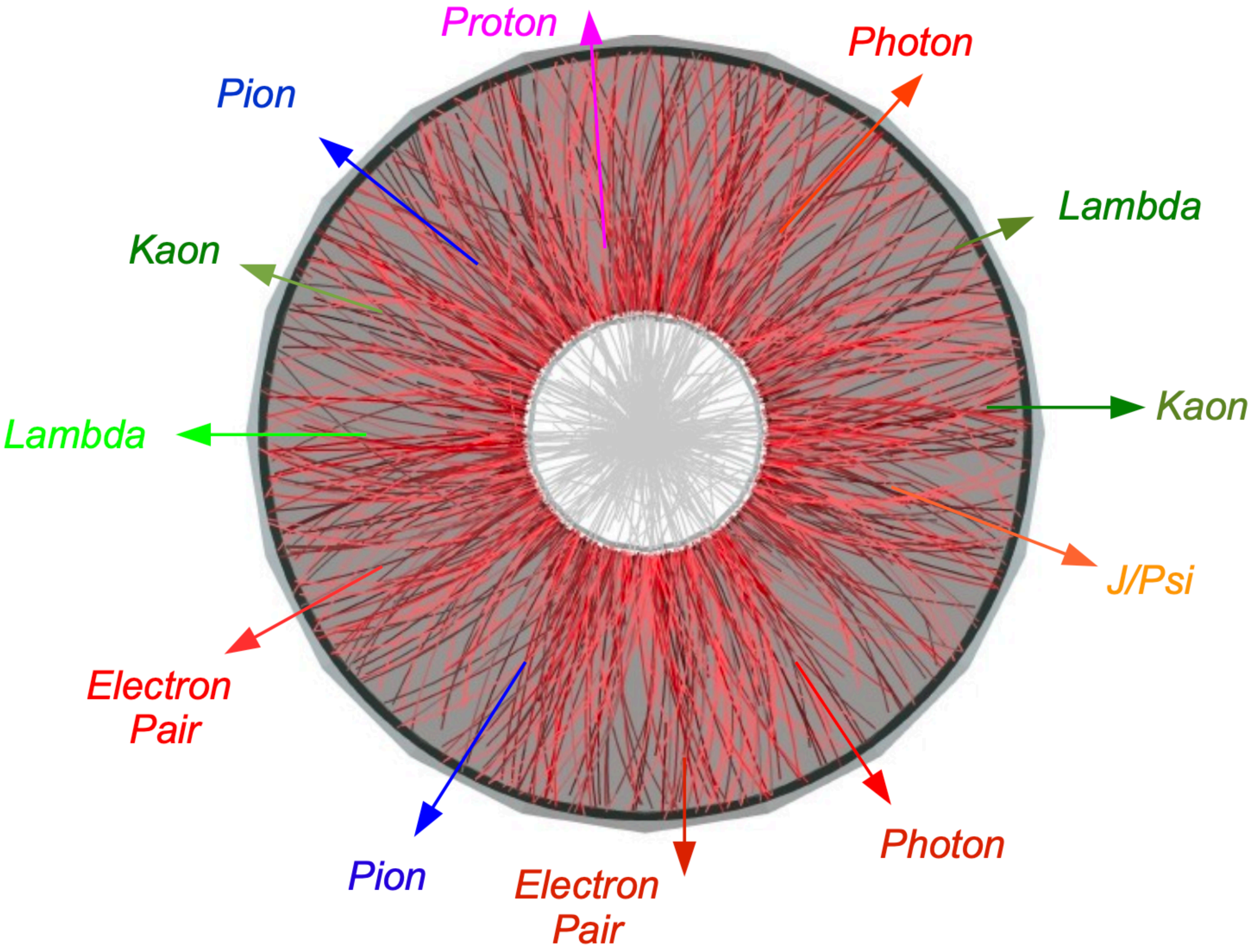

Fireball properties can be determined by measurement of the emitted particles

In this section:
hadrons with up, down, strange constituent quarks

Strangeness production in hadronic interactions

"hidden strangeness"

Particles with strange quarks:

$$K^+ = (u\bar{s}),\ K^- = (\bar{u}s),\ K^0 = (d\bar{s}),\ \bar{K}^0 = (\bar{d}s),\ \phi = (s\bar{s}),$$

$$\Lambda = (uds),\ \Sigma = (qqs),\ \Xi = (qss),\ \Omega^- = (sss)$$

Production in collisions of hadrons:

Example 1: $p + p \to p + K^+ + \Lambda, \quad Q = m_\Lambda + m_{K^+} - m_p \approx 670\,\mathrm{MeV}$

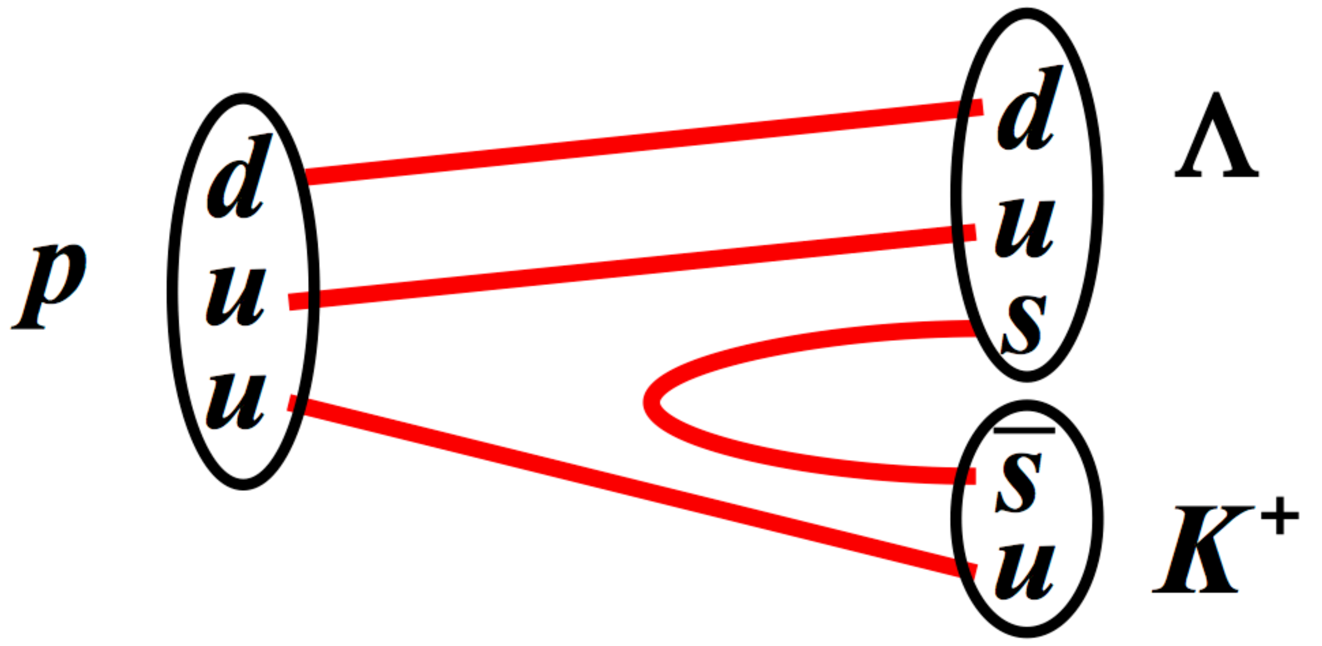

associated production of strangeness

Example 2: $p + p \to p + p + \Lambda + \bar{\Lambda}, \quad Q = 2m_\Lambda \approx 2230\,\mathrm{MeV}$

Strangeness production in the QGP

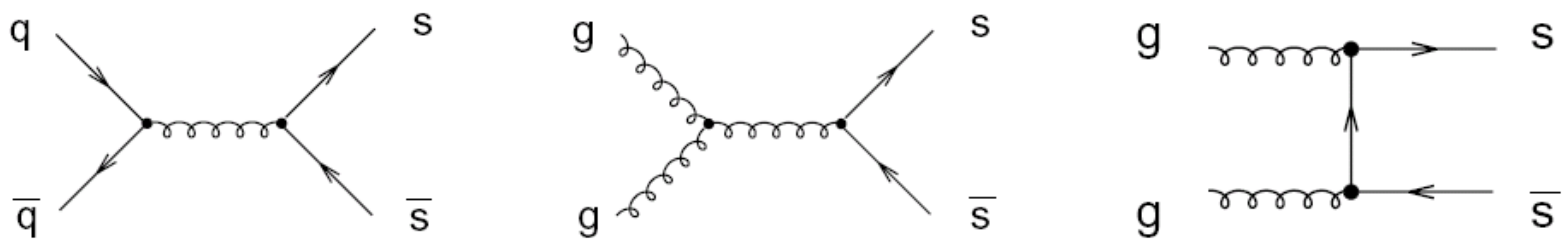

$$Q_{\mathrm{QGP}} \approx 2m_s \approx 200\,\mathrm{MeV}$$

Q value in the QGP significantly lower than in hadronic interactions

This reflects the difference between the current quarks mass (QGP) and the constituent quark mass (chiral symmetry breaking)

Strangeness Enhancement in Pb–Pb relative to p–Pb at $\sqrt{s_{NN}}$ = 17.3 GeV

0-40% Pb-Pb
at $\sqrt{s_{NN}}$ = 17.3 GeV

WA97,
PLB 449 (1999) 401,
CERN-EP/99-29

p-Be reference instead of p-Pb: similar behavior (NA57)

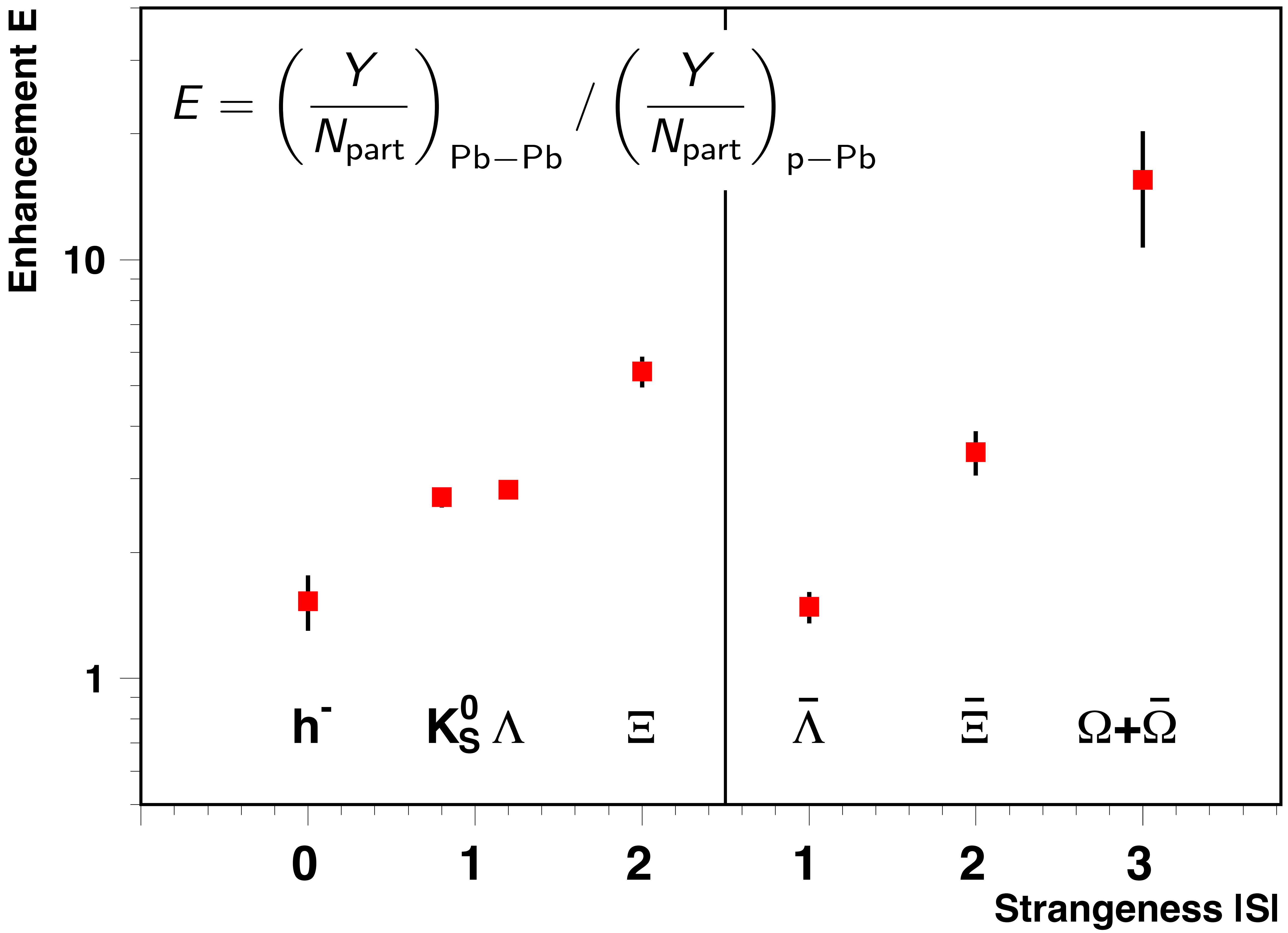

Strangeness enhancement increases with s-quark contents (up to factor 17 for the Ω baryon)

Thermal energy leads to population of hadronic states (1)

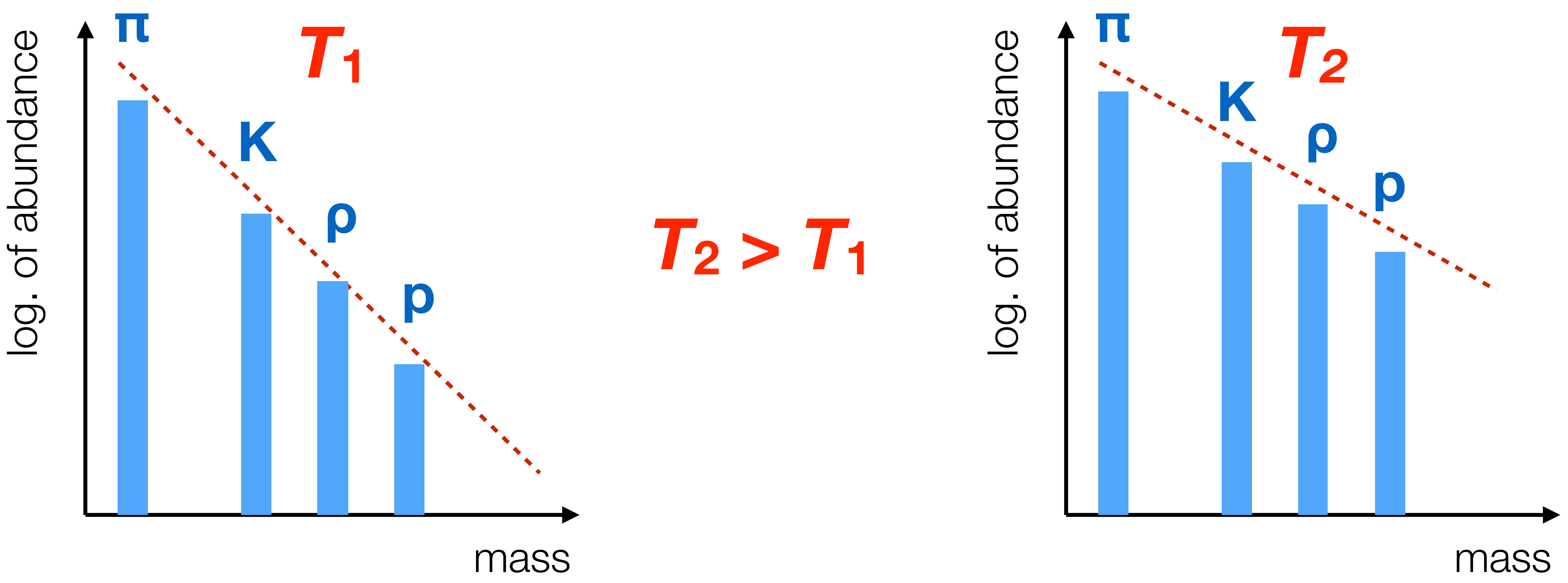

Assume phase space is filled thermally (Boltzmann) at hadronization:

Abundance of hadron species $\propto m^{3/2} \exp(-m/T)$

Determined by temperature (and density) at time of production of hadrons i.e. hadronization

Thermal energy leads to population of hadronic states (2)

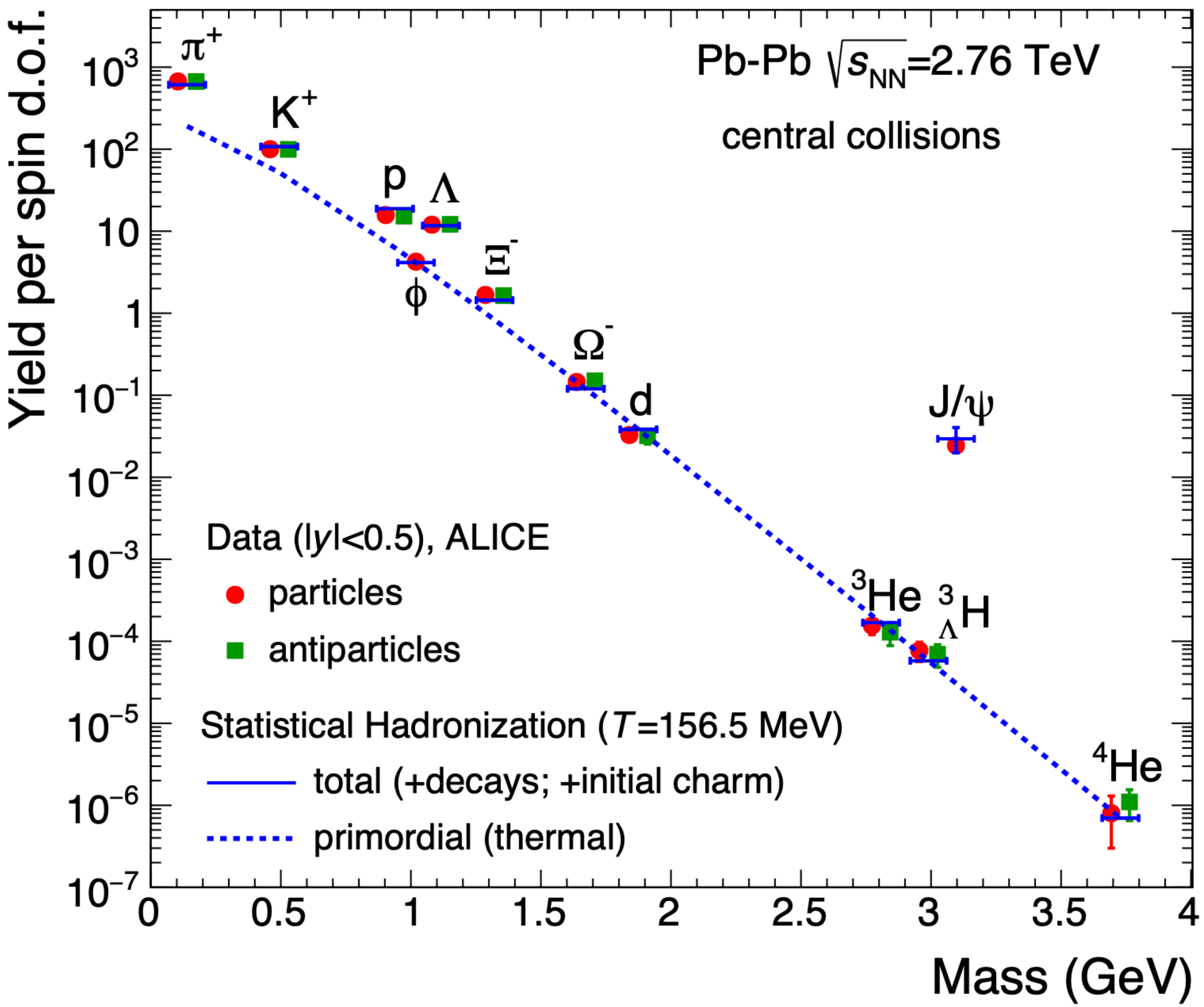

Need to calculate feeddown from decays of short-lived hadrons when comparing with data (e.g. $\rho \to \pi\pi$)

T_{ch} = 156.6 MeV gives a very good description of hadron yields in Pb–Pb at the LHC

Even the yields of large and loosely-bound particles like the hypertriton ($^3_\Lambda$H) are described well: *snowballs in hell* puzzle

[Braun-Munzinger, Dönigus, Nuclear Physics A 987 (2019) 144]

Hadron yields from in the hadron resonance gas model

Particle densities for a non-interacting massive gas of fermions (upper sign) / bosons (lower sign):

$$n_i \equiv \frac{N_i}{V} = g_i \frac{4\pi}{(2\pi)^3} \int_0^\infty \frac{p^2\,\mathrm{d}p}{\exp\left(\frac{\sqrt{p^2+m^2}-\mu_i}{T}\right) \pm 1} = \frac{g_i}{2\pi^2} m^2 T \sum_{k=1}^{\infty} \frac{(\mp 1)^{k+1}}{k} \lambda^k K_2\left(\frac{km}{T}\right)$$

$$\lambda = e^{\mu_i/T}$$

Formula for a grand canonical ensemble

"Boltzmann approximation"
(neglect "±1"): take only first term of the sum

Chemical potential: $\mu_i = \mu_\mathrm{B} B_i + \mu_\mathrm{S} S_i + \mu_{\mathrm{I}_3} I_i^{(3)},$

But can use conservation laws to constrain μ_S and μ_{I_3}.

Only 2 free parameters left: fit for each center-of-mass energy provides T and μ_B

$\sqrt{s_{NN}}$ dependence of T and μ_B

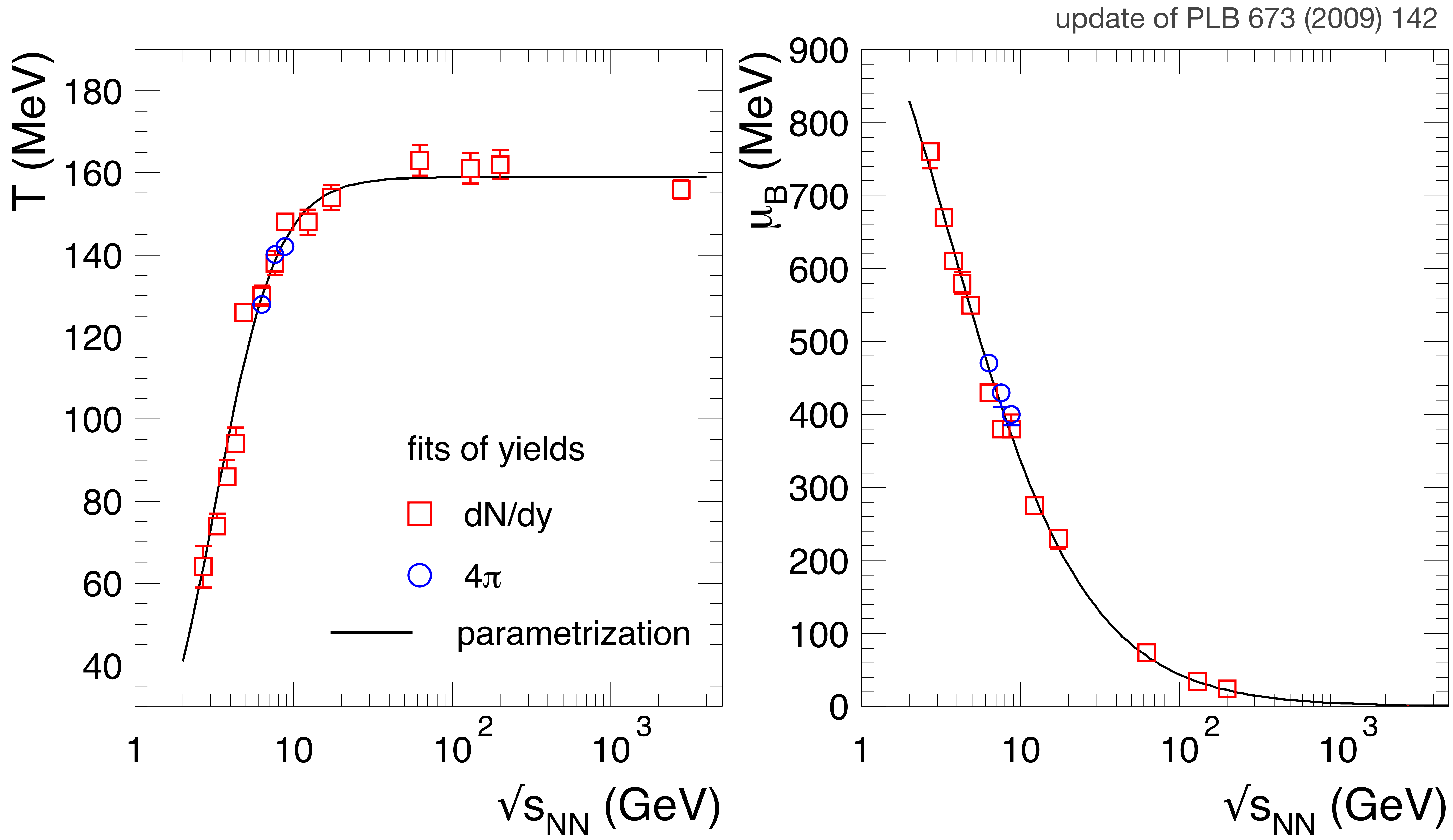

Smooth evolution of T and μ_B with $\sqrt{s_{NN}}$

T reaches limiting value close to T_{pc}

Chemical freeze-out parameters and the QCD phase diagram

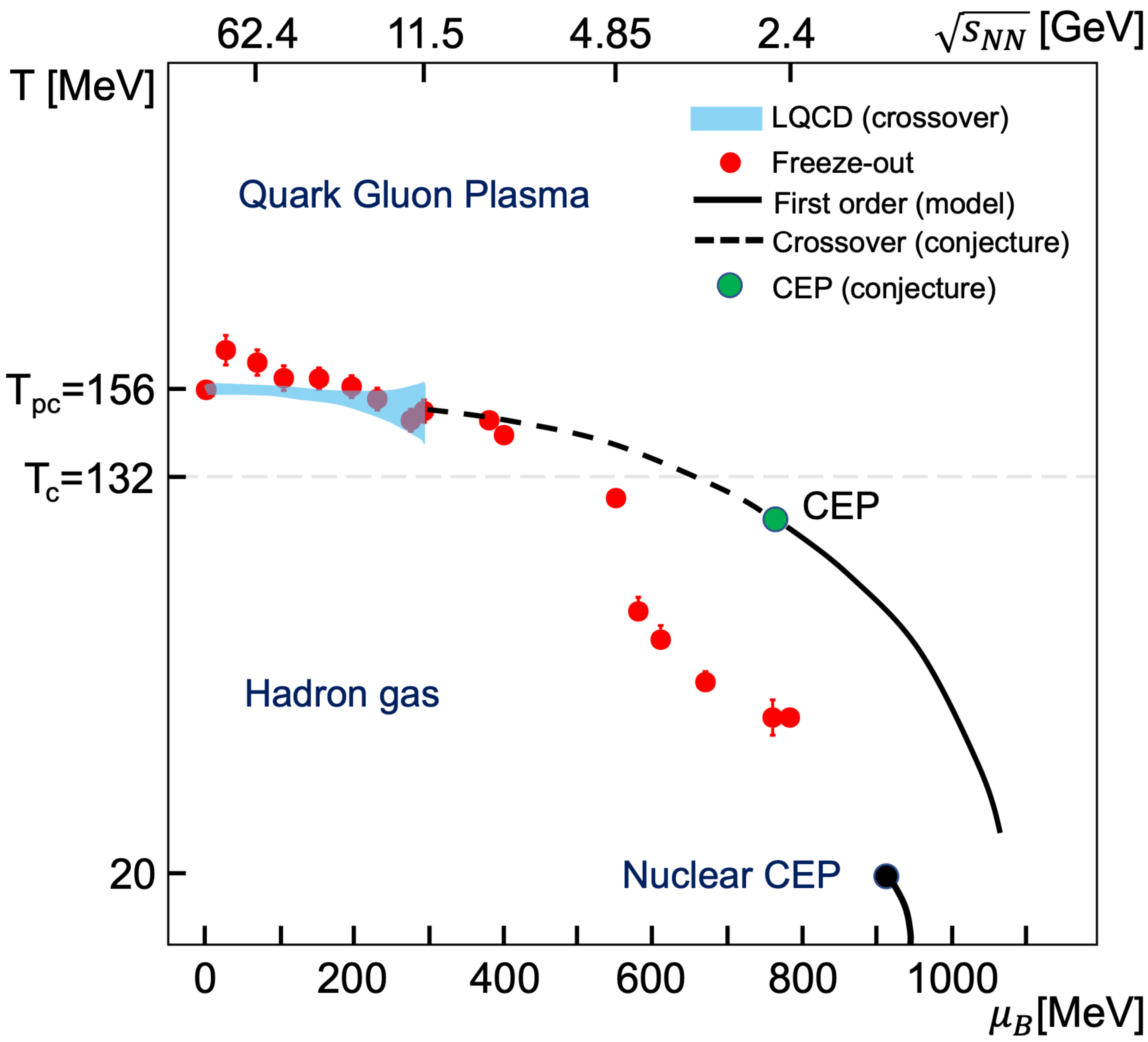

T_{ch} very close to T_{pc}:
produced hadrons cease to interact inelastically within a narrow temperature interval at RHIC and LHC energies

Search for the critical endpoint (CEP) is an ongoing research topics

Space-time evolution

Radial flow

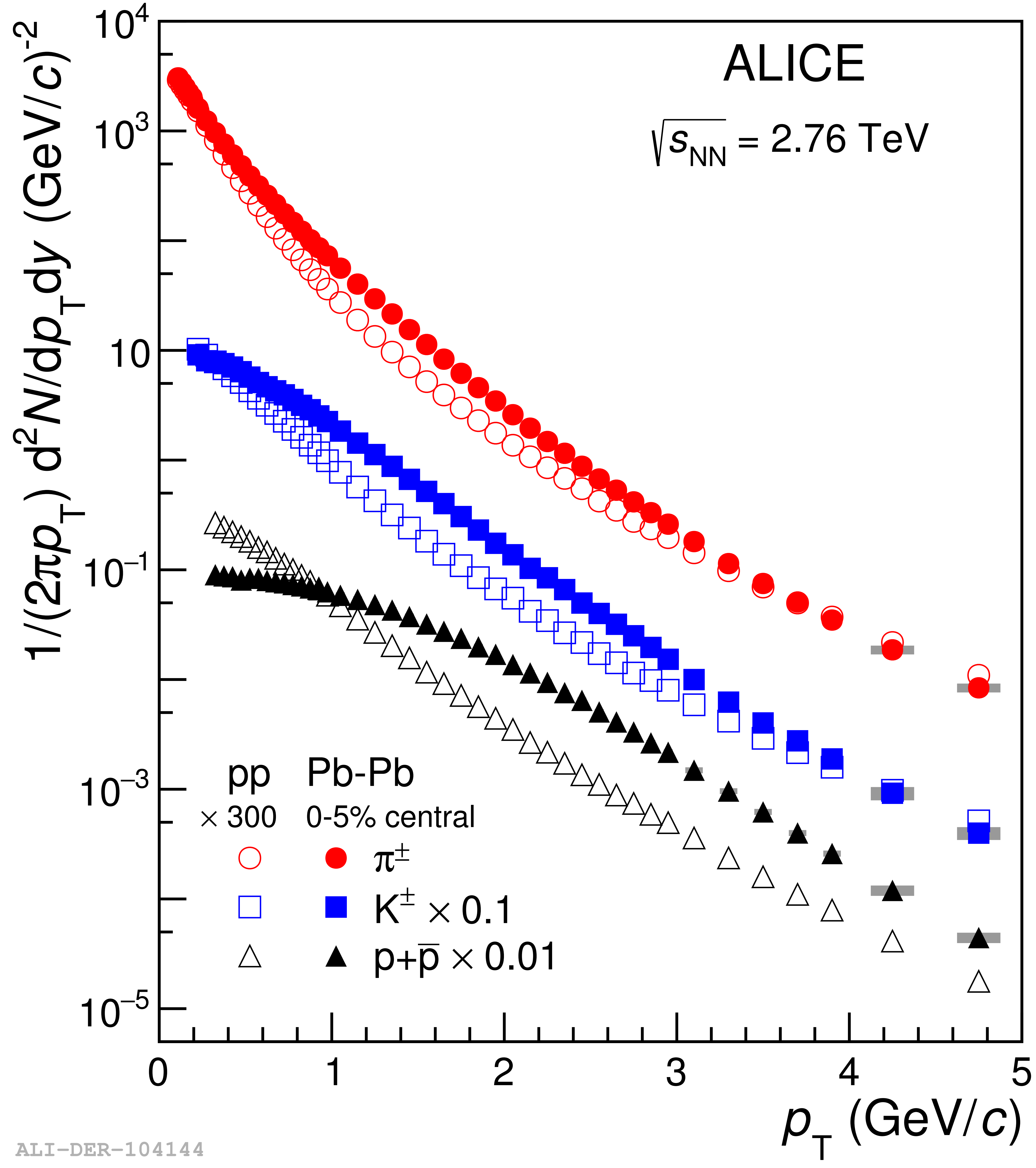

Shape is different in pp and A–A

Stronger effect for heavier particles

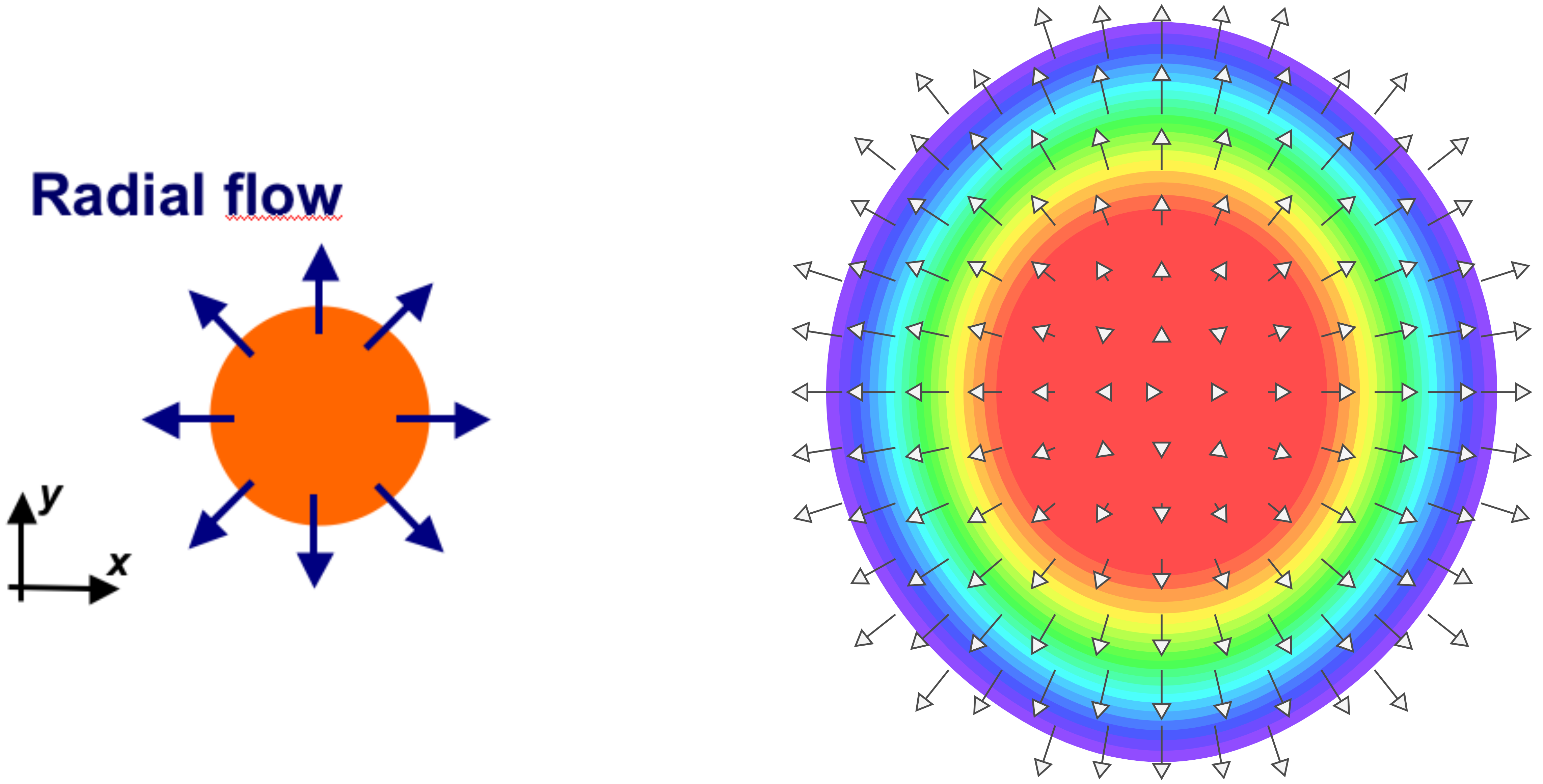

average transverse velocity correlated with the position in the transverse plane

Elliptic flow

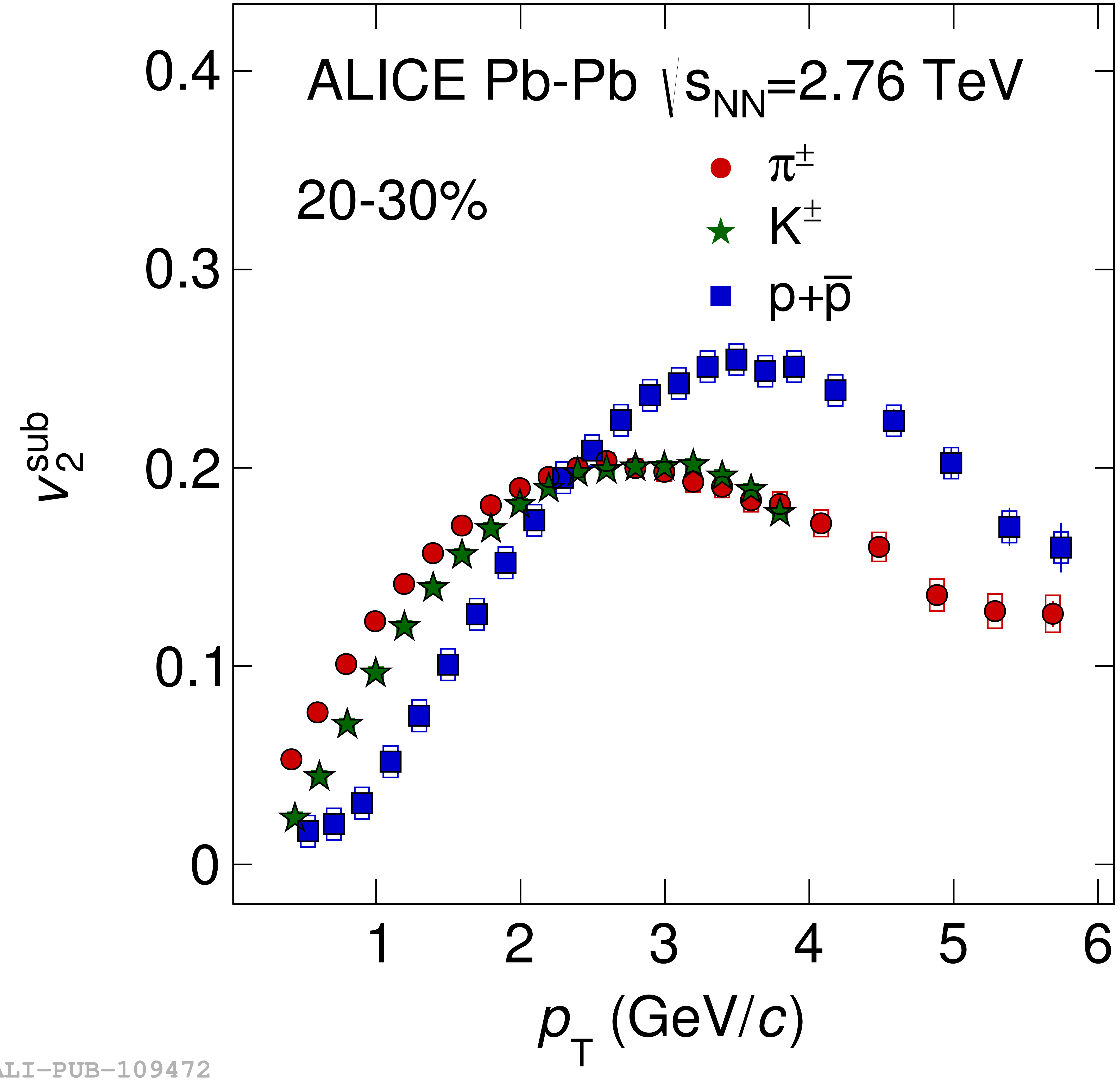

ALI-PUB-109472

Good explanation:
Azimuthal variation of the flow velocity

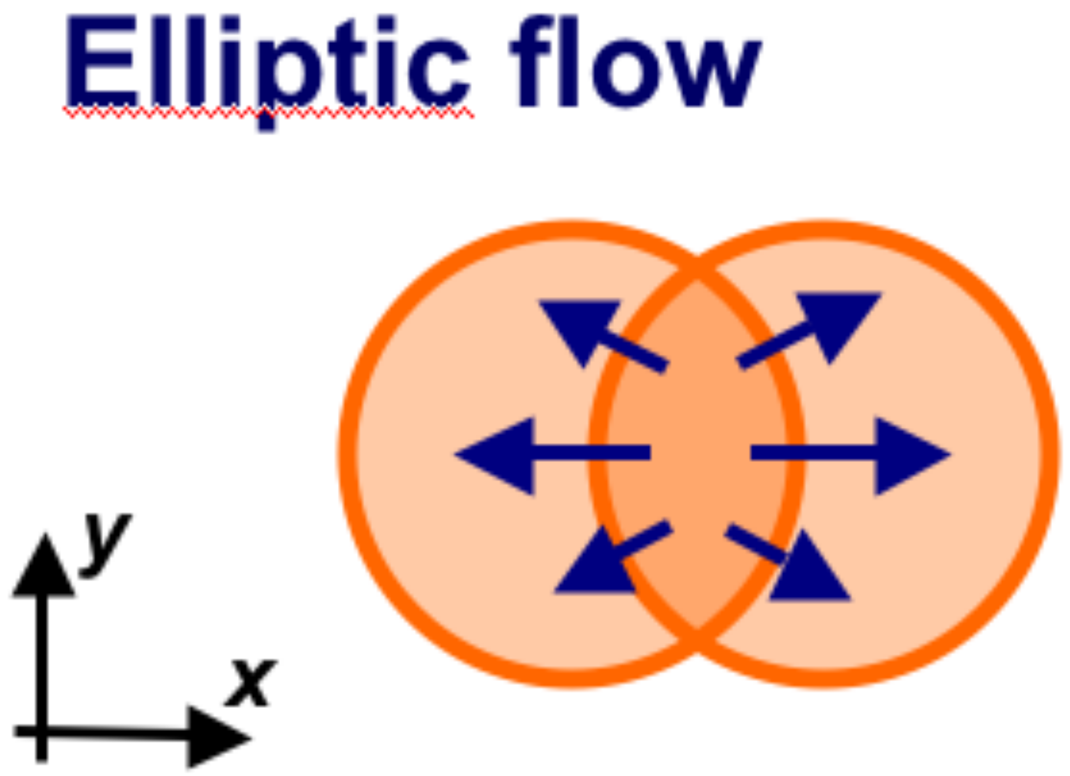

Relativistic hydrodynamics

See e.g. Ollitrault, arXiv:0708.2433

Hydrodynamics assumes **local thermodynamic equilibrium**: $P(x^\mu)$, $T(x^\mu)$, $\mu(x^\mu)$

Local thermodynamic equilibrium only possible if mean free path between two collisions much shorter than all characteristic scales of the system: $\boldsymbol{\lambda_{mfp} \ll L}$

Ideal hydrodynamics ($\lambda_{mfp} \to 0$): vanishing viscosity ($\eta/s \approx 0$)

Hydro equations closed by **equation of state** $\boldsymbol{P(\varepsilon, n_B)}$, usually taken from lattice QCD.

What can we learn from hydro modeling:

Initial state:	**unknown** (use another model)
Equation of state:	**want to study**
Transport coefficients:	**want to study**
Freeze-out:	**unknown** (use another model)

Transverse expansion of the fireball in a hydro model (temperature profile)

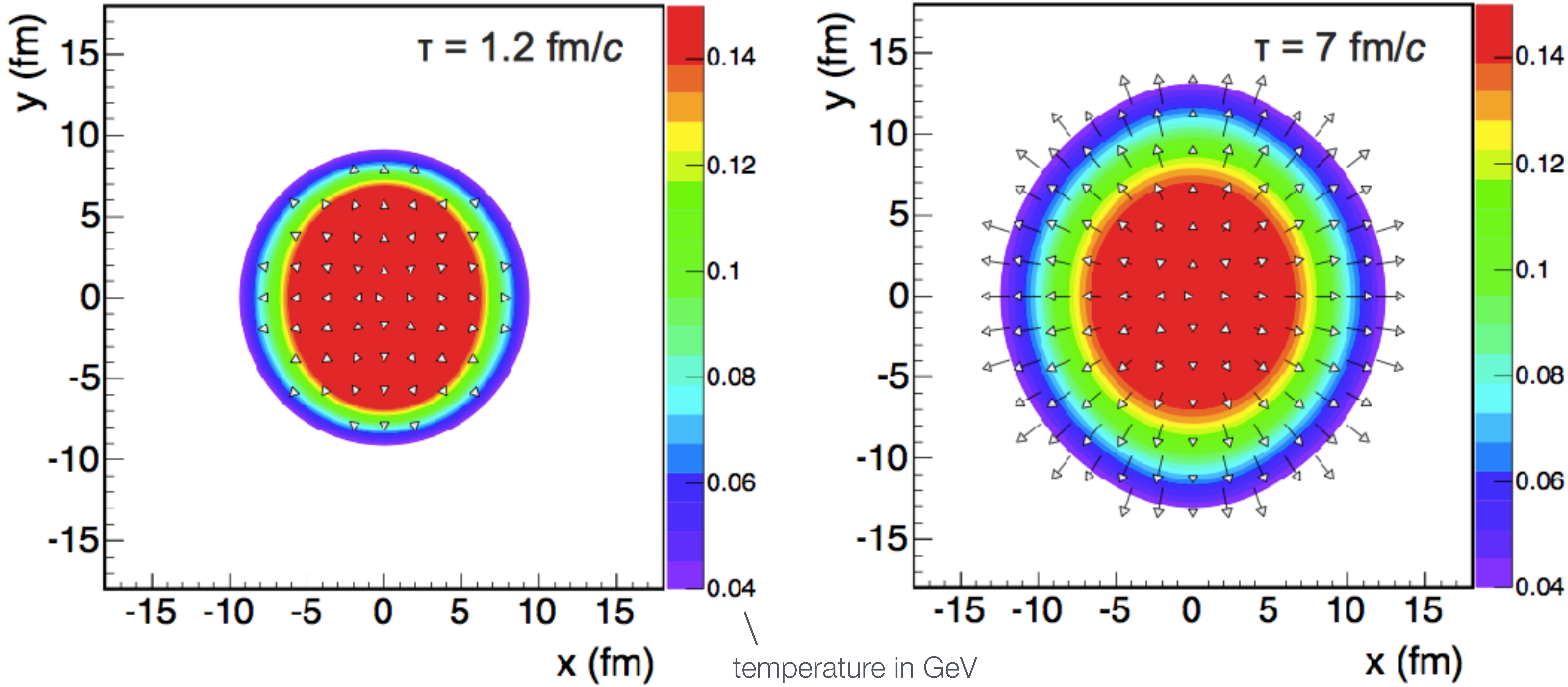

temperature in GeV

Good description of low-p_T π, K, p spectra with hydro models

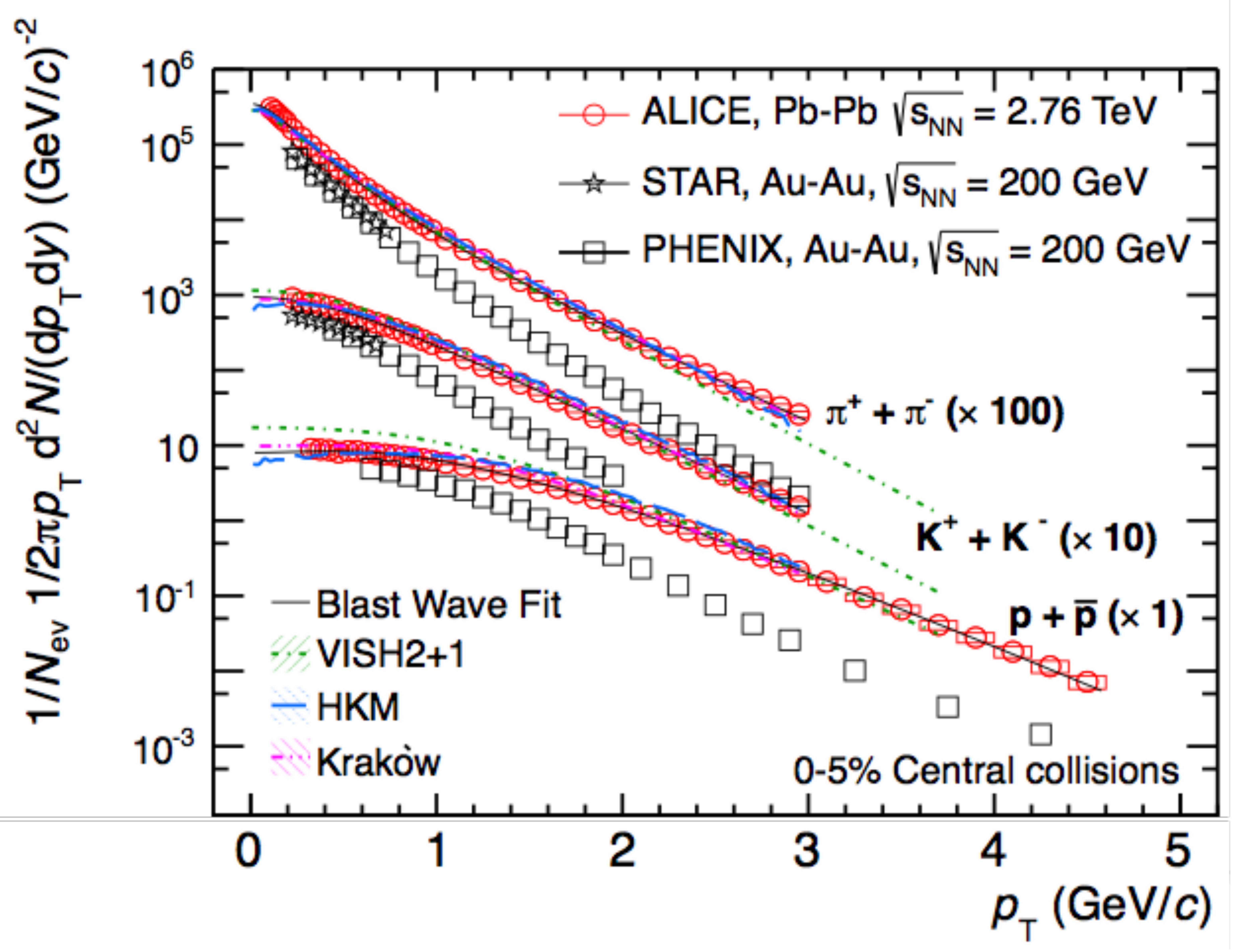

Kinetic freeze-out temperatures and transverse velocity from blast-wave fits

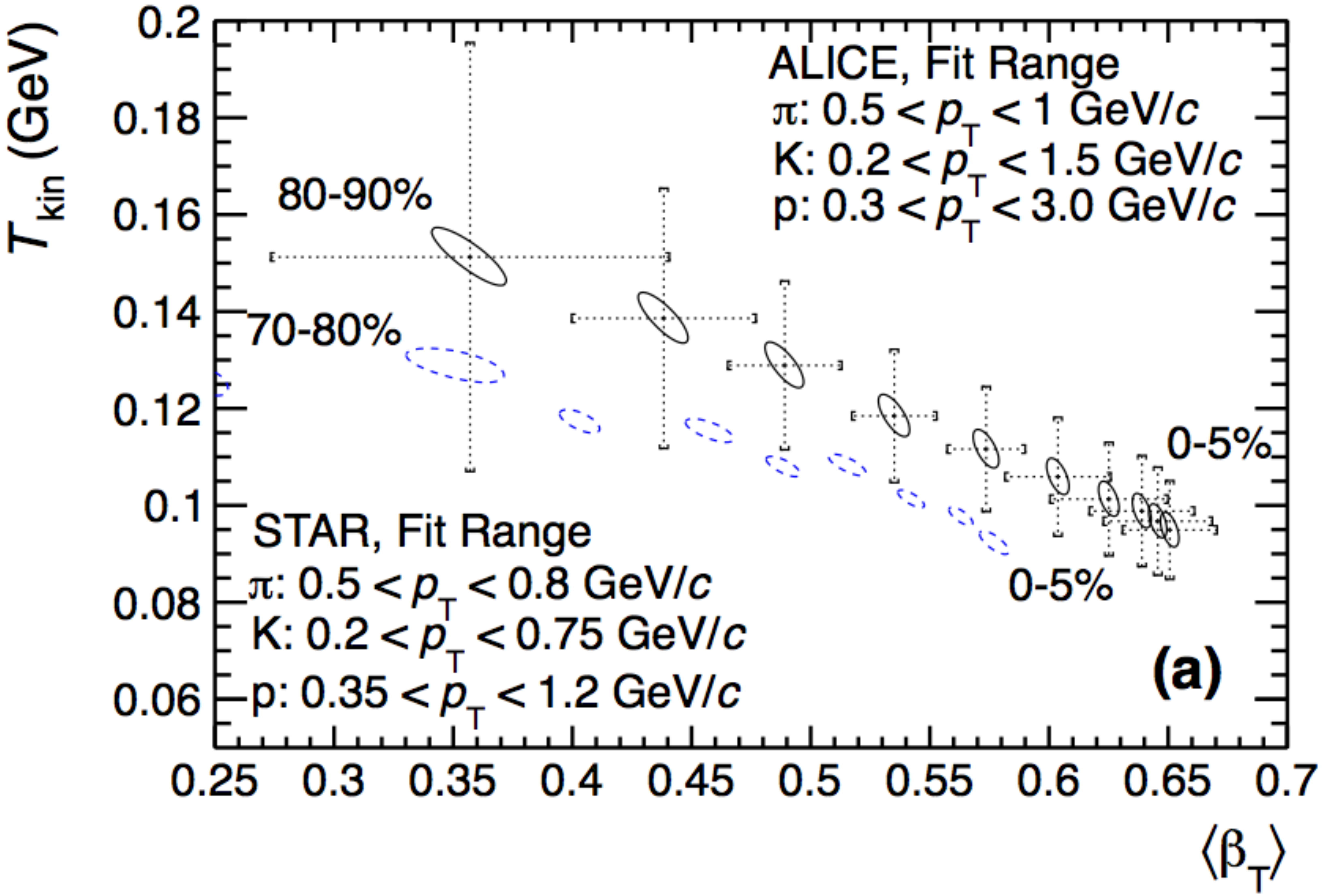

Blastwave model:
based on simplified model of the freeze-out hyper-surface and the corresponding flow velocities of the fluid cells

A–A collisions are like an explosion: **average transverse flow velocity is ~65% of the speed of light** in central Pb–Pb collision at the LHC

Azimuthal distribution of produced particles

spatial anisotropy → momentum anisotropy

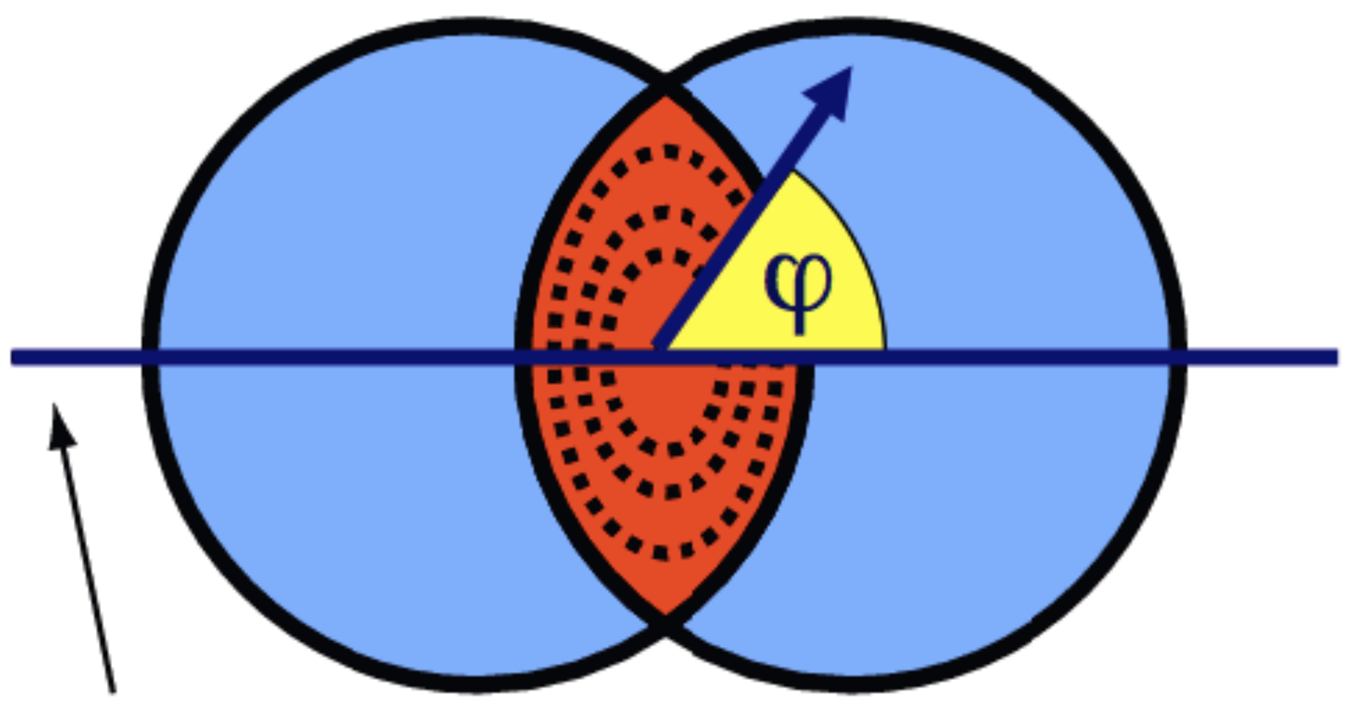

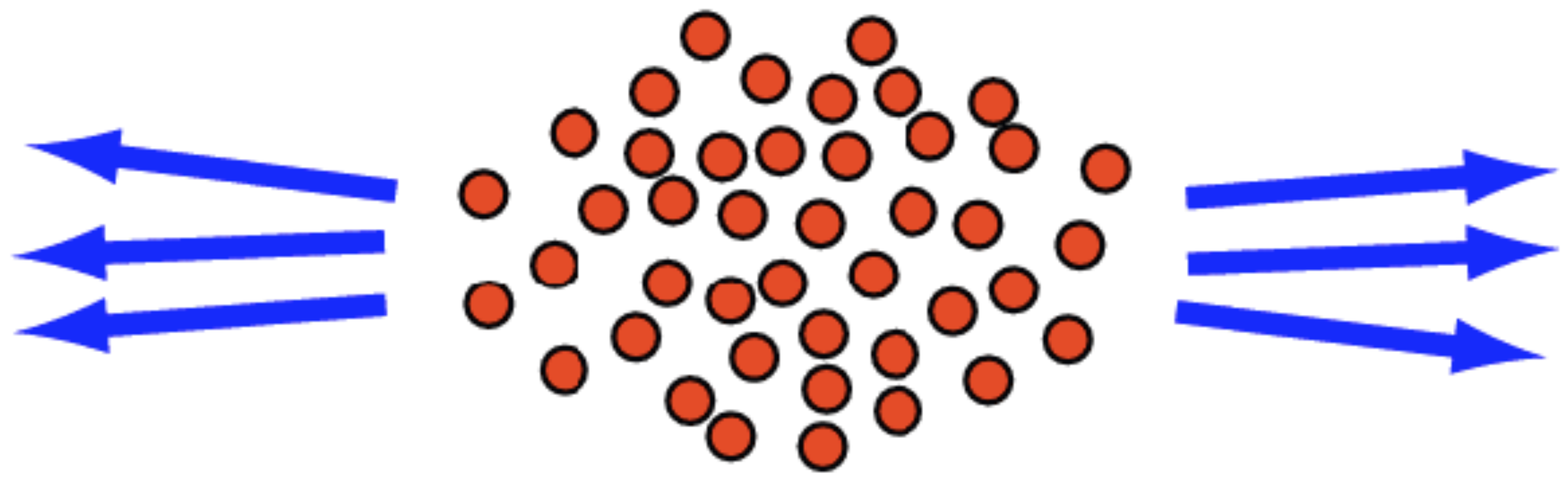

$$\frac{dN}{d\varphi} \propto 1 + 2\sum_{n=1}^{\infty} v_n \cos[n(\varphi - \Psi_n)]$$

Fourier coefficients: $v_n(p_T, y) = \langle \cos[n(\varphi - \Psi_n)] \rangle$

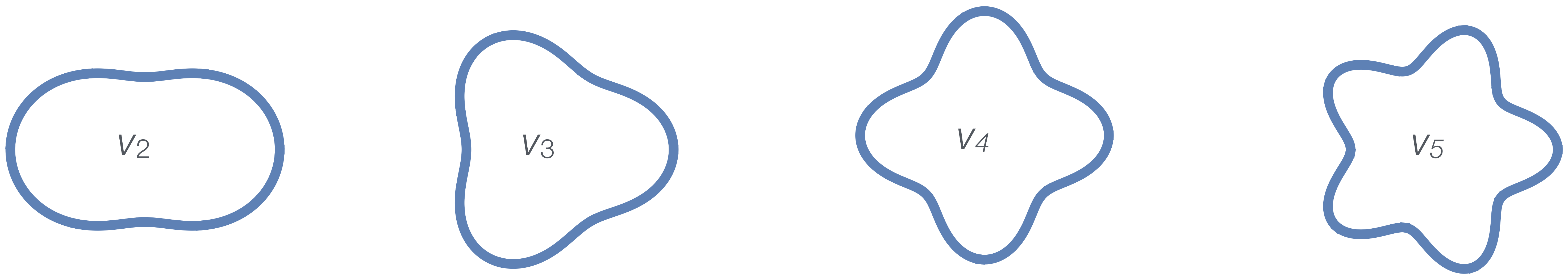

elliptic flow

triangular flow

$f(\varphi) = 1 + 2v_n \cos(n\varphi)$

Measuring the hydrodynamics of the QGP (1)

CMS-DP-2013-018
D. Teaney, Soft pions and the dynamics of the chiral phase transition

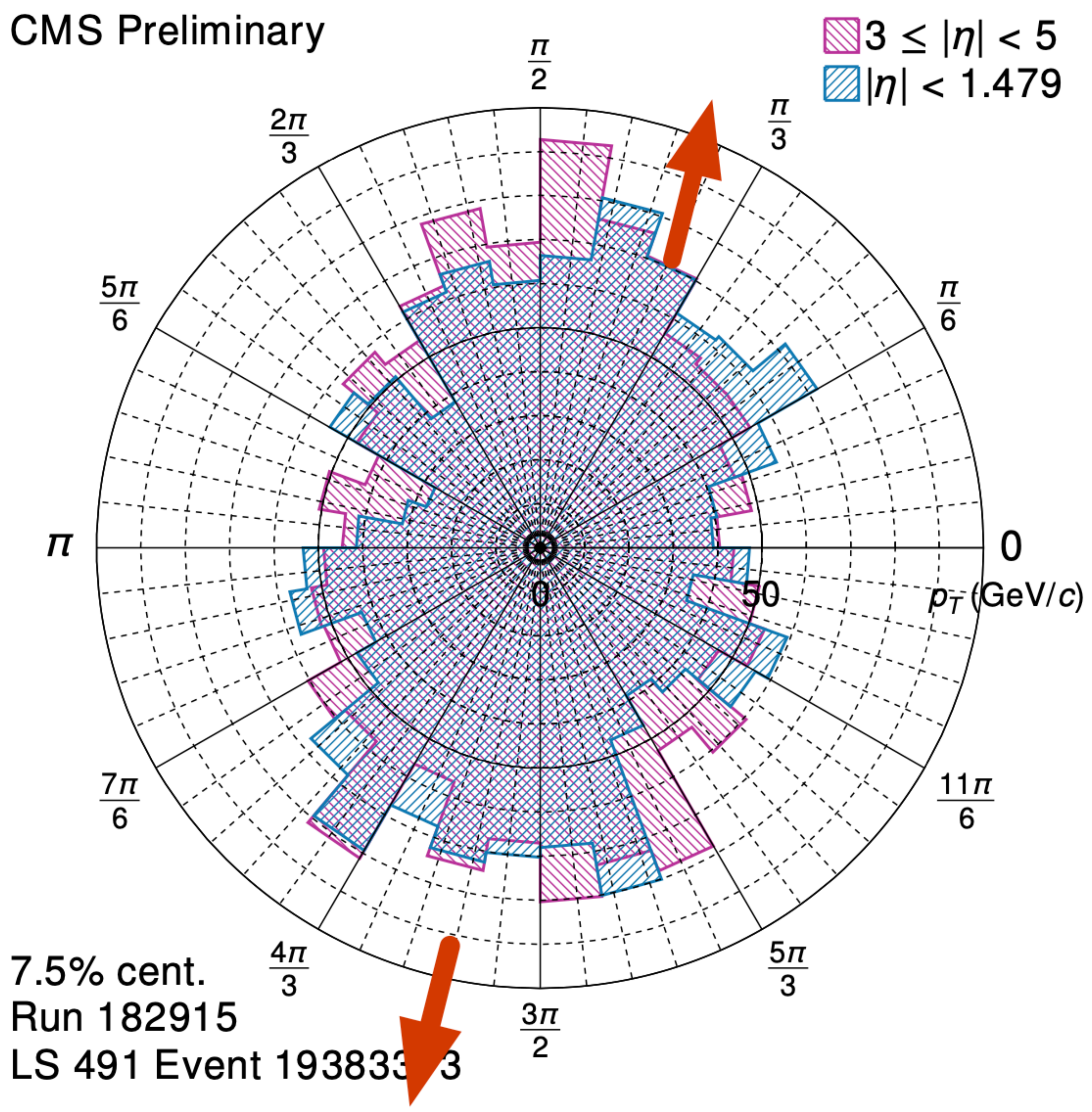

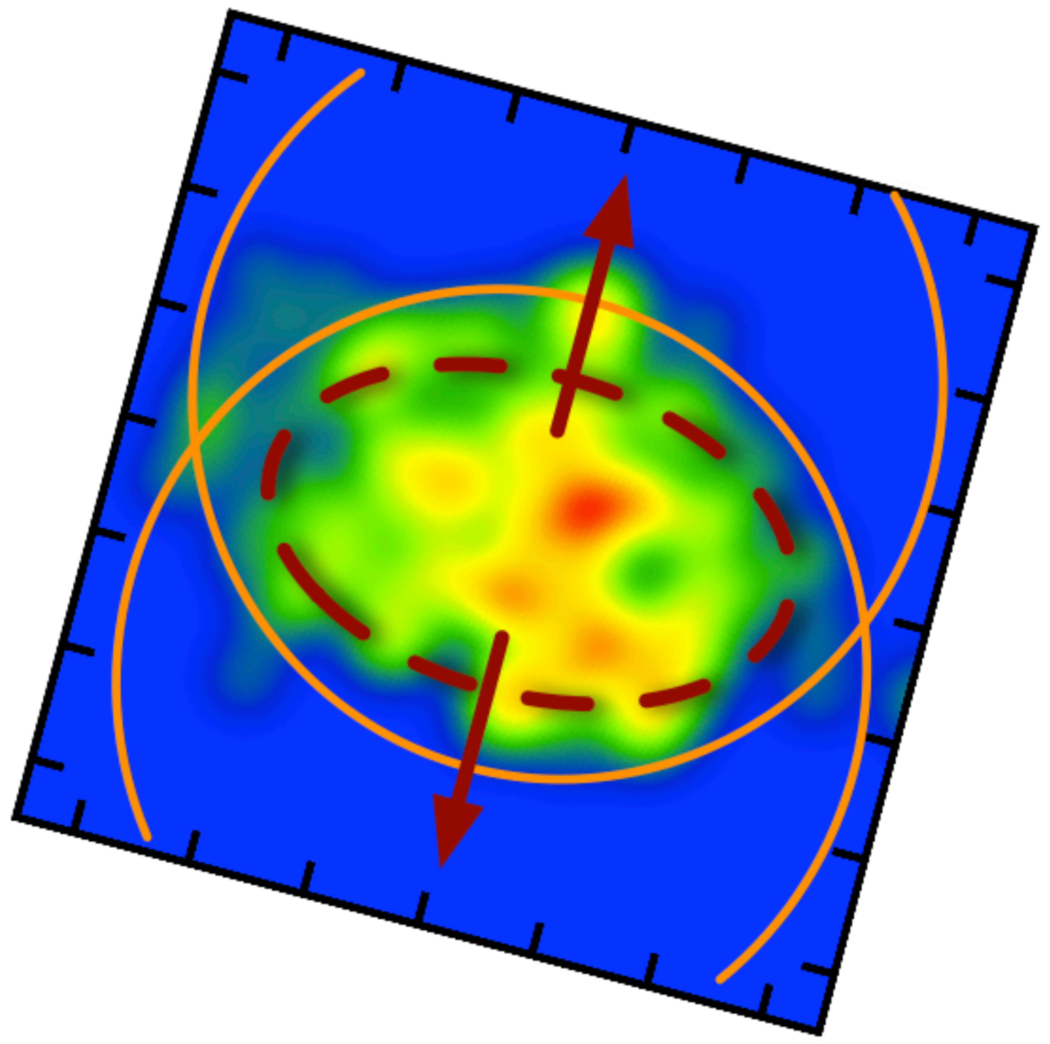

V_2

Measuring the hydrodynamics of the QGP (2)

CMS-DP-2013-018
D. Teaney, Soft pions and the dynamics of the chiral phase transition

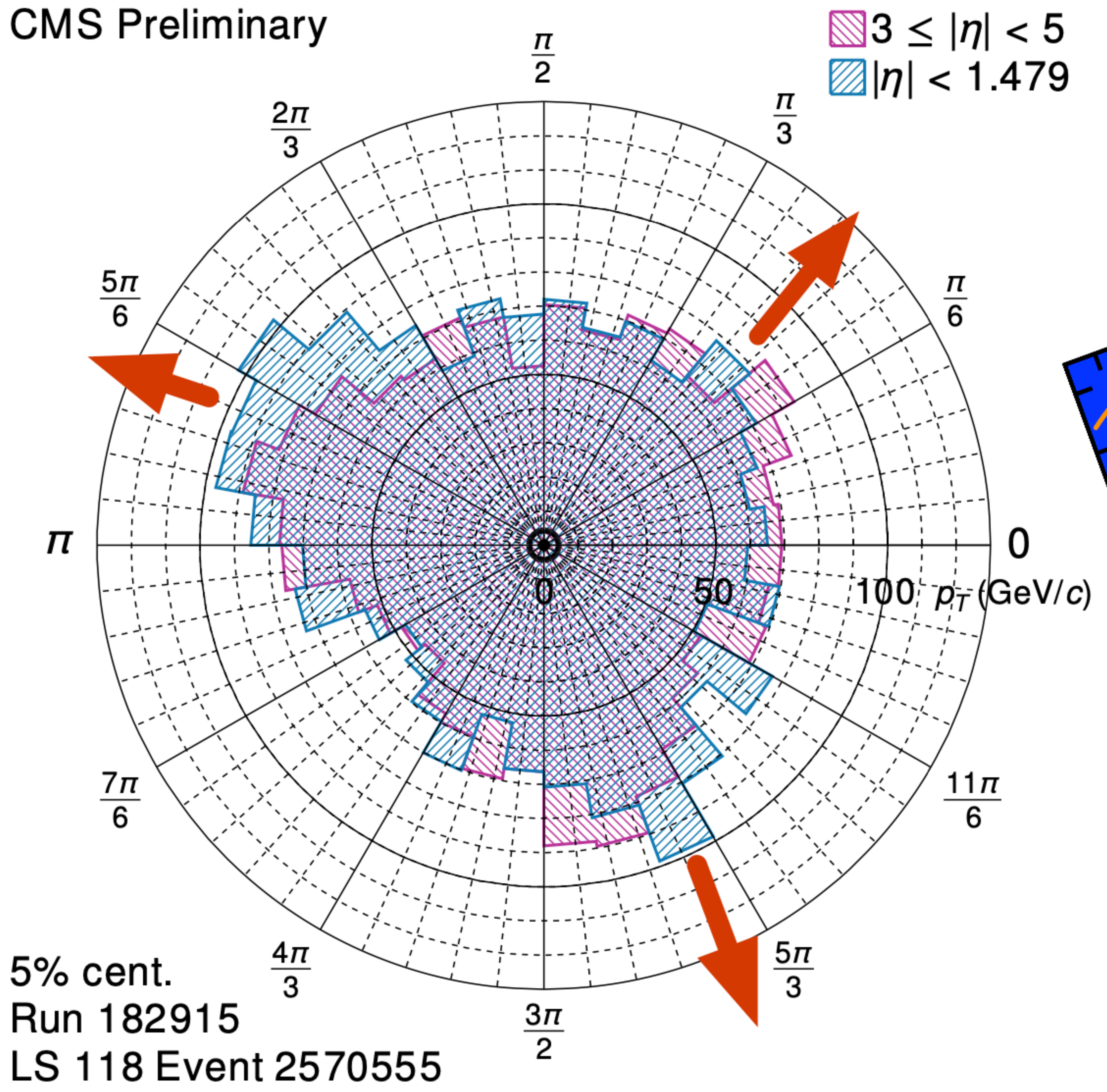

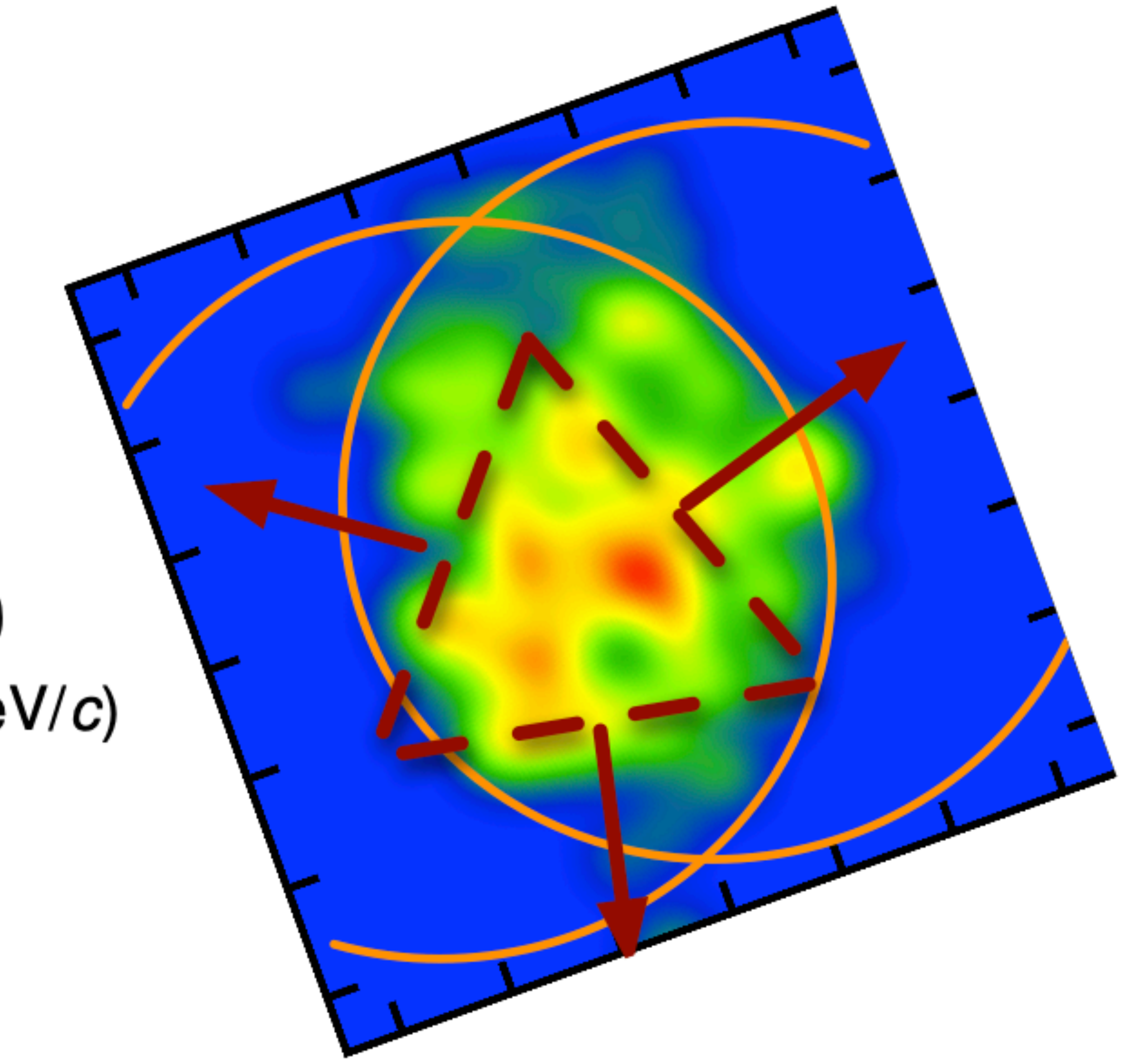

V_3

Elliptic flow of identified hadrons: Reproduced by viscous hydro with η/s = 0.2

final results: arXiv:1405.4632

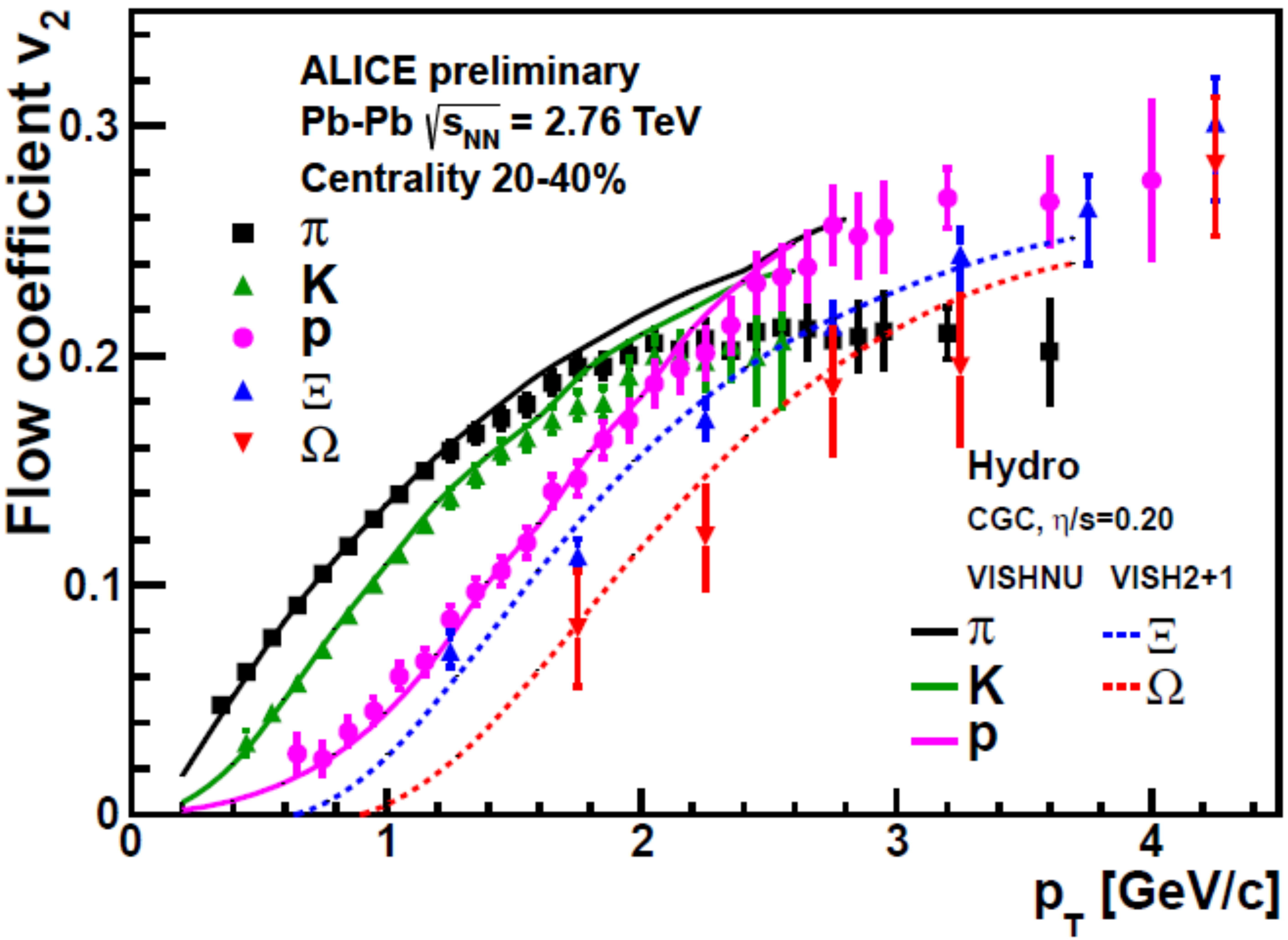

Dependence of v_2 on particle mass (**"mass ordering"**) is considered to be a strong indication for hydrodynamic space-time evolution

Current constraints on shear and bulk viscosity

ALICE, arXiv:2211.04384

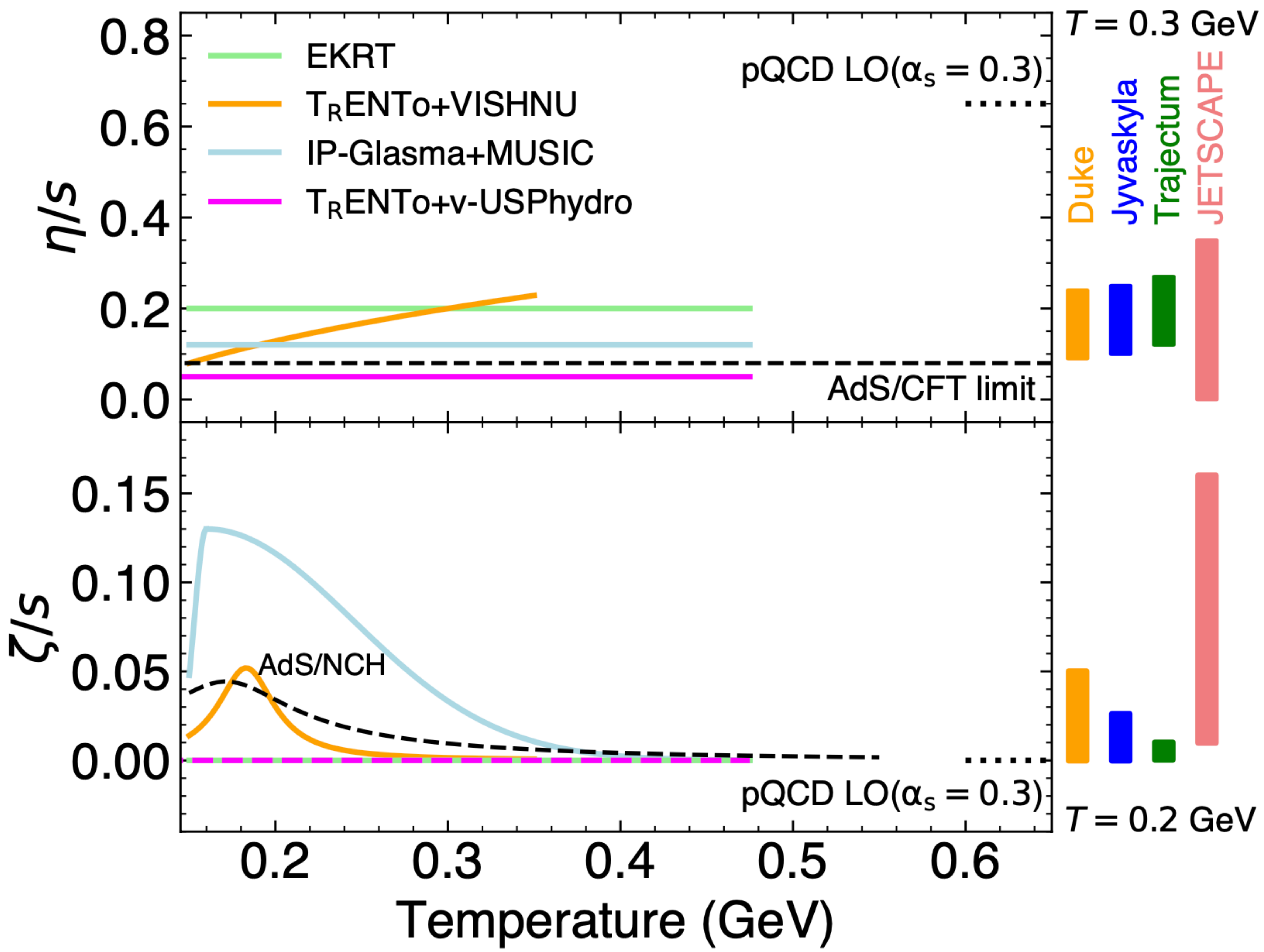

Model parameters like η/s constrained by applying a **Bayesian analysis**.

Credible intervals for model parameters from posterior distribution

$$P_{\text{posterior}}(\theta|\text{data}) \propto L(\text{data}|\theta) P_{\text{prior}}(\theta)$$

Hard Scattering and Jet Quenching

Theoretical description of High-p_T particle production: Perturbative QCD

Scattering of pointlike partons described by QCD perturbation theory (pQCD)

Soft processes described by universal, phenomenological functions

- Parton distribution function from deep inelastic scattering
- Fragmentation functions from e+e- collisions

Particle production dominated by hard scattering for $p_T \gtrsim 3$ GeV/*c*. *However, 99% or so of all particle from soft processes*

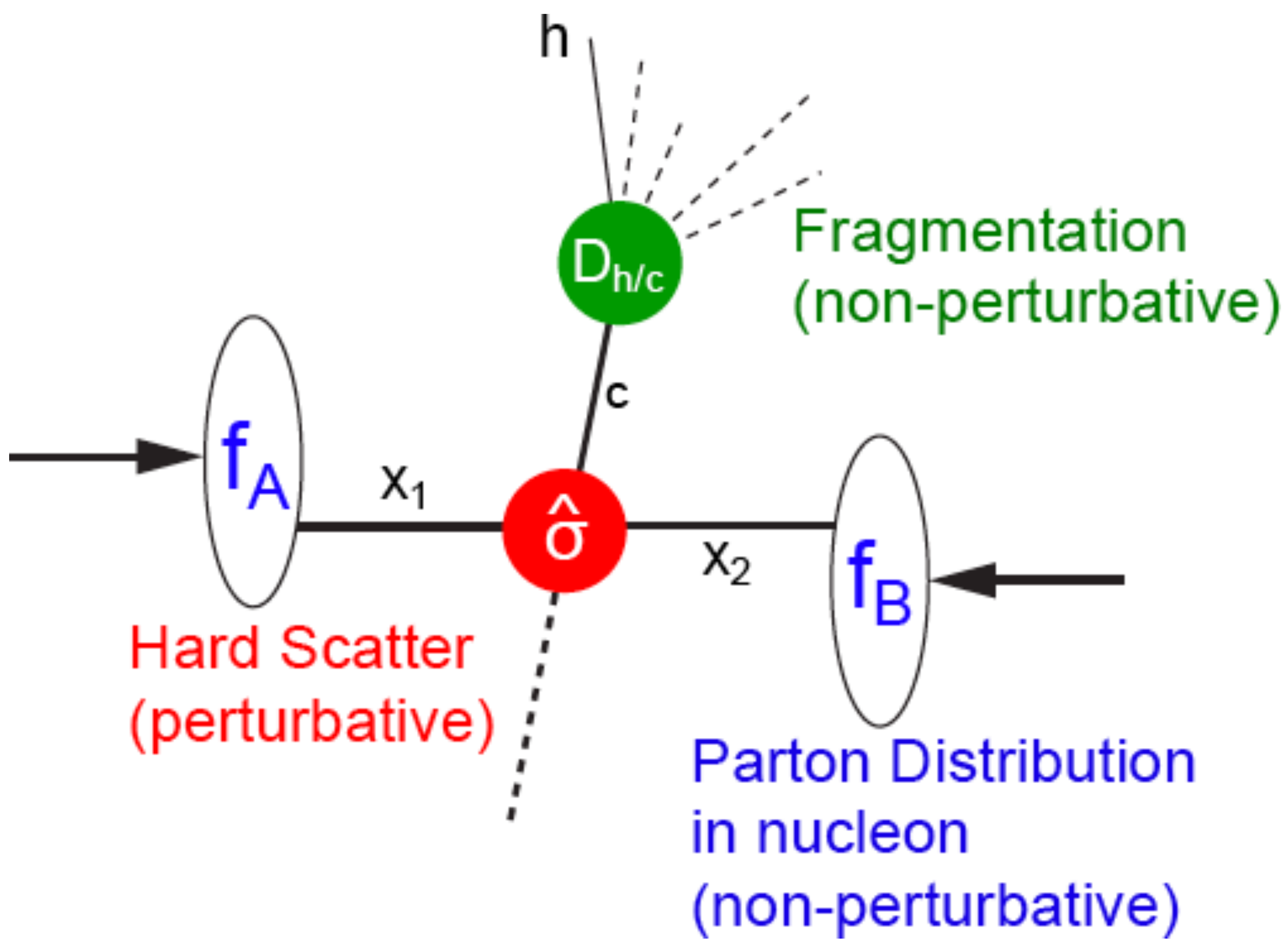

$$d\sigma = \sum_{a,b,c} f_a \otimes f_b \otimes d\hat{\sigma}^c_{ab} \otimes D^{Hadron}_c$$

Jet quenching in heavy-ion collisions

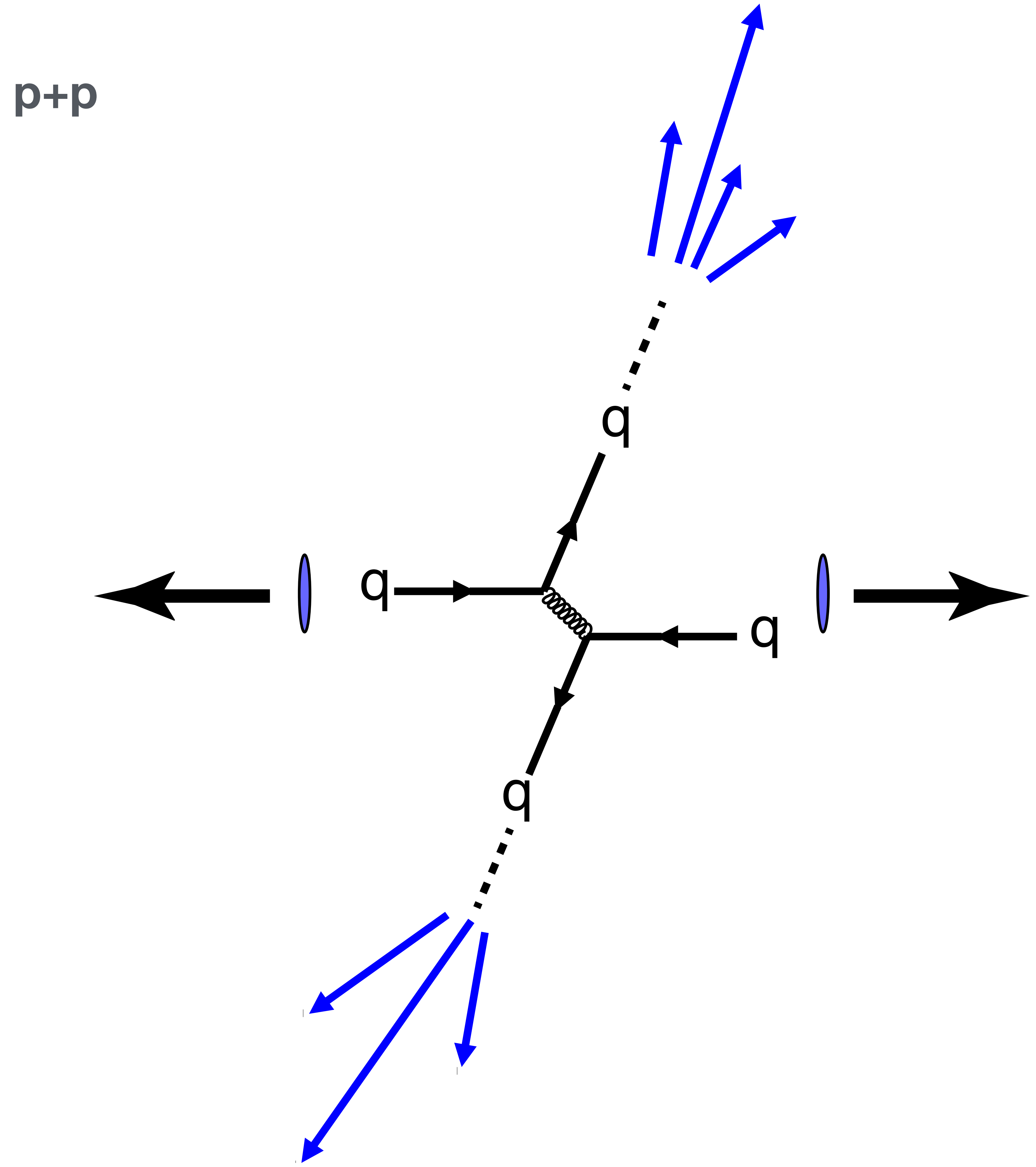

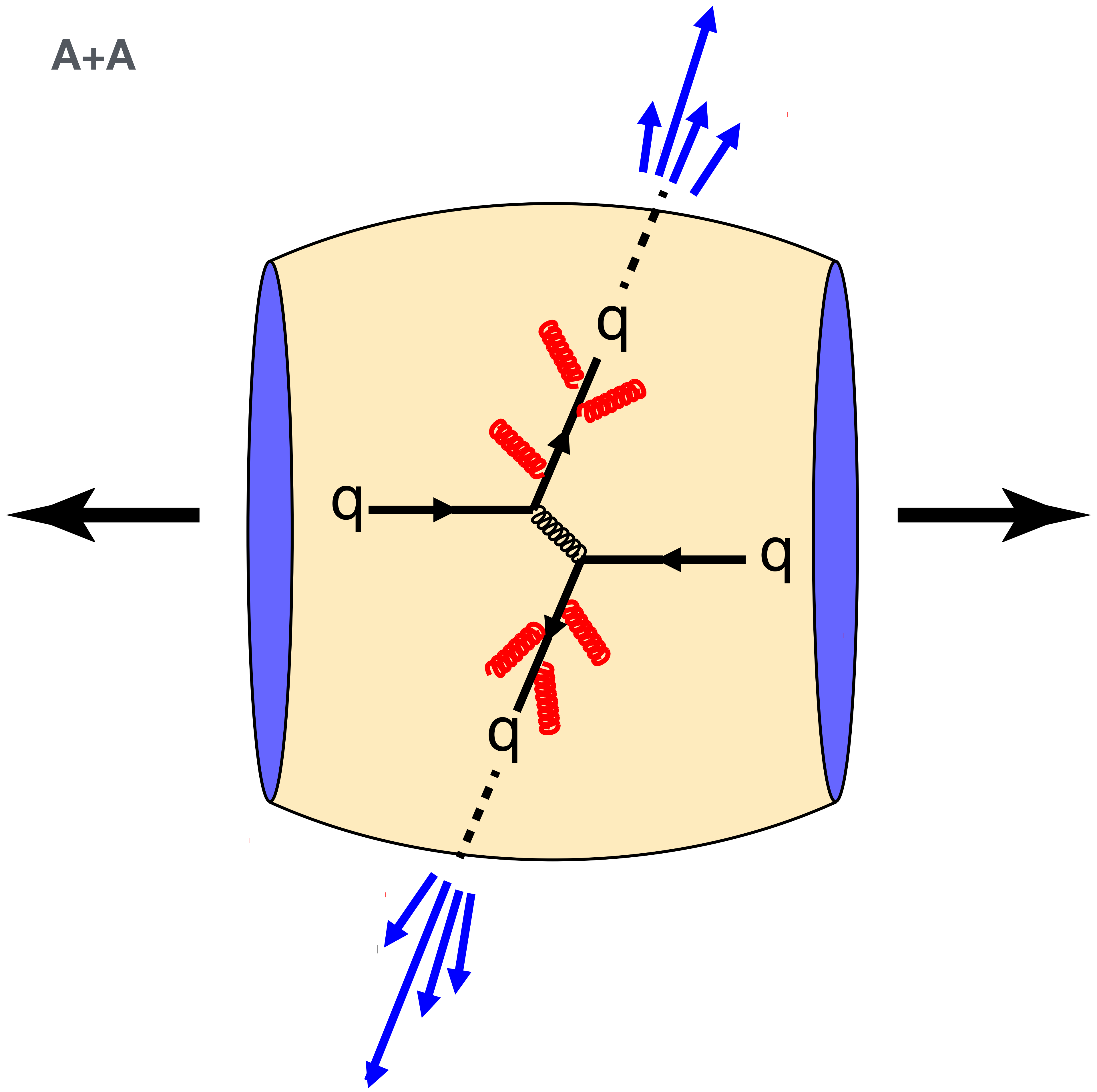

A-A collision: shower evolution in the medium, energy loss of the leading parton

Jet quenching history

Energy Loss of Energetic Partons in Quark-Gluon Plasma:
Possible Extinction of High p_T Jets in Hadron-Hadron Collisions.

FERMILAB-Pub-82/59-THY
August, 1982

J. D. BJORKEN
Fermi National Accelerator Laboratory
P.O. Box 500, Batavia, Illinois 60510

Abstract

High energy quarks and gluons propagating through quark-gluon plasma suffer differential energy loss via elastic scattering from quanta in the plasma. This mechanism is very similar in structure to ionization loss of charged particles in ordinary matter. The dE/dx is roughly proportional to the square of the plasma temperature. For this effect. An interesting signature may be events in which the hard collision occurs near the edge of the overlap region, with one jet escaping without absorption and the other fully absorbed.

It is now believed that radiative energy loss (gluon bremsstrahlung) is more important than elastic scattering

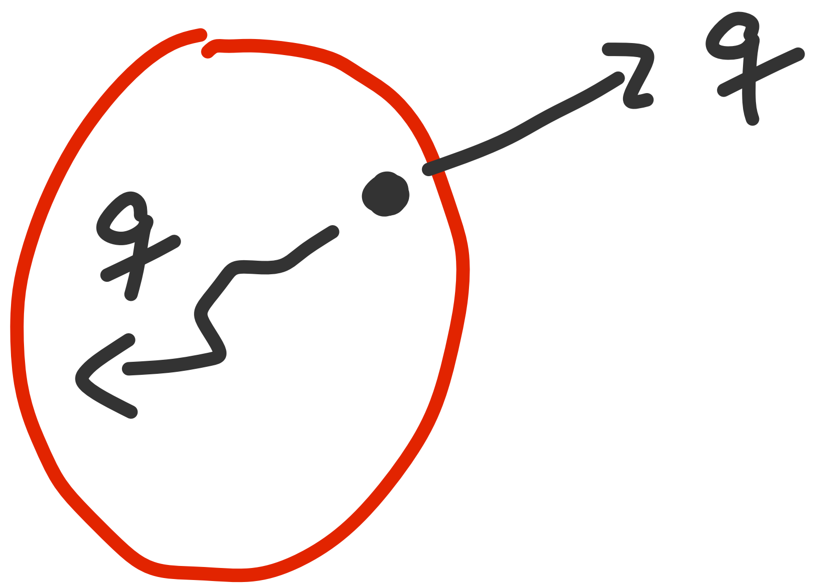

Collisional vs. radiative parton energy loss

Collisional energy loss:

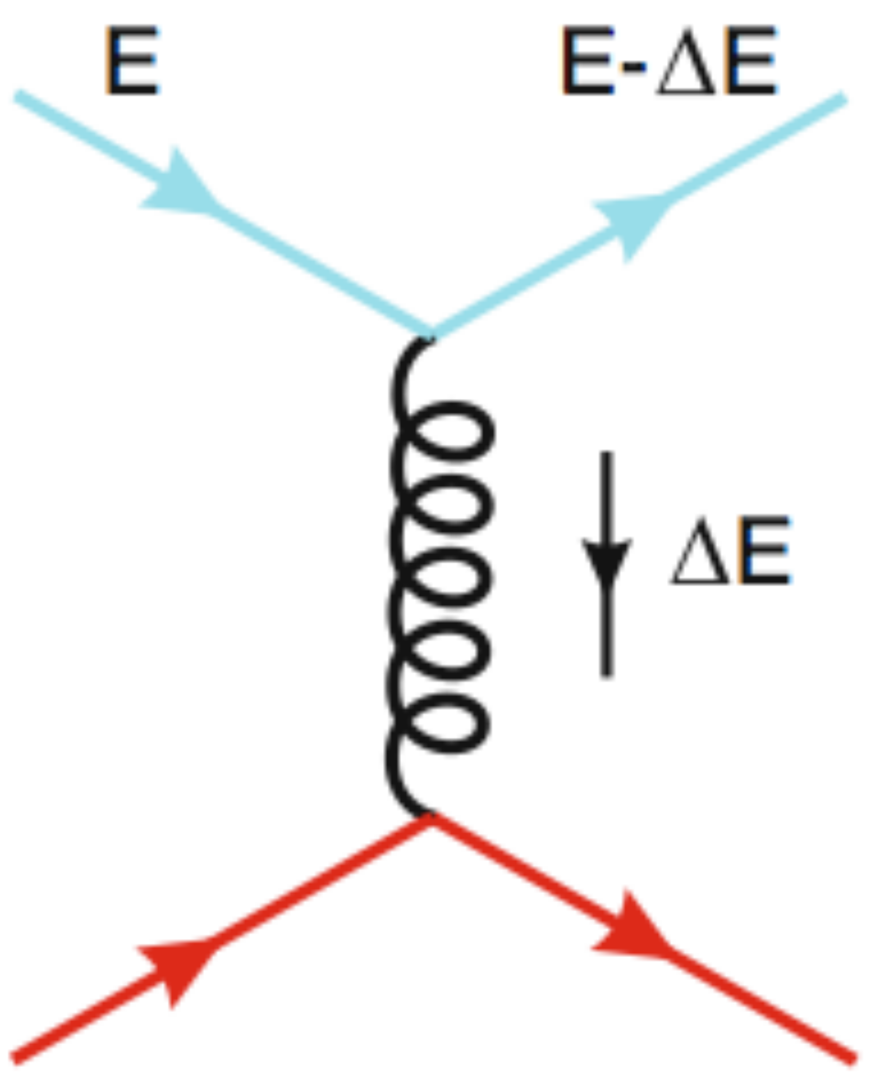

Elastic scatterings with medium constituents

Dominates at low parton momenta

Radiative energy loss:

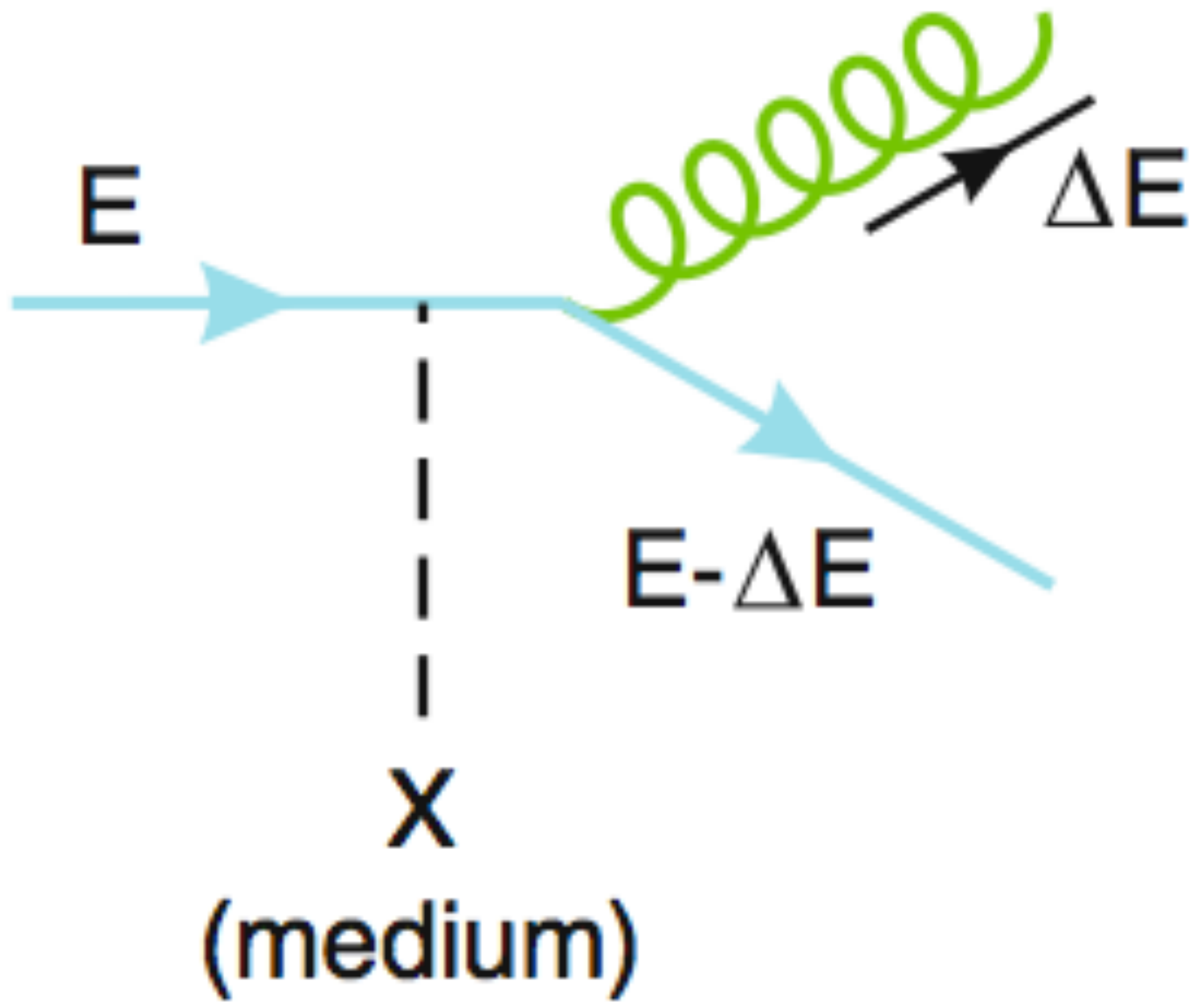

Inelastic scatterings within the medium

Dominates at higher momenta

N_coll-scaled π^0 yields in pp compared to Au-Au

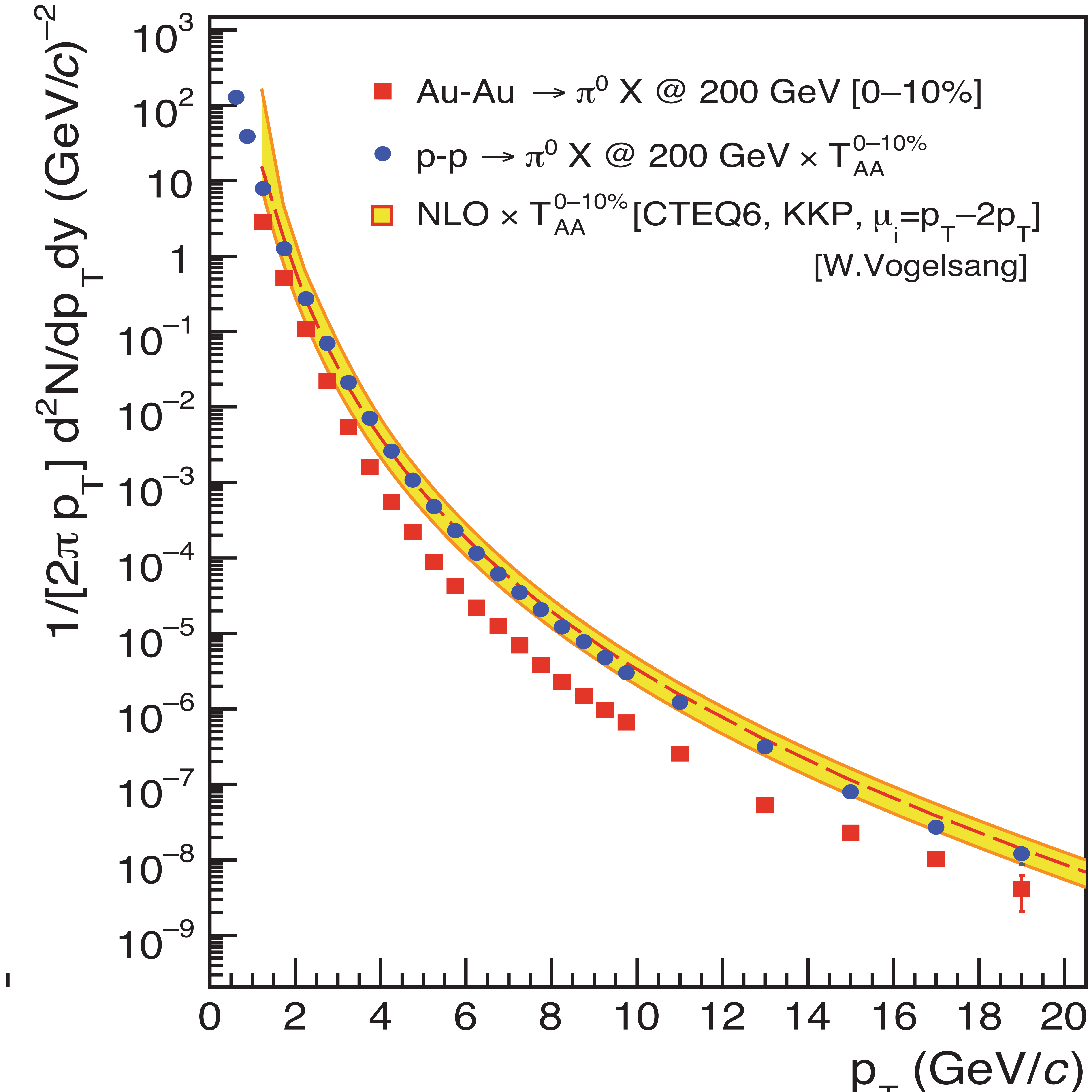

$$T_{AA} = \langle N_\text{coll} \rangle / \sigma_\text{inel}^\text{NN}$$

"increase in parton luminosity" per collision when going from pp to AA"

Without a medium, hadron yields for $p_T \gtrsim$ 2-3 GeV/c are expected to scale with Ncoll

Observation:
Clear suppression w.r.t. Ncoll scaling

Discovery of Jet Quenching at RHIC (ca. 2000–2003)

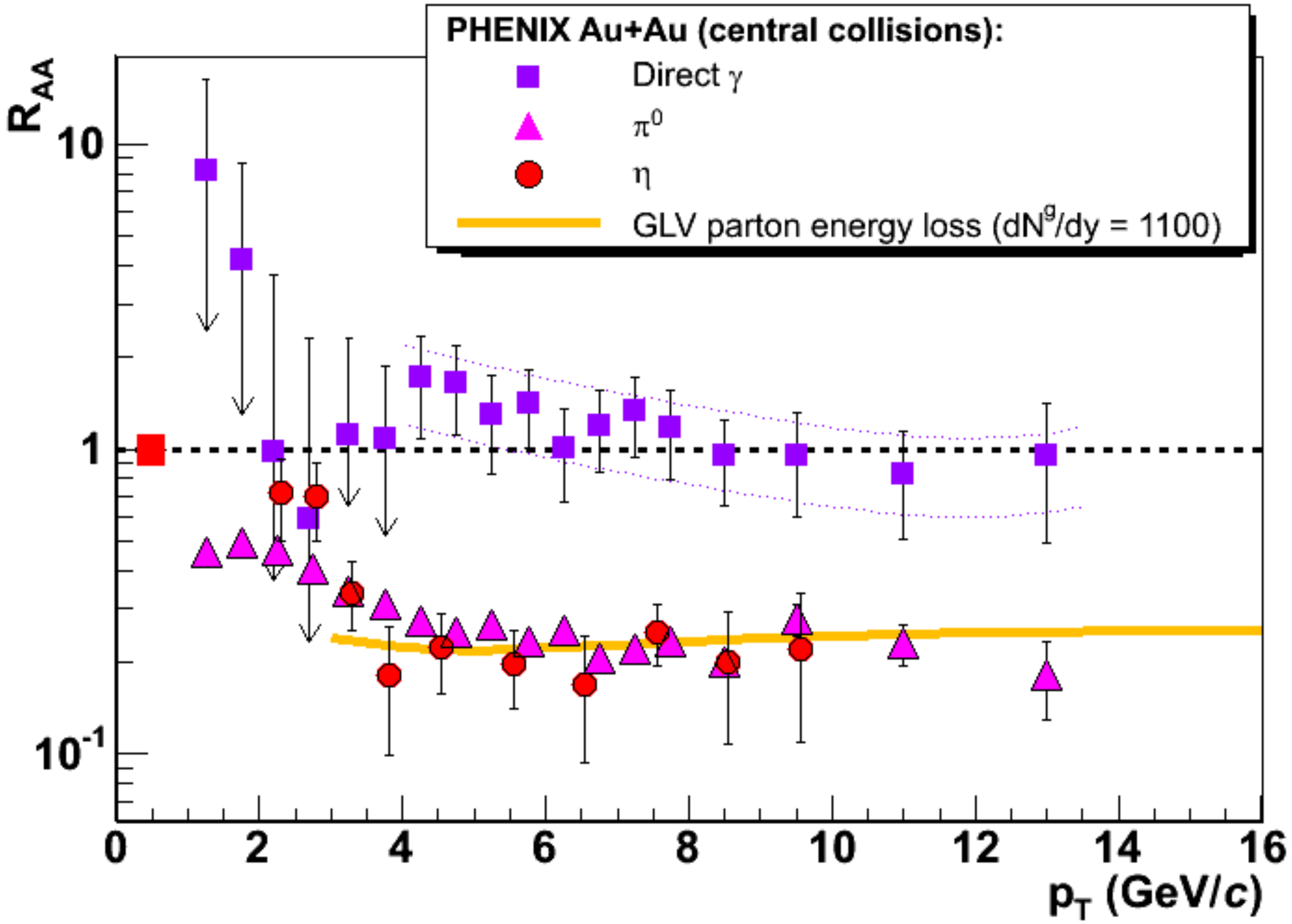

$$R_{AB} = \frac{dN/dp_T|_{A+B}}{\langle T_{AB}\rangle \times d\sigma_{inv}/dp_T|_{p+p}},$$

$$\text{where} \quad \langle T_{AB}\rangle = \langle N_{coll}\rangle / \sigma_{inel}^{NN}$$

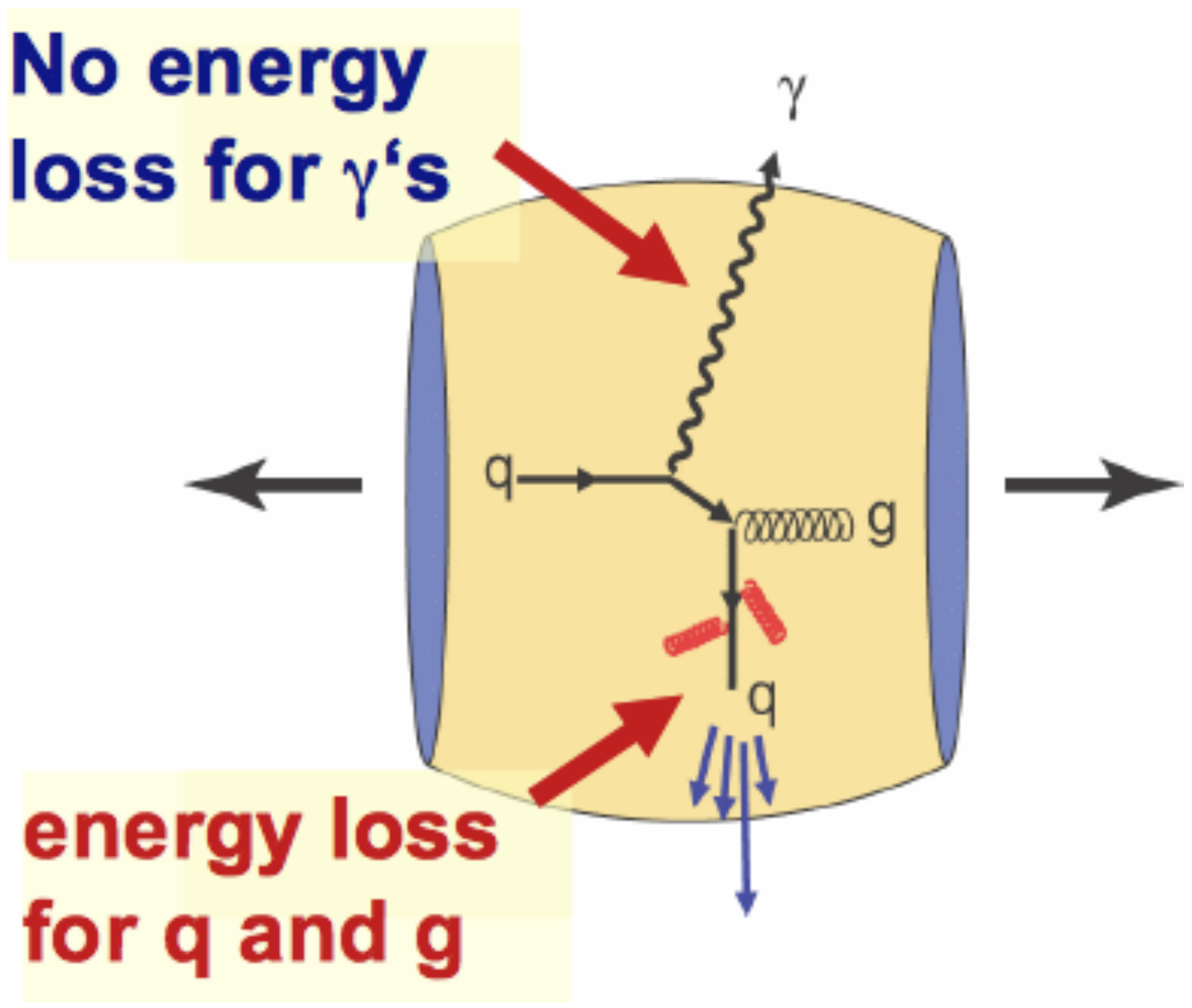

- Hadrons are suppressed, direct photons are not
- Evidence for parton energy loss

Single-particle R_{AA} in Pb–Pb at the LHC: Qualitatively similar observation as for RHIC energies

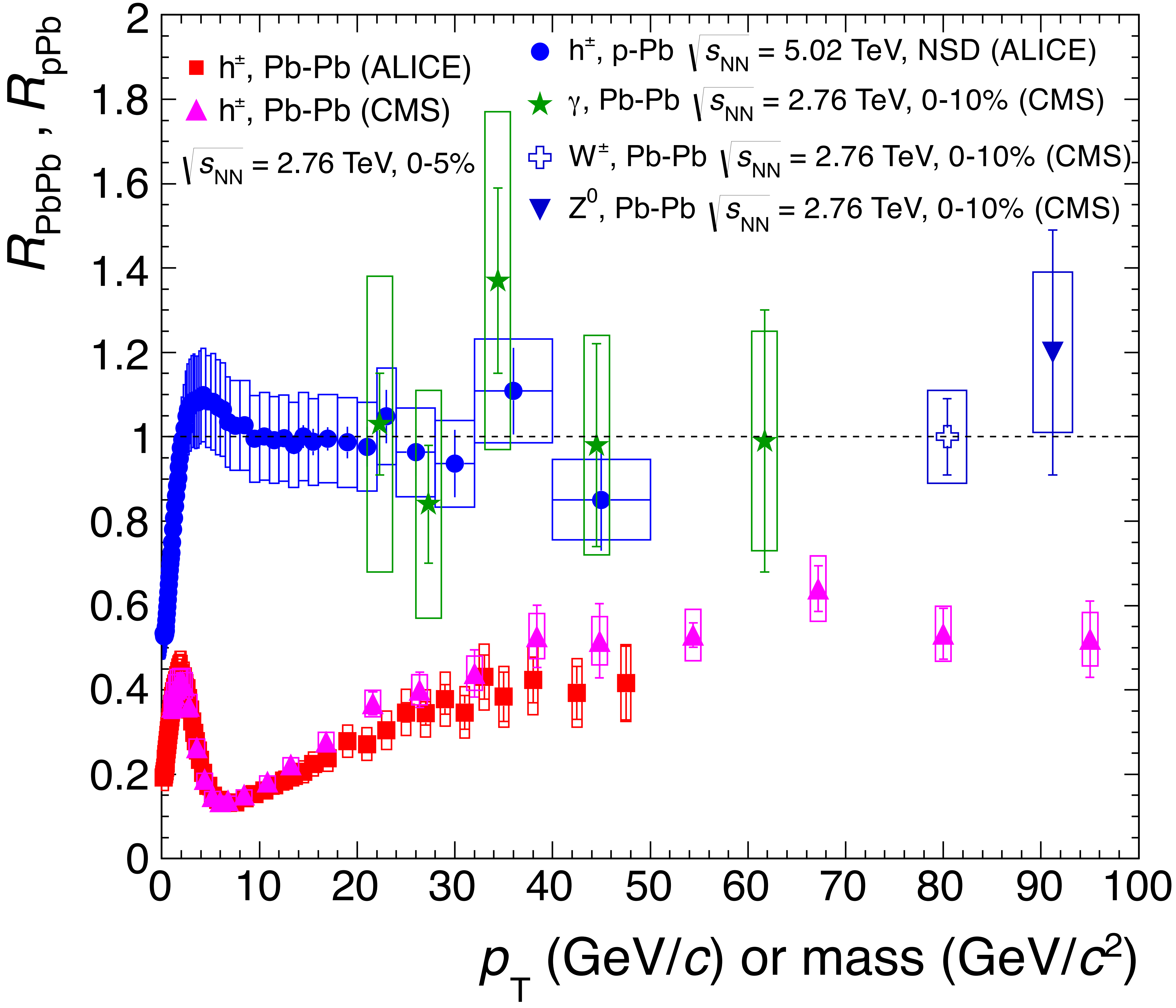

No suppression for γ, W^{+-}, Z^0 in Pb–Pb

No suppression of hadrons in p–Pb

Strong suppression of hadrons in Pb–Pb

Quark mass dependence of the parton energy loss

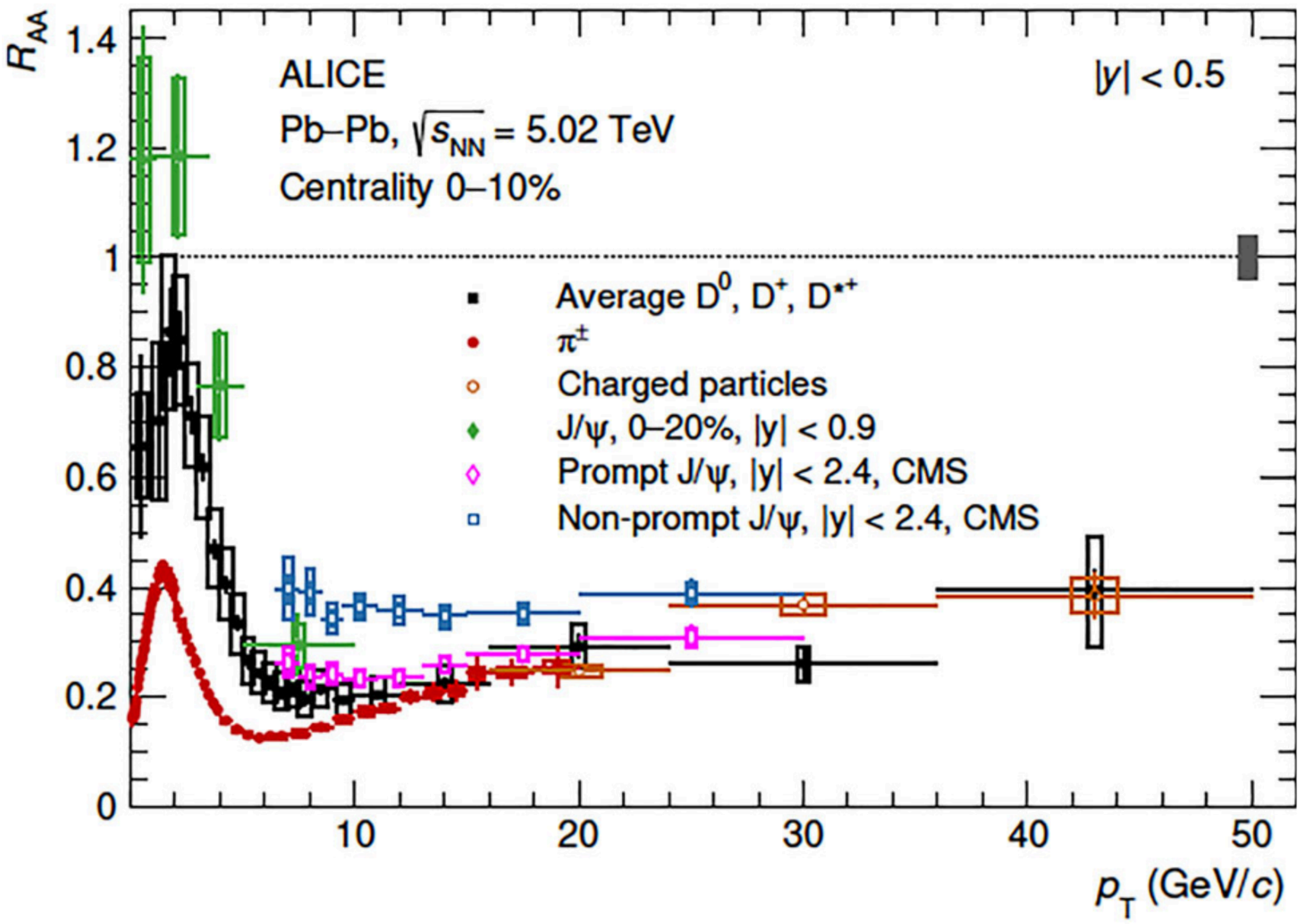

Expect smaller energy loss for heavier quarks due to **dead-cone effect**

$$\Delta E_{\mathrm{b}} < \Delta E_{\mathrm{c}} < \Delta E_{\mathrm{u,d,s}}$$

Dead-cone effect:
suppression of gluon bremsstrahlung radiation for $E_{gluon} \lesssim m_{quark}/E_{quark}$

D mesons less suppressed than pions at low p_T

J/ψ from B meson decays less suppressed than prompt J/ψ

However, harder p_T spectrum and different fragmentation function of charm quarks compared to light quarks and gluons: detailed model calculation needed to interpret the data

Studying jet quenching with jets: Large dijet energy asymmetries in Pb-Pb

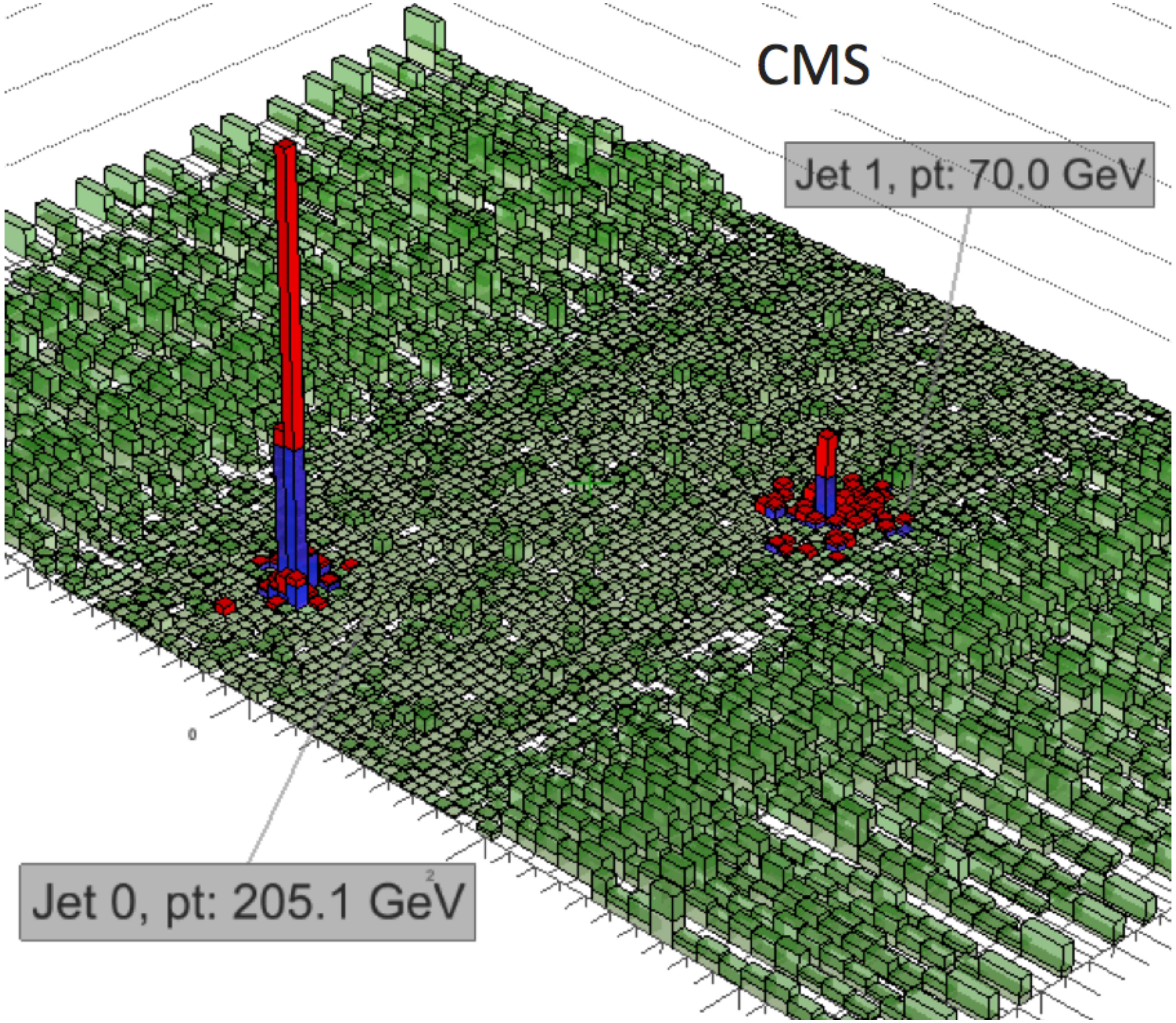

Pb–Pb at $\sqrt{s_{NN}}$ = 5.02 TeV: Jet RAA up to p_T = 1 TeV

ATLAS-CONF-2017-009, http://cds.cern.ch/record/2244820

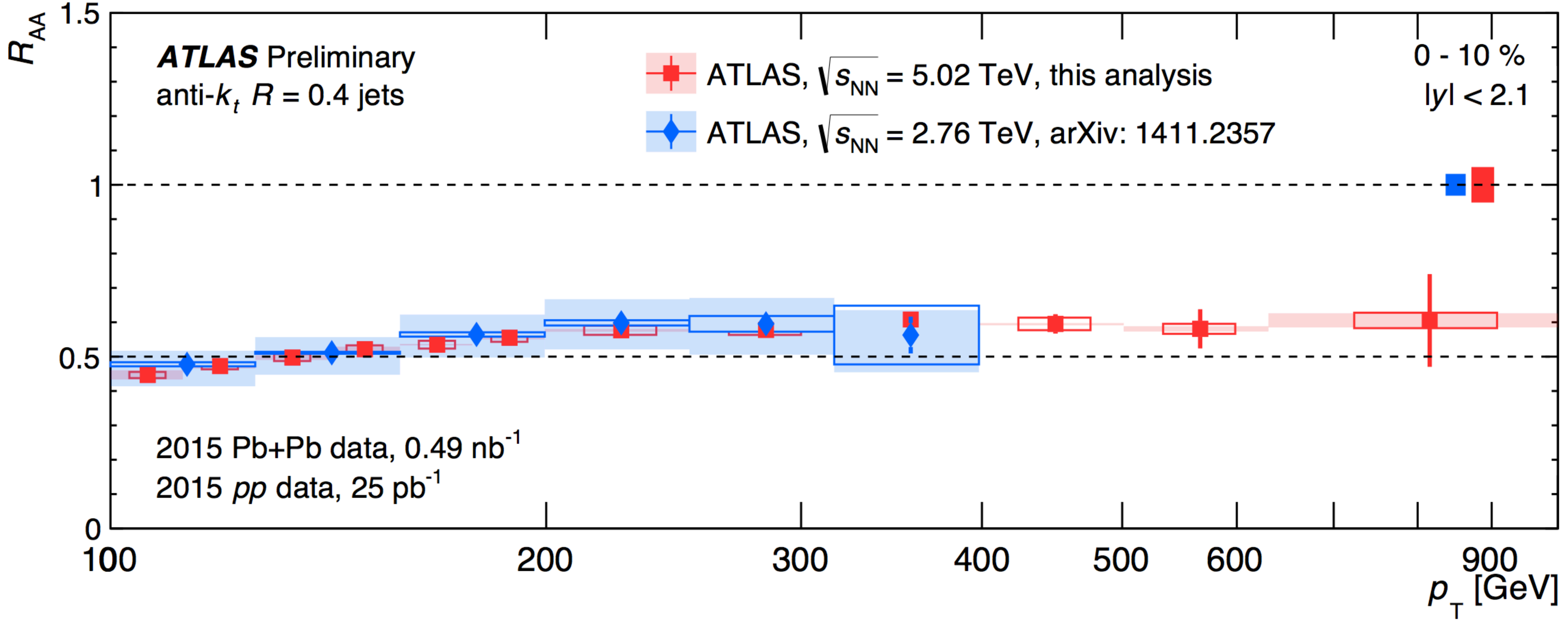

Bayesian parameter extraction of $\hat{q}/T^3$ from inclusive hadron suppression

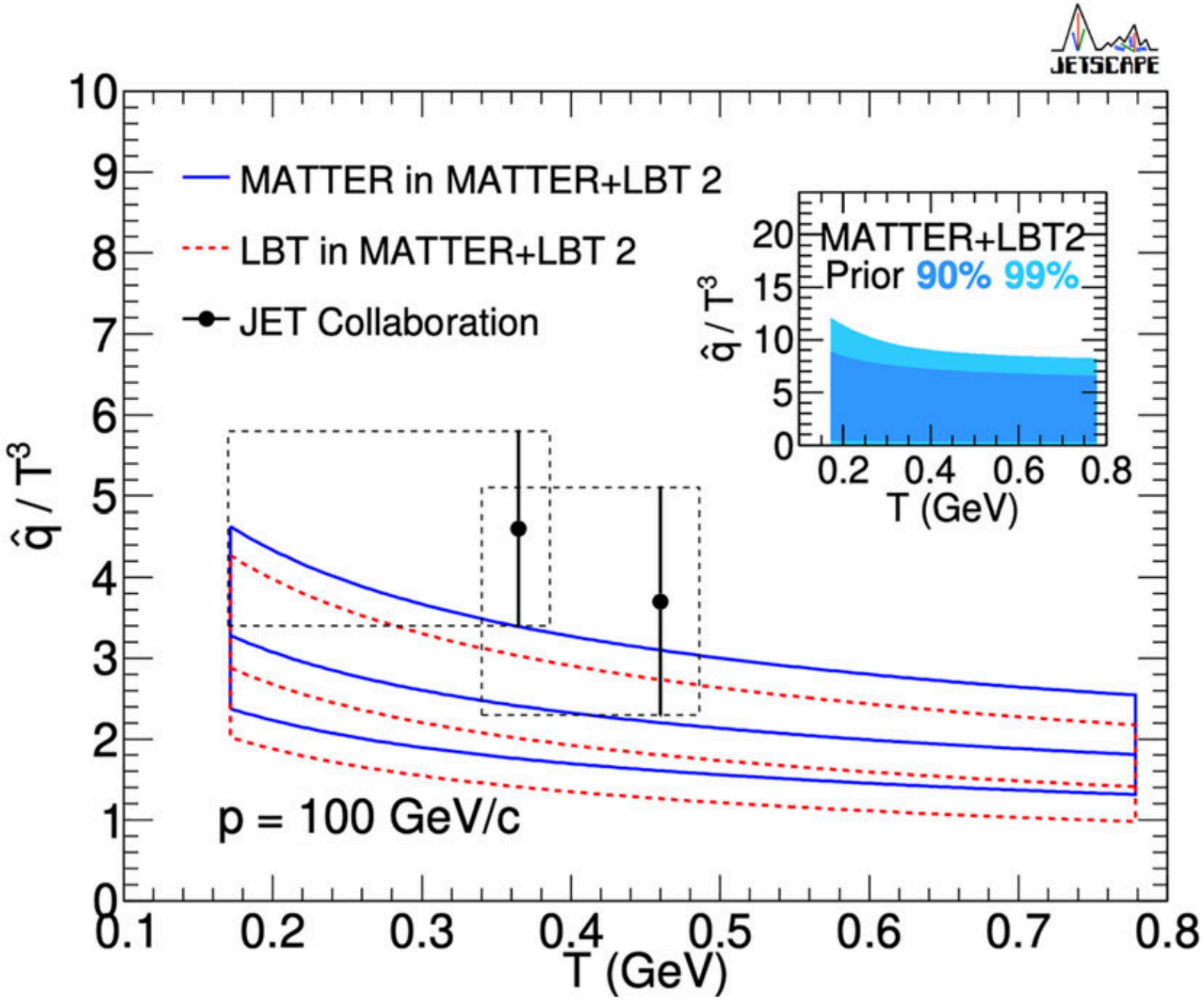

Energy loss E in a static medium of length L for a parton energy $E \to \infty$:

$$\Delta E \propto \alpha_s C_F \hat{q} L^2 \qquad \hat{q} = \frac{\mu^2}{\lambda}$$

$$C_F = \begin{cases} 3 & \text{for gluon jets} \\ 4/3 & \text{for quark jets} \end{cases}$$

μ^2 : typical momentum transfer from medium to parton per collision

λ : mean free path length in the medium

***T* = 400 MeV:** $\hat{q} \approx 1.3\,\mathrm{GeV}^2/\mathrm{fm}$

BDMPS result, Nucl. Phys. B 483, 291, 1997

Quarkonia

Charmonium and bottomium

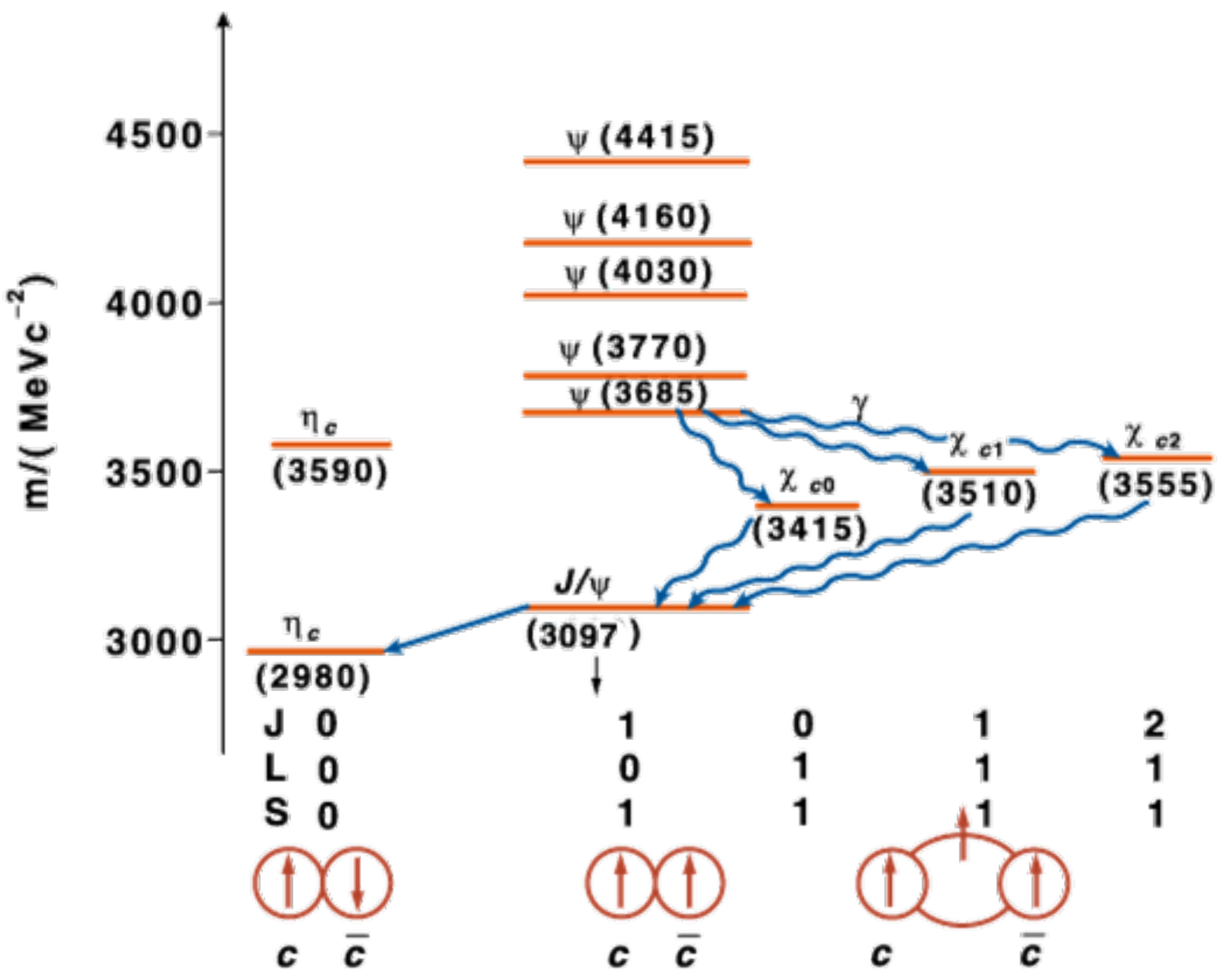

Quarkonia: tightly bound, smaller radius than light mesons

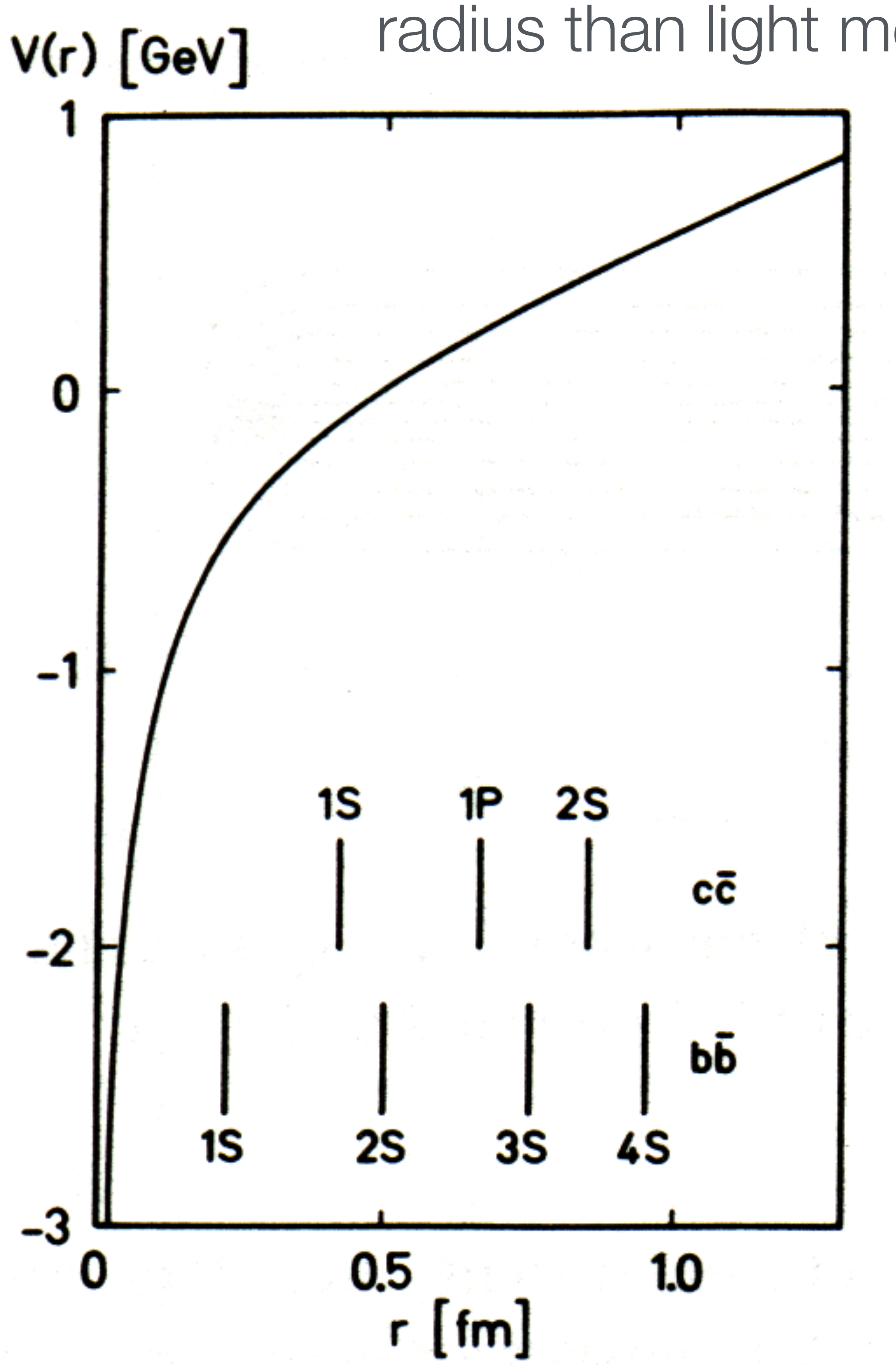

$$V(r) = -\frac{\alpha}{r} + \sigma r$$

$\sigma \approx 1$ GeV/fm, $\alpha \approx \pi/12$

Non-relativistic treatment for heavy quarks ($m_c \approx 1.3$ GeV, $m_b \approx 4.7$ GeV)

Charmonium and bottomium states reproduced by solving Schrödinger equation using Cornell potential

Debye screening in the QGP

Matsui, Satz (Phys. Lett. B 178 (1986)):

- Potential between two heavy quarks is modified in the QGP, preventing initially produced charm anticharm quarks to form a J/ψ
- J/ψ suppression is a QGP signal

Simple parameterization of the screened potential ("Debye screening"):

$$V(r,T) = -\frac{\alpha}{r}e^{-\mu r} + \sigma r \frac{1-e^{-\mu r}}{\mu r}$$

Debye mass

screening radius depends on temperature: $r_D = 1/\mu$ $\qquad \mu = \mu(T) \propto g(T)T$

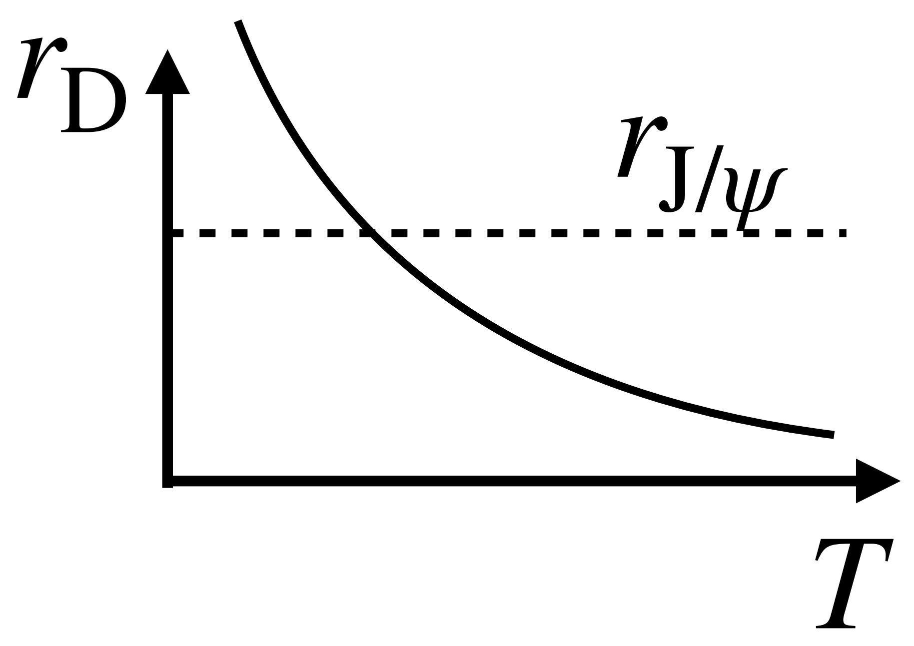

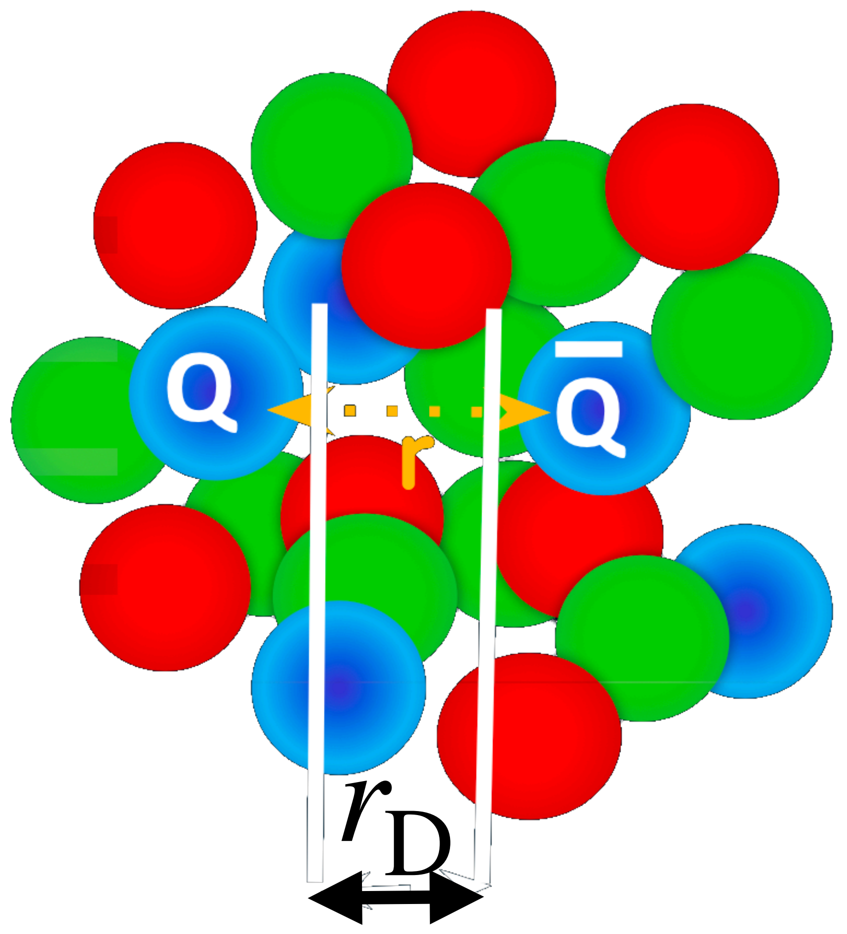

Basic idea: heavy-quark bound state melts in the QGP if $r_{\bar{Q}Q} \gtrsim r_\mathrm{D}$

There is a dissociation temperate T_{dis} for each state ("sequential melting"):

state	χ_c	ψ'	J/ψ	Υ'	χ_b	Υ
T_{dis}	$\leq T_c$	$\leq T_c$	$1.2T_c$	$1.2T_c$	$1.3T_c$	$2T_c$

arXiv:0706.2183

Can the different T_d's serve as a QGP thermometer?

Screened potential as a function of *T* from lattice QCD

TUMQCD, arXiv:1804.10600, “Color screening in (2+1)-flavor QCD”

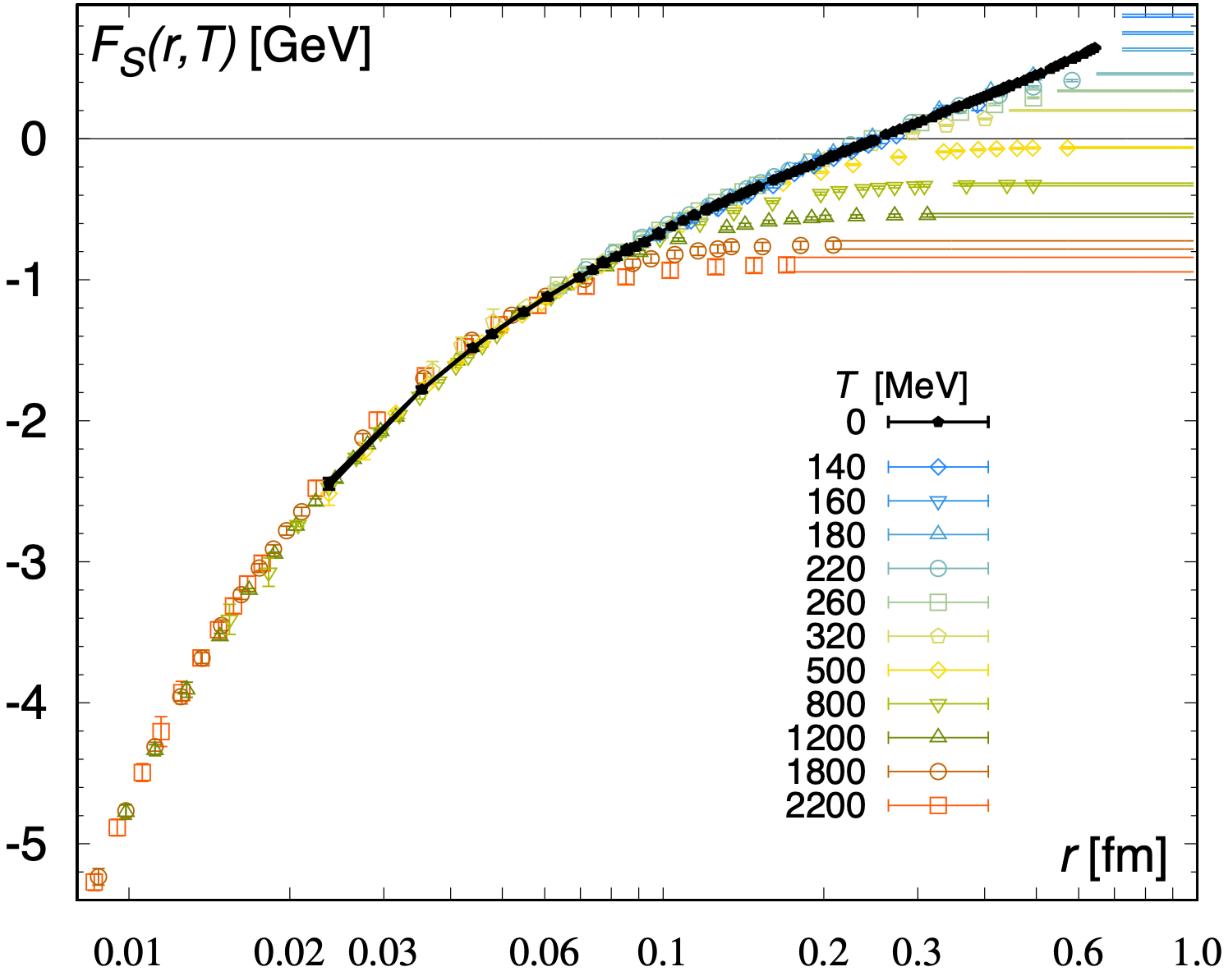

At the LHC, all quarkonia should be Debye screened.

Considering the formation time of hadrons, they should not form at high *T* at all

A new twist: J/ψ can form from deconfined charm quarks

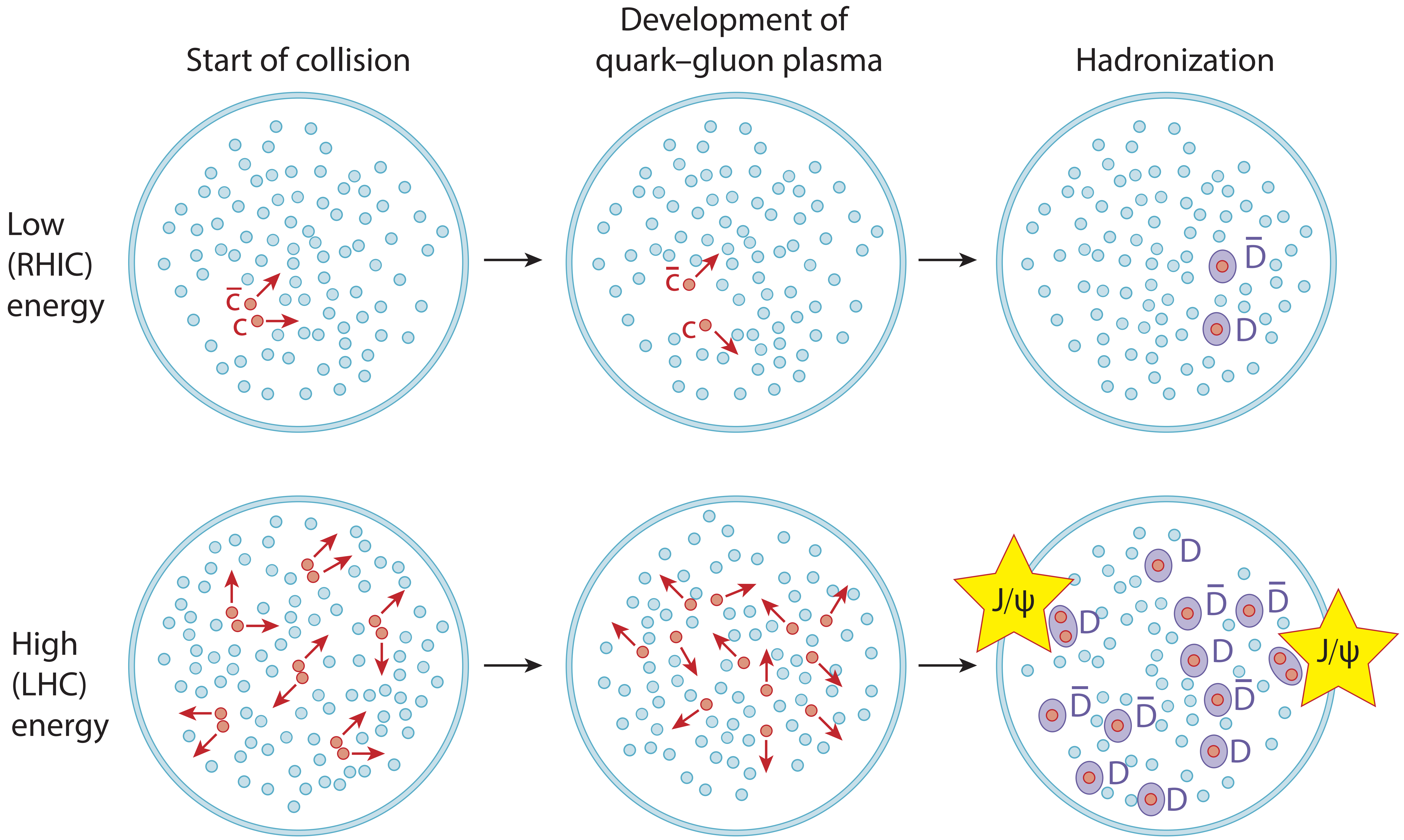

Requires large number of initially produced $c\bar{c}$ pairs:

$$N_{J/\psi} \propto N_{c\bar{c}}^2$$

Expect J/ψ suppression at SPS, RHIC and J/ψ enhancement at high energies (LHC)

Central AA coll	Ncc	Nbb
SPS, 17 GeV	~0.2	0
RHIC, 200 GeV	~10	~1
LHC, 5.02 TeV	~115	~10

Braun-Munzinger, Stachel, Nature 448 (2007) 302
Braun-Munzinger, Stachel, PLB490(2000)196
Thews et al, PRC63:054905(2001)

Expected J/ψ signal with or without statistical recombination of charm quarks

Kluberg, Satz, 0901.3831

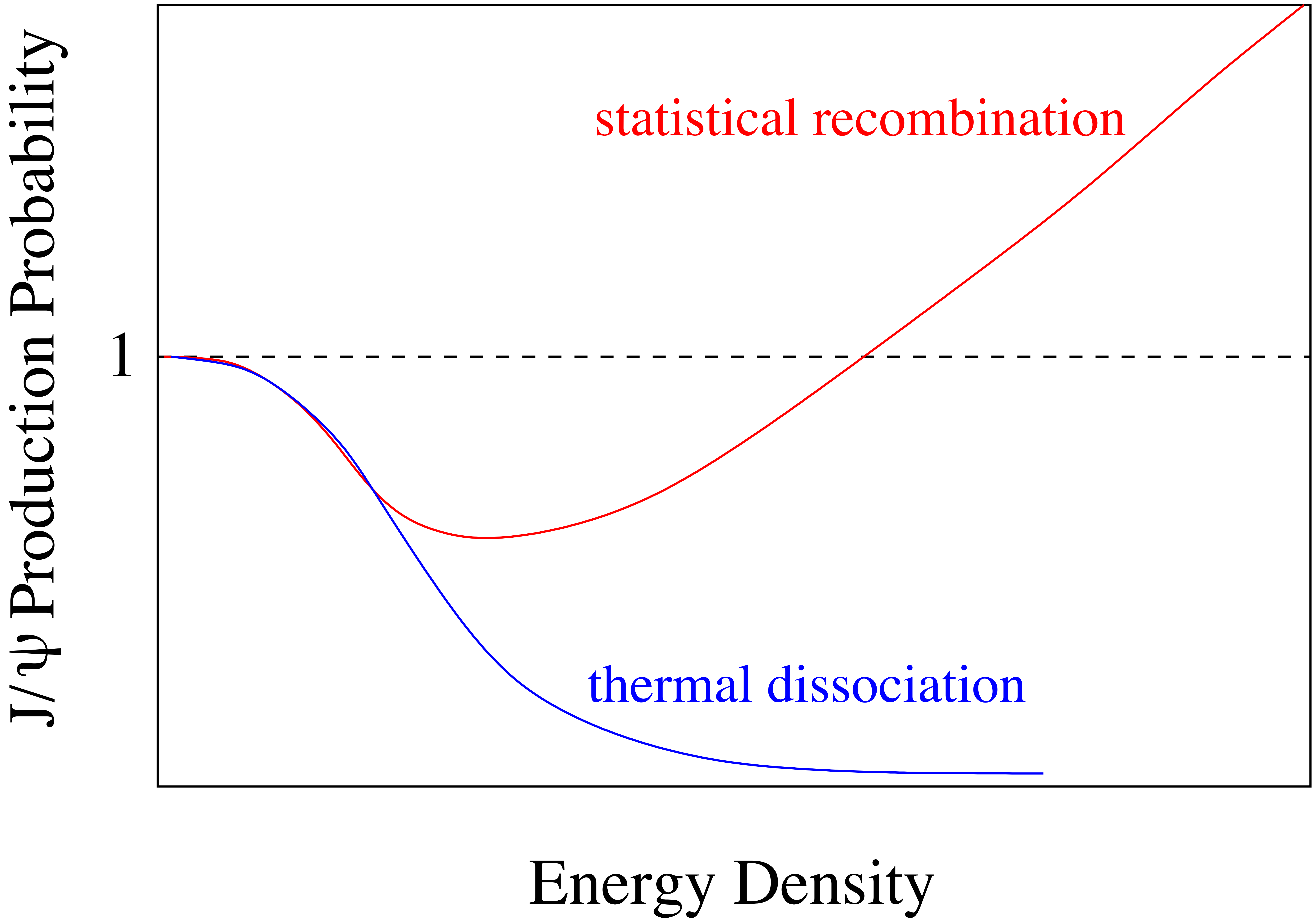

Observation of J/ψ suppression at the CERN SPS (Pb–Pb at $\sqrt{s_{NN}}$ = 17 GeV)

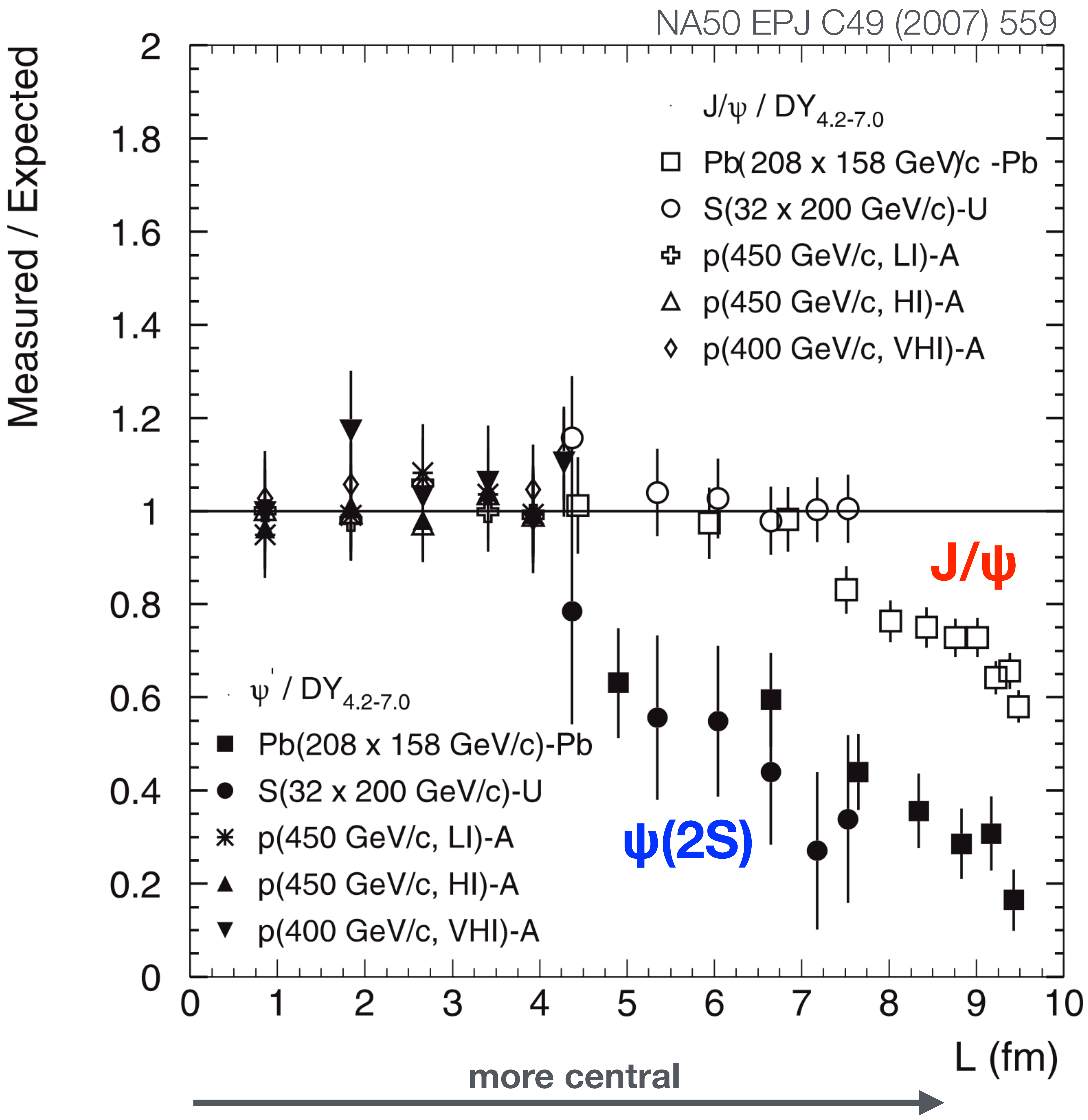

First observation of ***anomalous* J/ψ suppression** (more suppression than can be explained by cold nuclear matter effects)

Size of J/ψ suppression quantitatively consistent with melting of ψ(2S) and χc

Evidence of sequential suppression

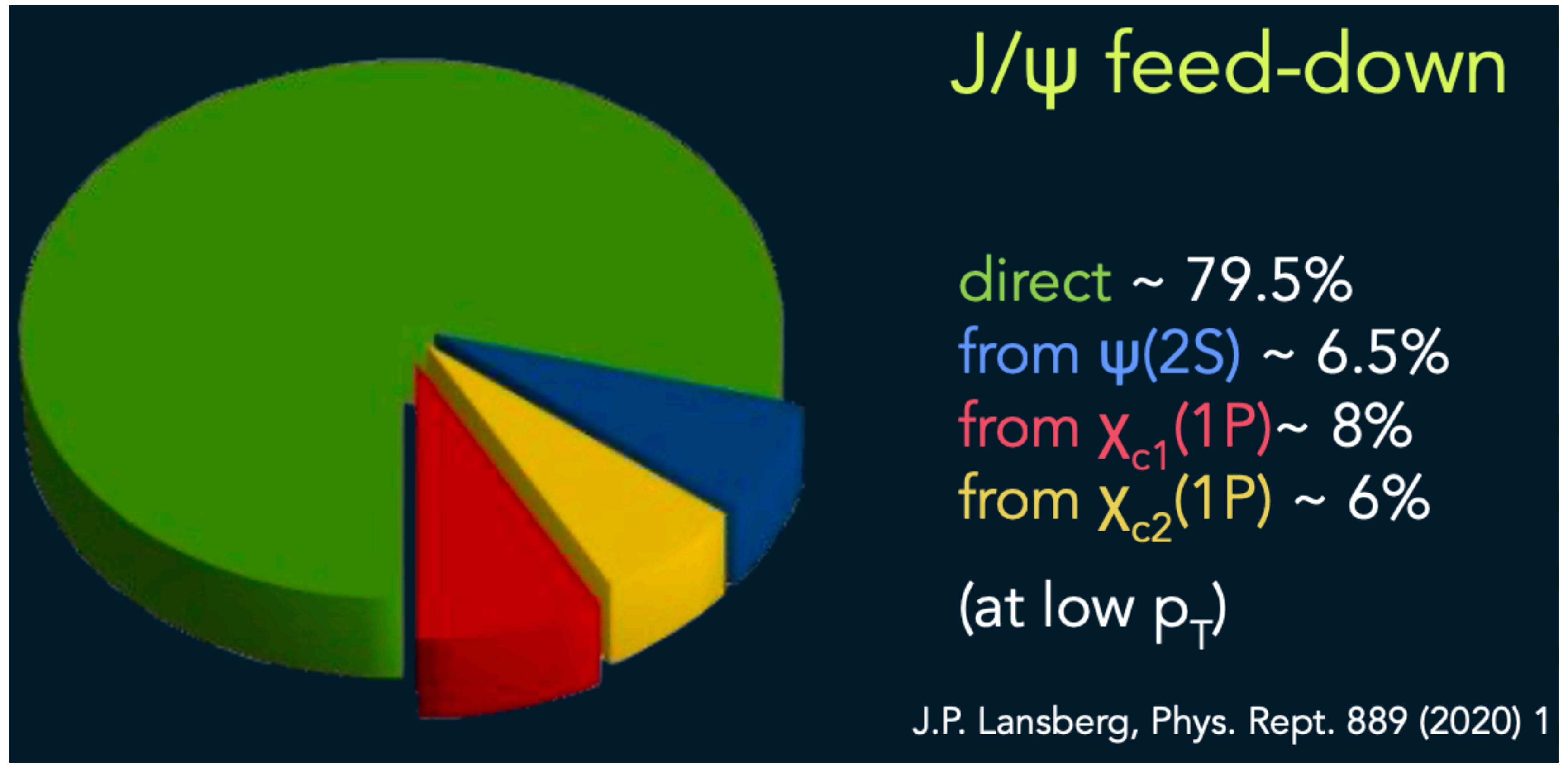

J/ψ R_{AA} vs p_T at the LHC

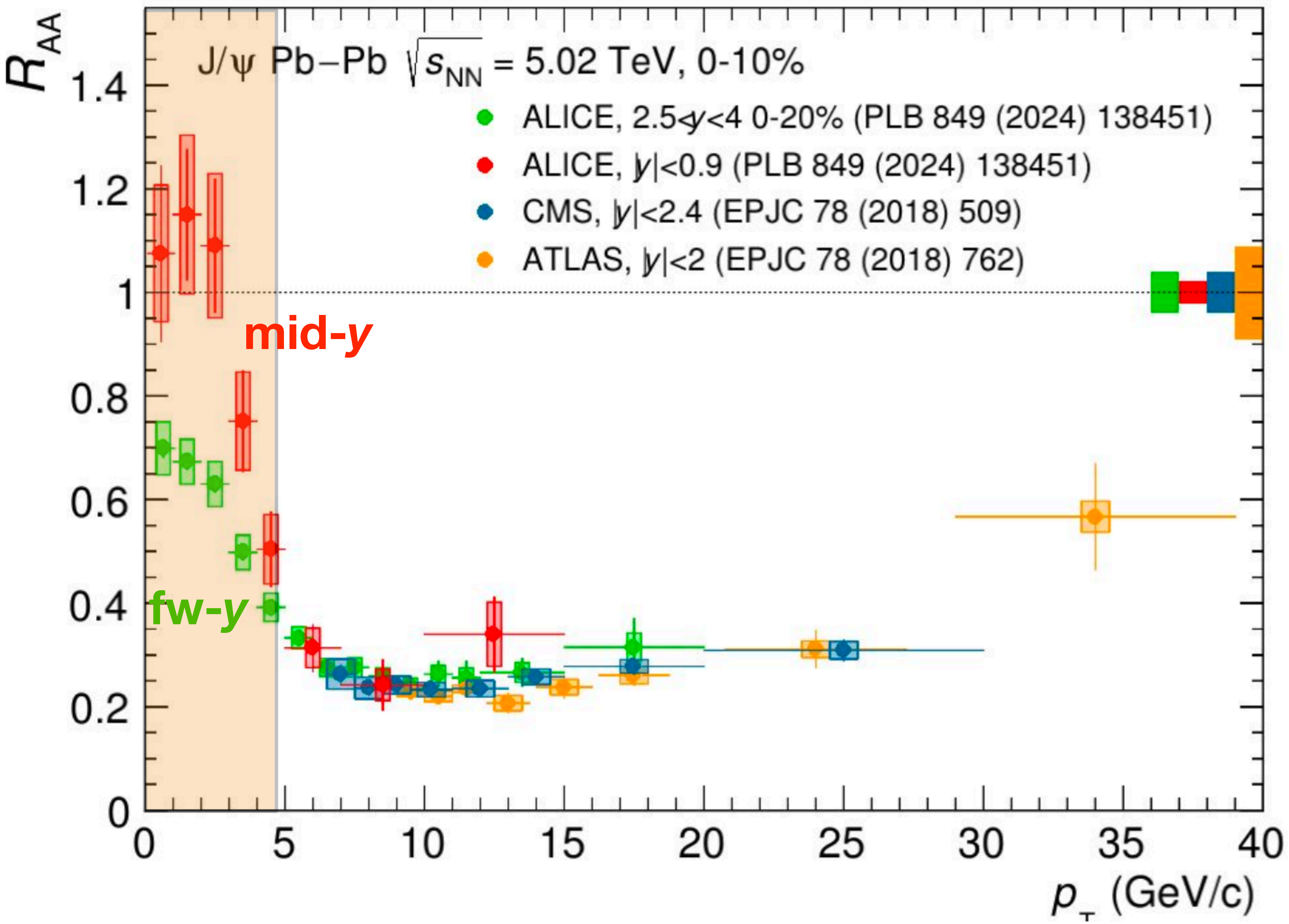

No suppression at low p_T at midrapidity

Suppression at low p_T at forward rapidity expected due to lower charm quark yield

Consistent with recombination picture

J/ψ R_{AA} at SPS, RHIC, and LHC

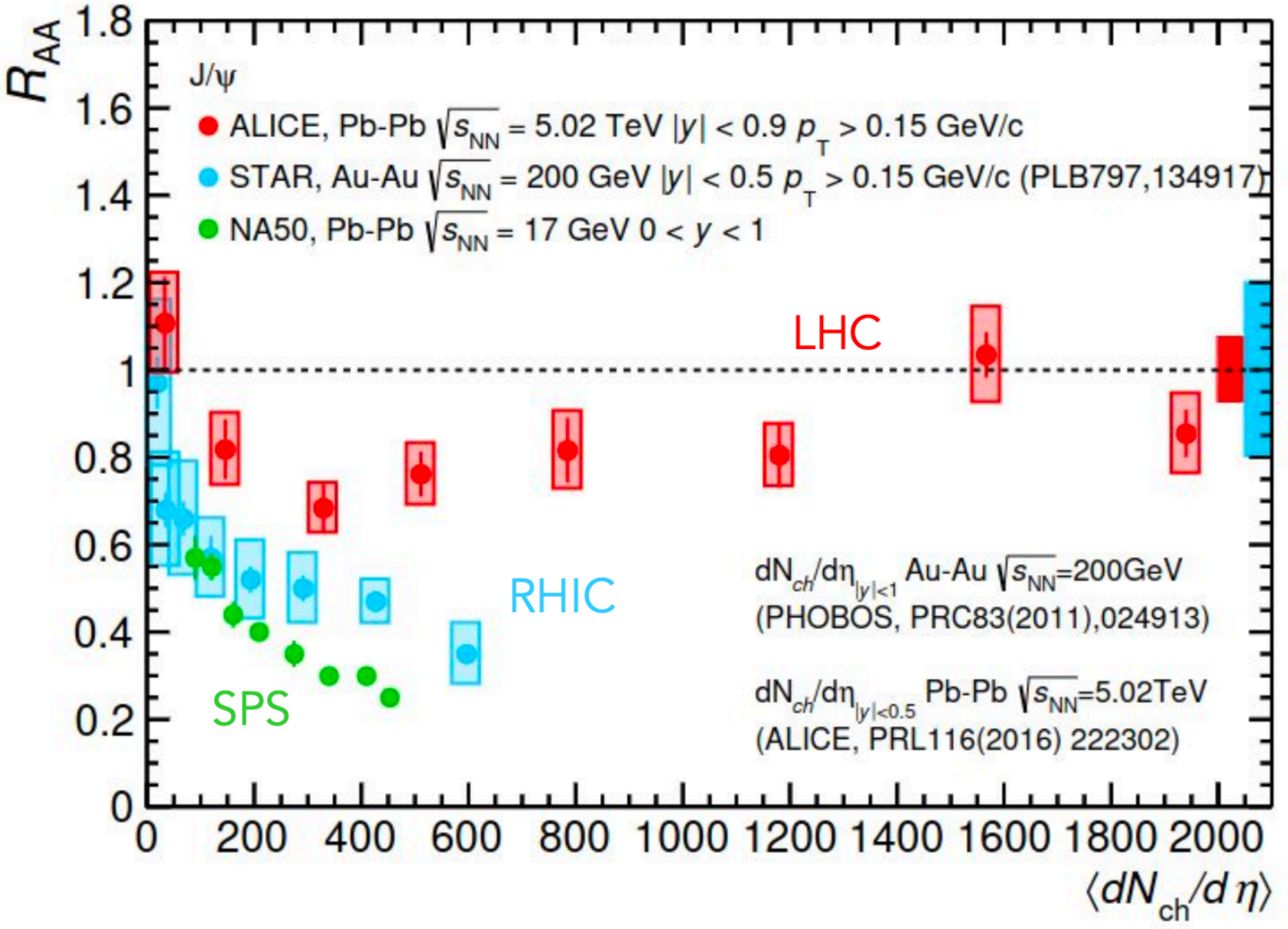

Less suppression when going low to high center-of-mass energies

LHC: no suppression in central collisions

Consistent with regeneration picture

Centrality dependence reproduced by recombination models

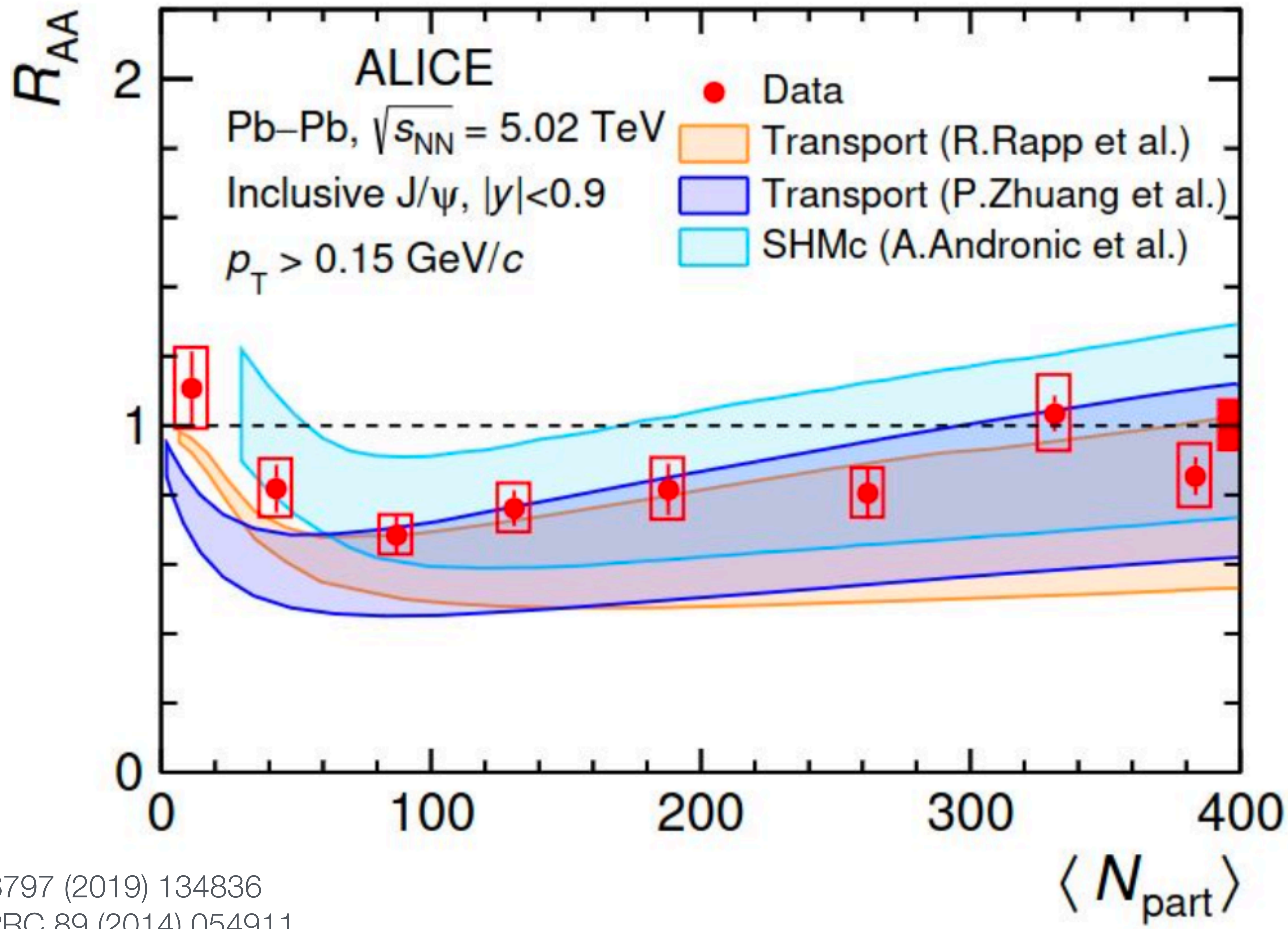

SHM: A. Andronic et al. PLB797 (2019) 134836
Transport: P. Zhuang et al. PRC 89 (2014) 054911
TAMU: R. Rapp et al. PLB664 (2008) 253

R_{AA} for J/ψ and ψ(2S): sequential suppression pattern

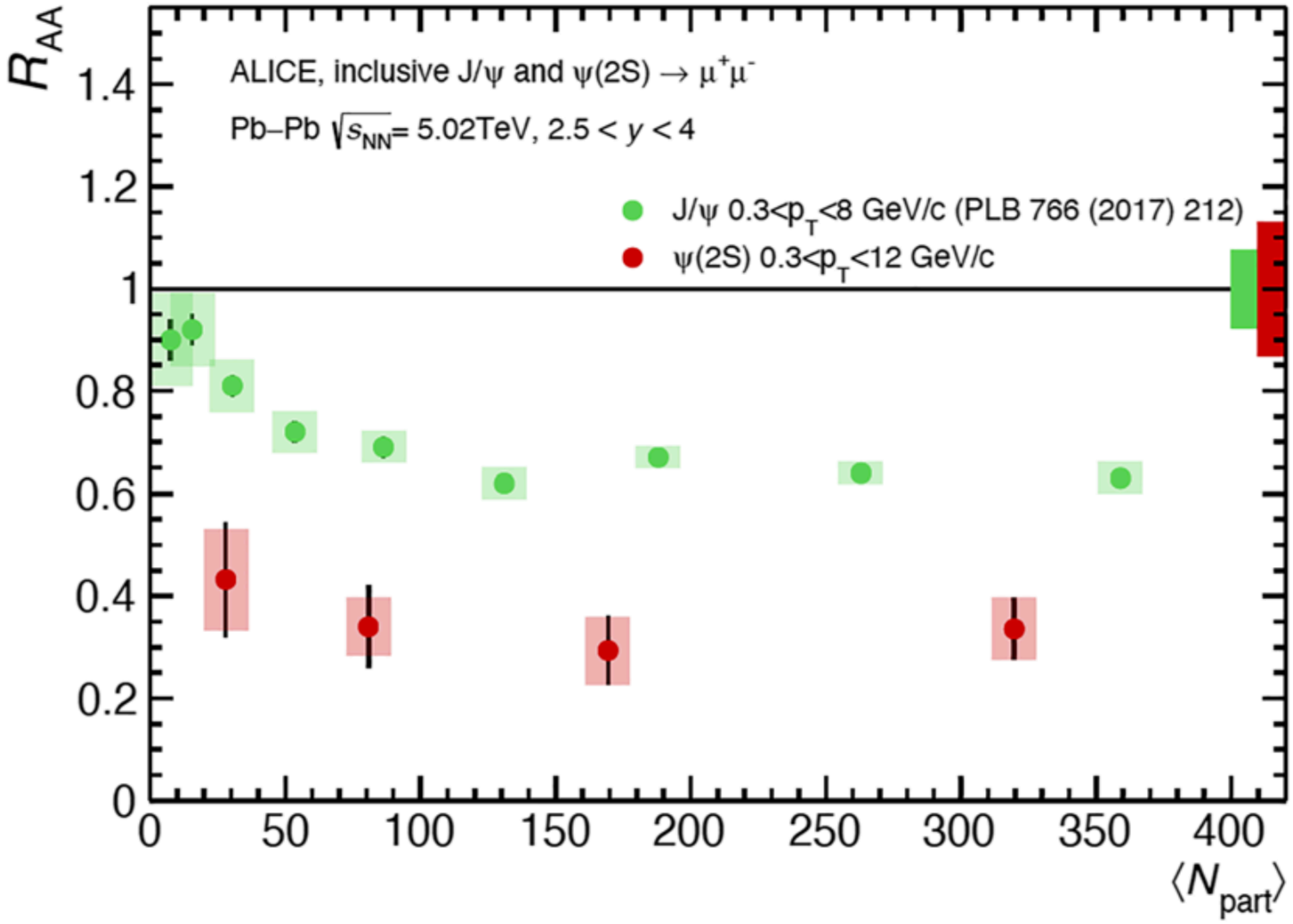

Y(*n*S) suppression

CMS, arXiv:2303.17026

pp

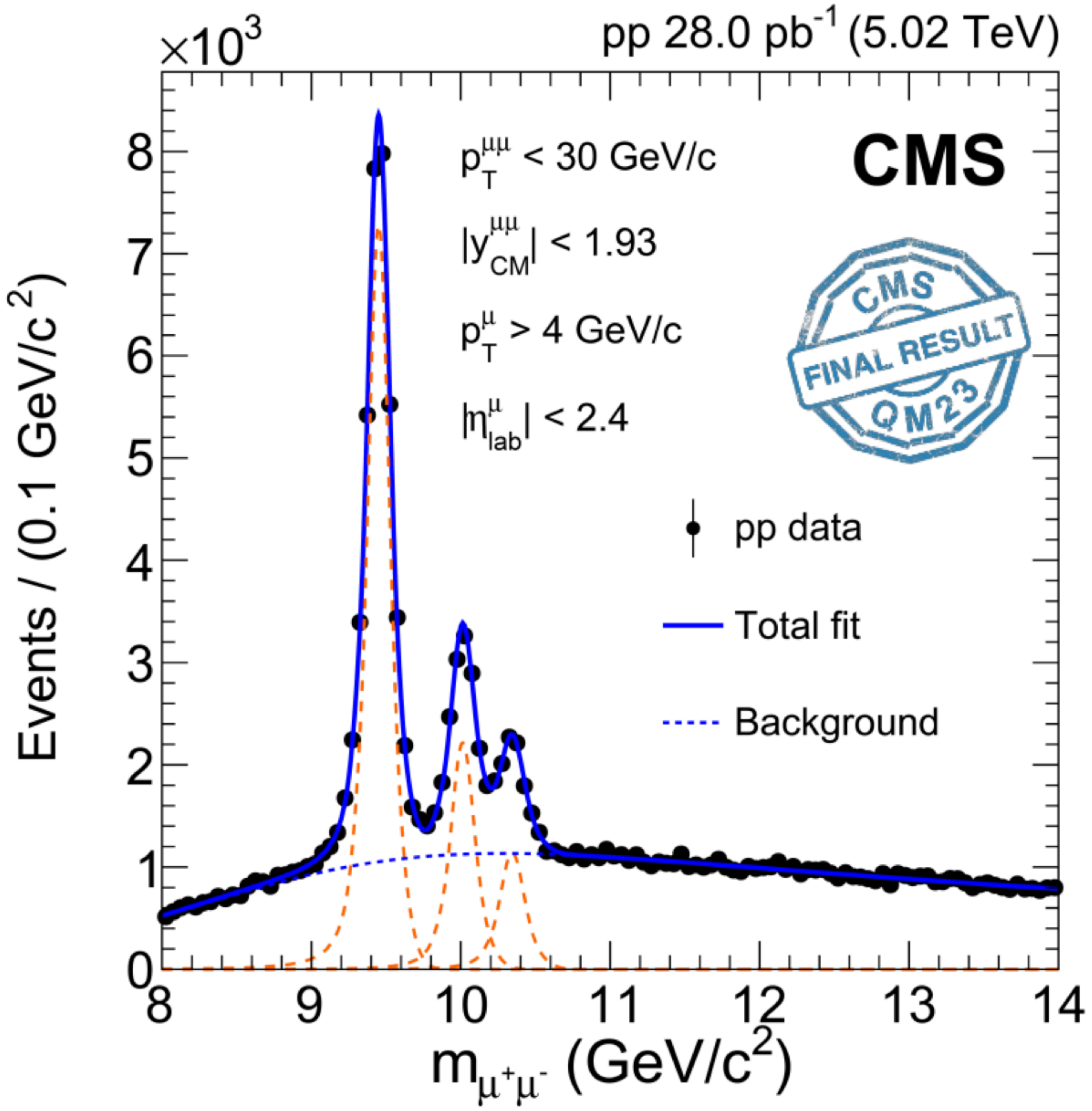

Pb–Pb

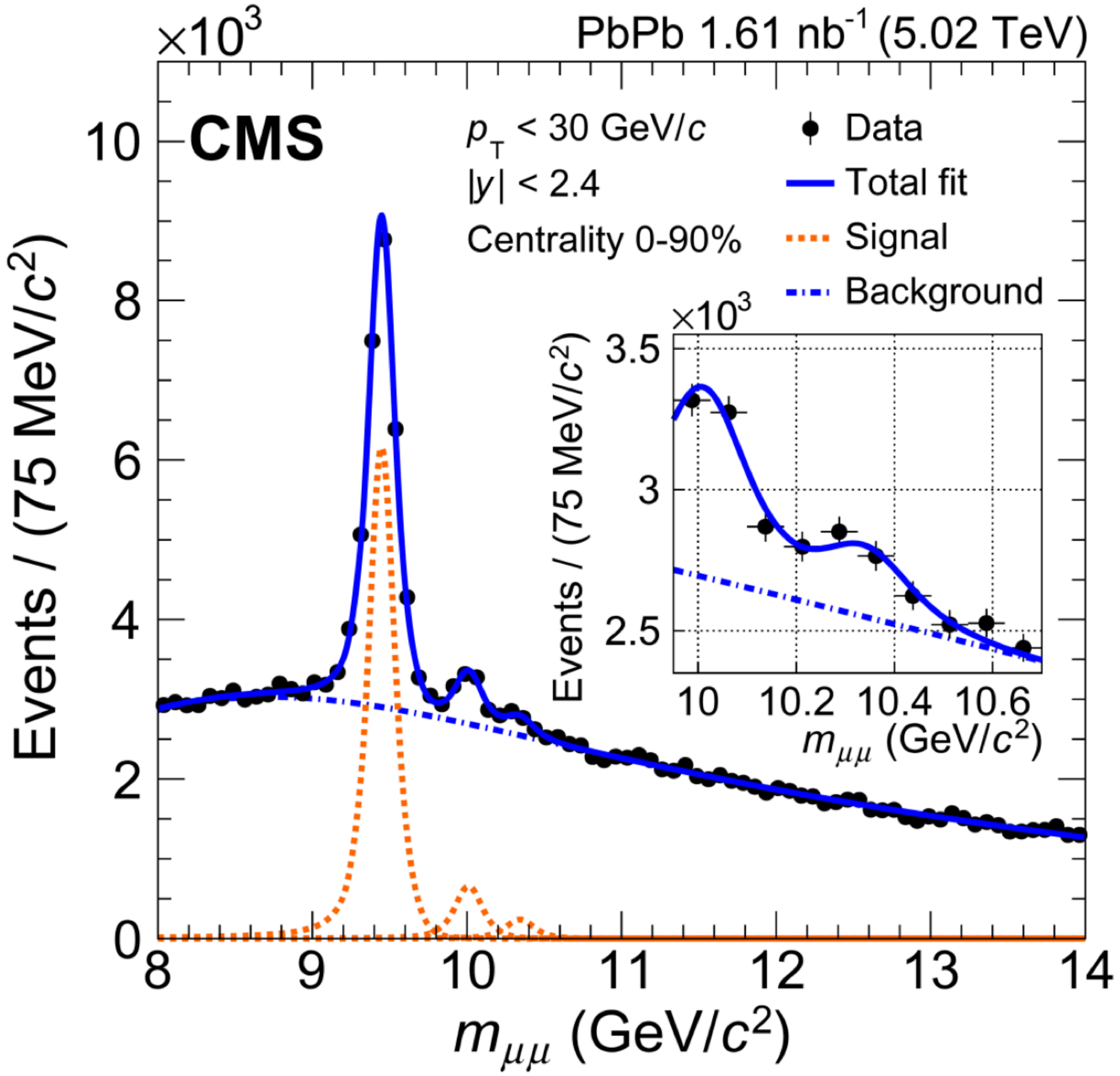

Evidence for sequential suppression of Y(*n*S) states

Electromagnetic Probes

The role of direct photons in heavy-ion physics

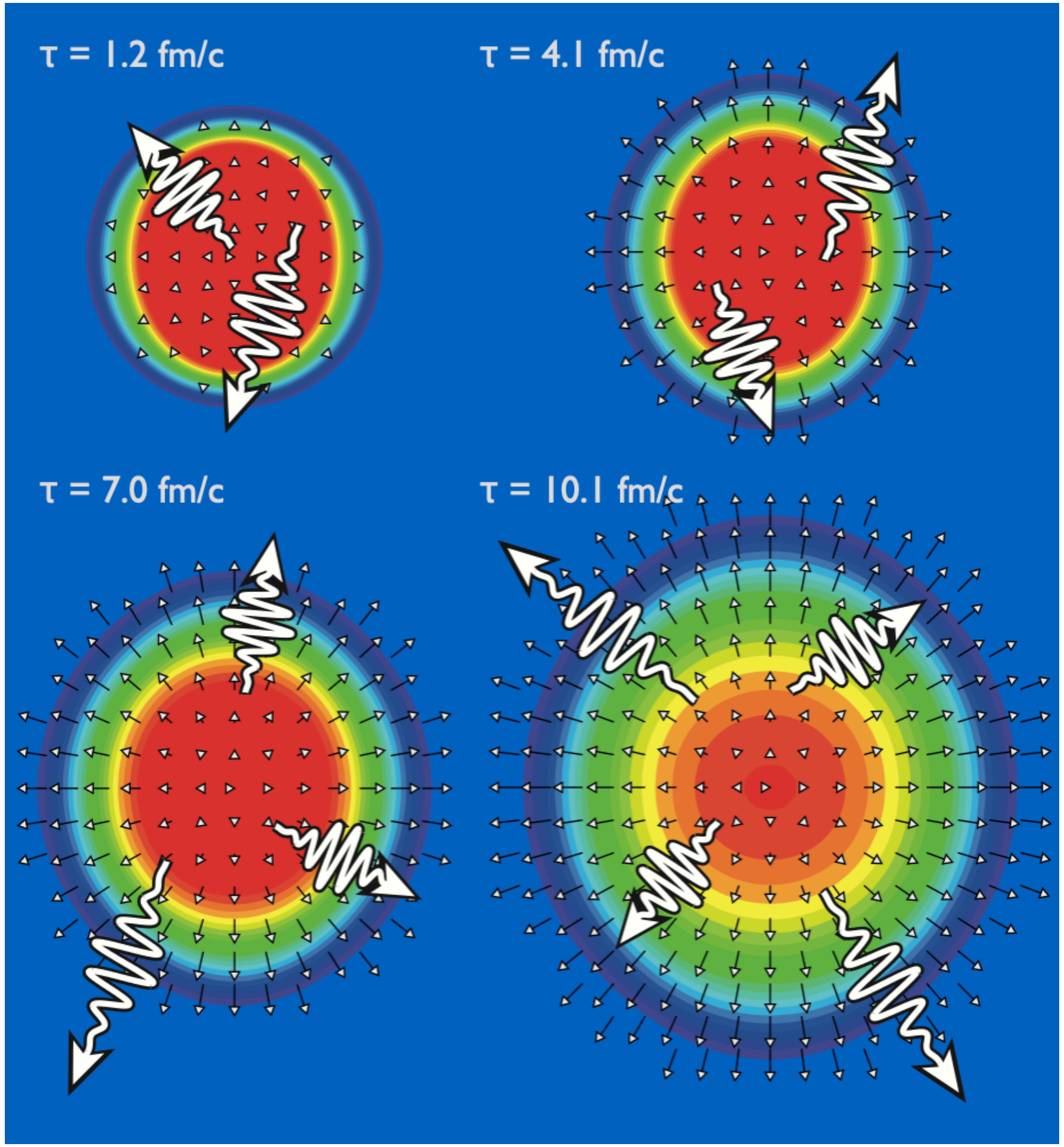

Escape medium unscathed

Produced over the entire duration of the collision (unlike low-p_T hadrons)

Direct photons test of the space-time evolution, in particular of the hydro

Experimental access to initial QGP temperature

QGP photon rate r_γ (lowest order):

$$E_\gamma \frac{dr_\gamma}{d^3p} \propto \alpha \alpha_s T^2 e^{-E_\gamma/T} \log \frac{E_\gamma T}{k_c^2}$$

Total emission rate (thermal photons per unit time and volume):

$$r_\gamma \propto T^4$$

Feynman diagrams: Photon production in the QGP and in the HG

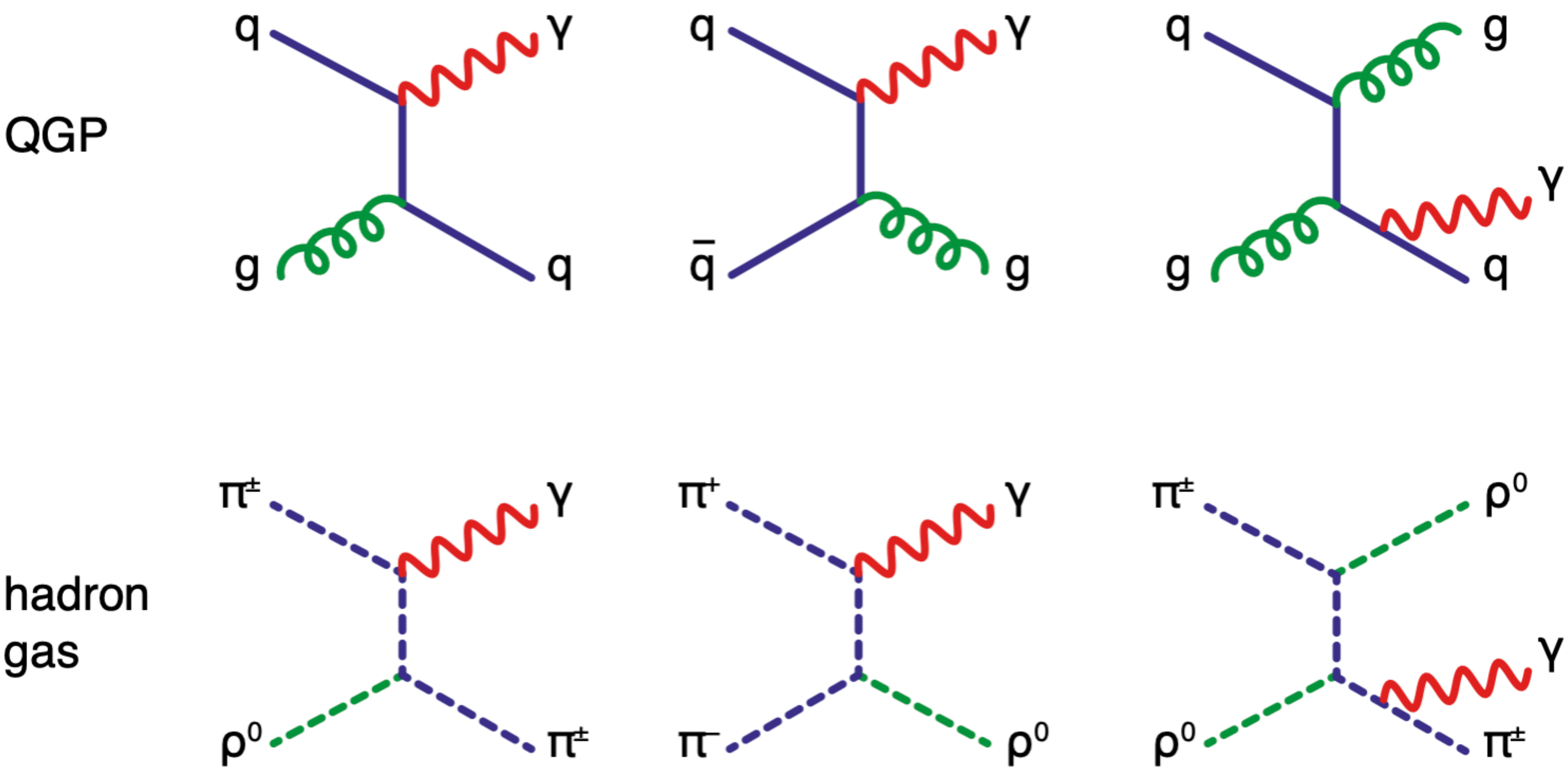

Example: Temperature of the universe from Planck spectrum

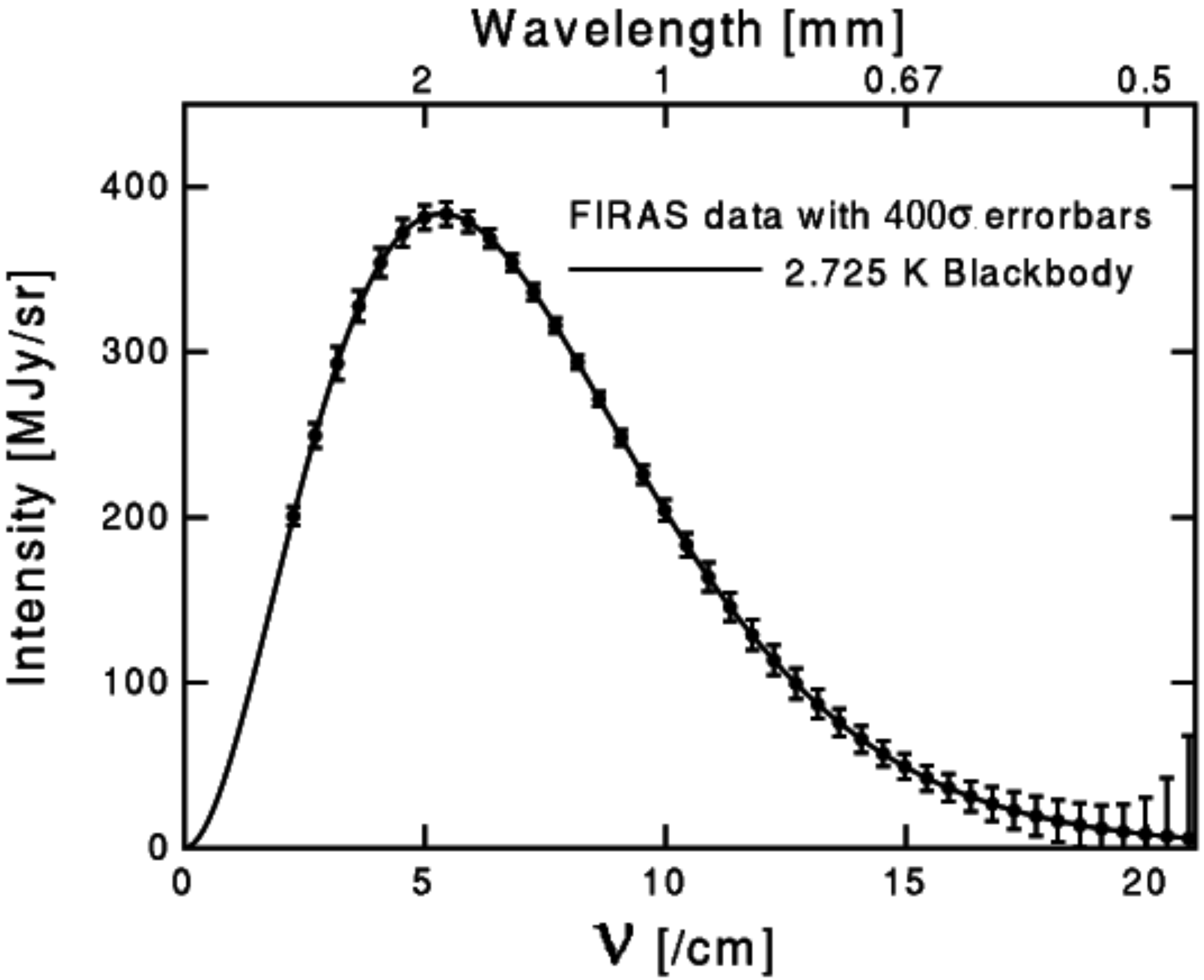

Difference in heavy-ion collisions: photons not in thermal equilibrium (but quarks and gluons are)

Expected photon spectrum

Schematically:

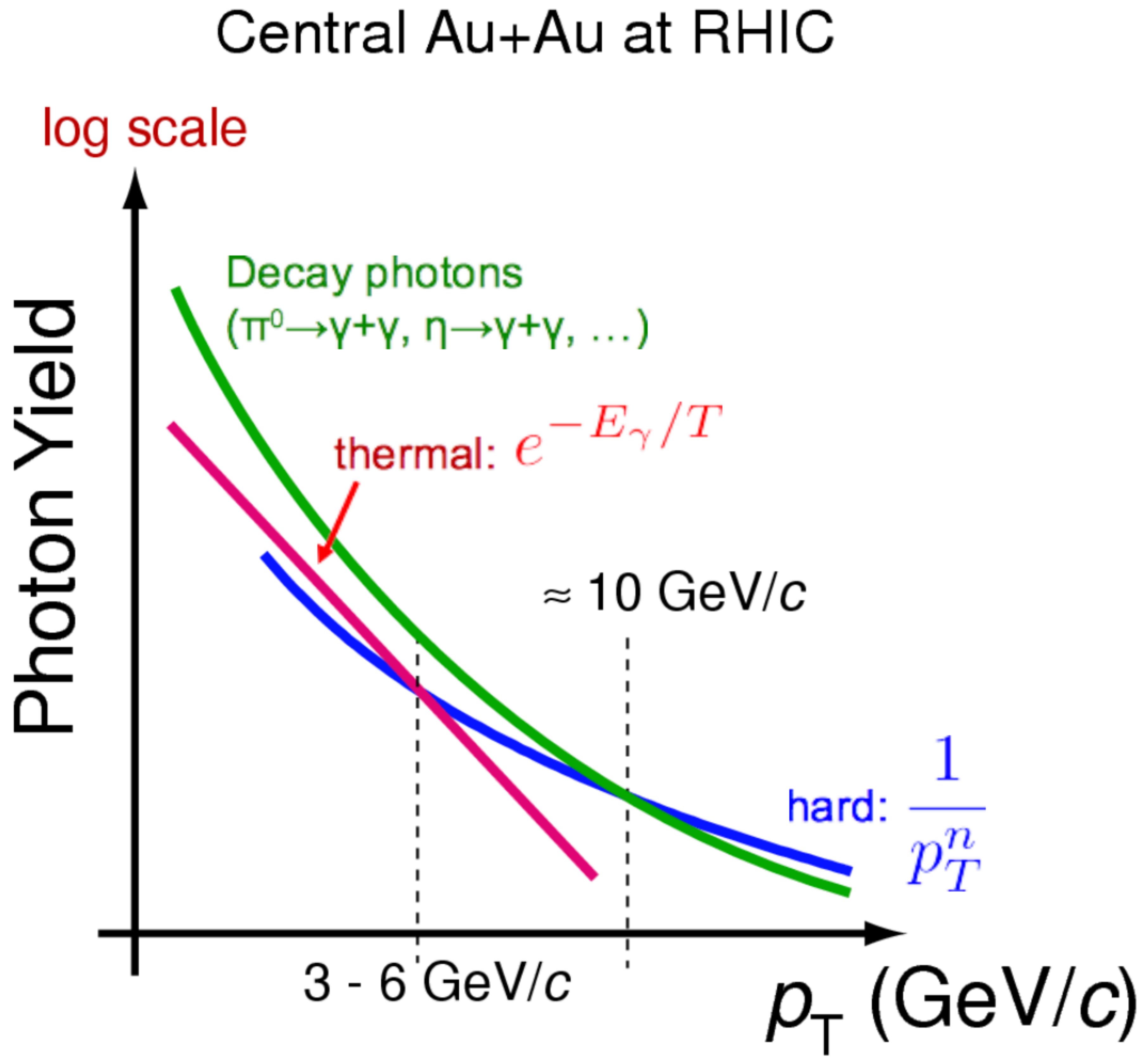

Actual calculation for Au–Au at RHIC:

Turbide, Rapp, Gale, Phys. Rev. C 69 (014902), 2004

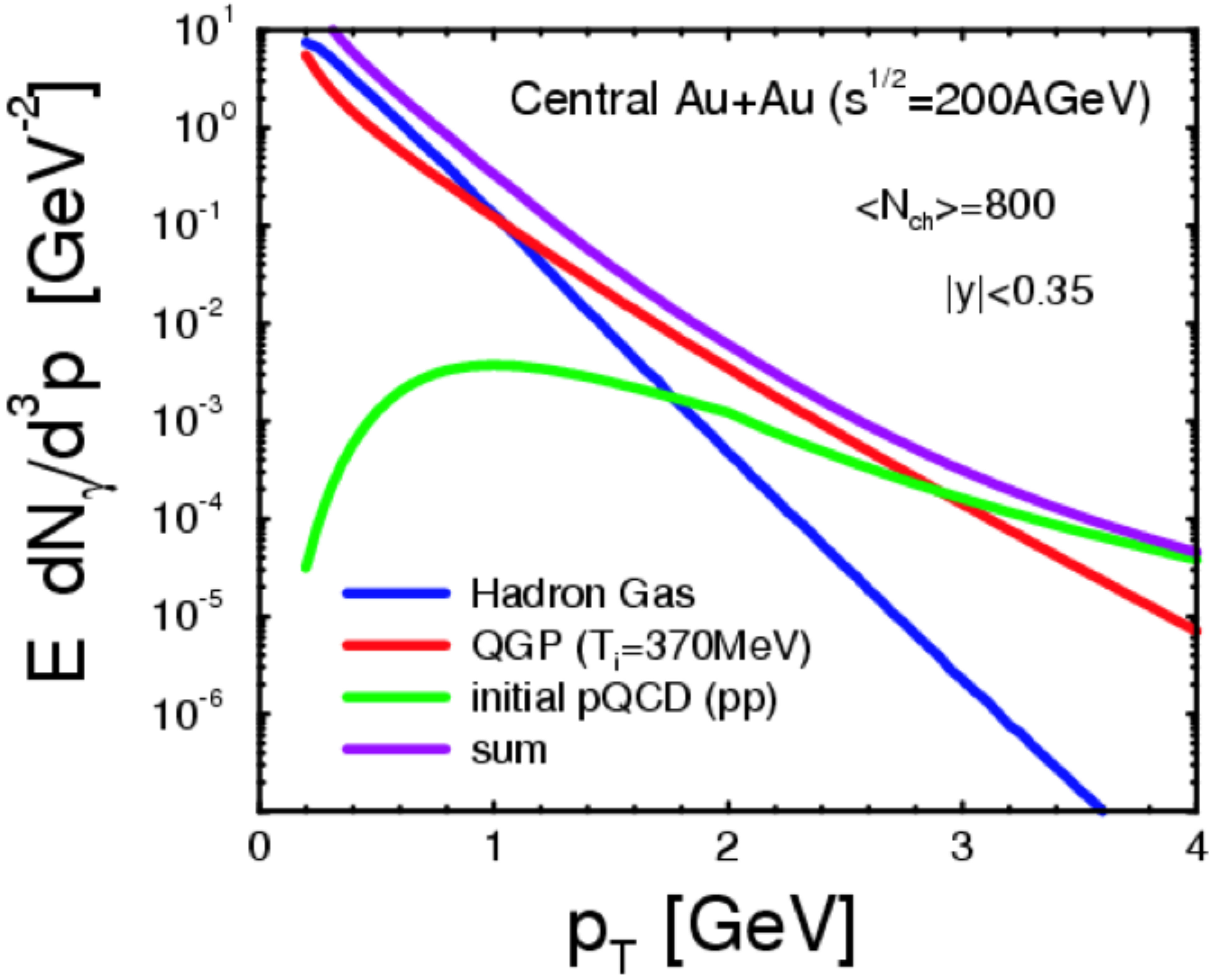

Direct photons in central Pb–Pb at the LHC

ALICE, Physics Letters B 754 (2016) 235

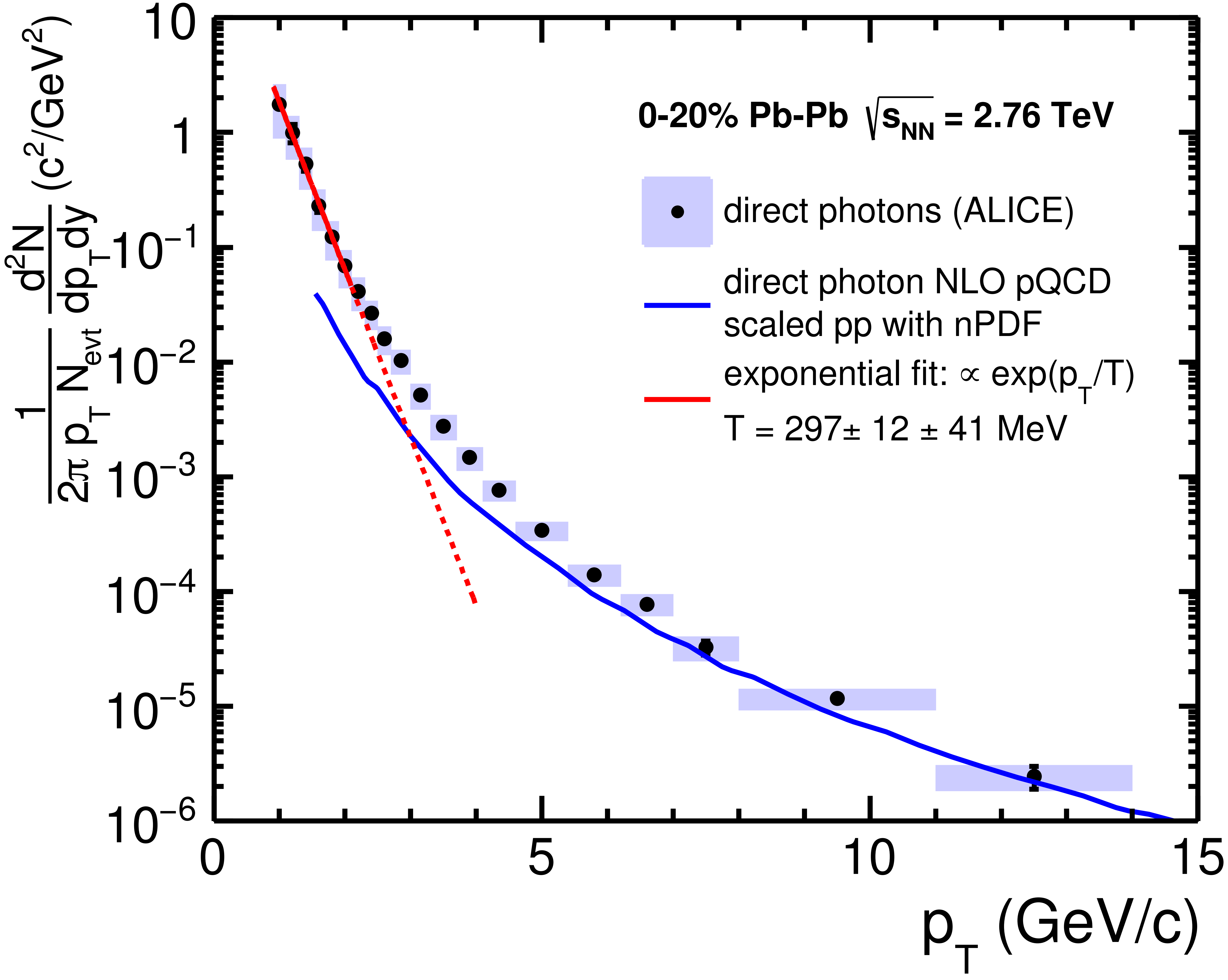

Inverse slope parameter of $T \approx 300$ MeV greater than T_{pc} = 150–160 MeV
→ Evidence for QGP formation

Summary and outlook

Status after ~30 years of ultrarelativistic heavy-ion physics (1)

- Prime goal: **discovery and characterization of the quark-gluon plasma**
- Modeling A–A collisions assuming QGP formation works well
- **Hydrodynamic models** for the space-time evolution of the QGP involving a **equation-of-state from lattice QCD** in good agreement with the data
- Viscous hydro models allow one to extract transport parameters like η/s (shear viscosity-to-entropy ratio):
  - $0.05 < \eta/s < 0.2$ (depending on T/T_{pc})
  - QGP is the most perfect fluid known in nature
- **Hadron yields** described by a production from a **thermal source with $T_{ch} \approx$ 156 MeV**, wich is very close to the transition temperature from a QGP to a hadron gas as calculated with lattice QCD
- Hadron suppression at high p_T allows one to extract the **jet quenching quenching parameter**:
  - $3.4 < \hat{q}/T^3 < 5.8$ at RHIC
  - $2.4 < \hat{q}/T^3 < 5.0$ at the LHC

Status after ~30 years of ultrarelativistic heavy-ion physics (2)

- Strong evidence for J/ψ through recombination/coalescence: confirms production of deconfined medium
- QGP in small systems like high-multiplicity pp collisions?
  - Collective effects observed in these systems
  - But no jet quenching
  - Interpretation?
  - Likely no QGP in min. bias pp collisions

Outlook: ALICE 3 (2035+)

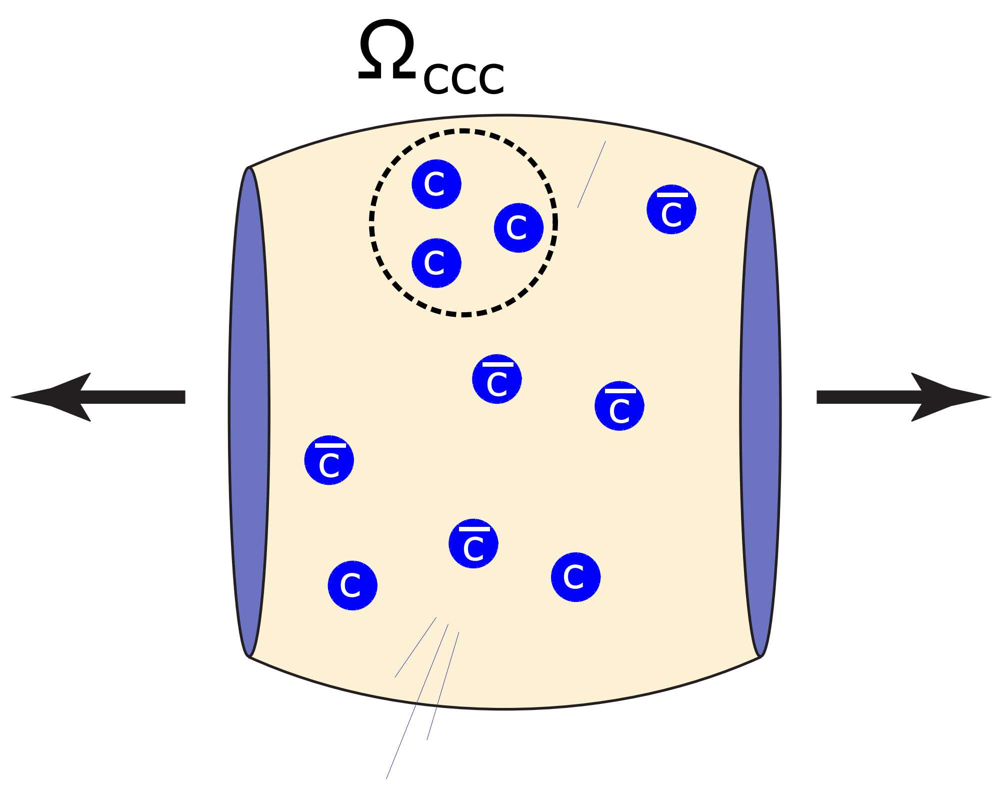

Deconfinement and hadronization

Multiple charm hadrons, quarkonia, X(3872): extremely enhanced in the QGP

Vary charm quark density through large rapidity coverage

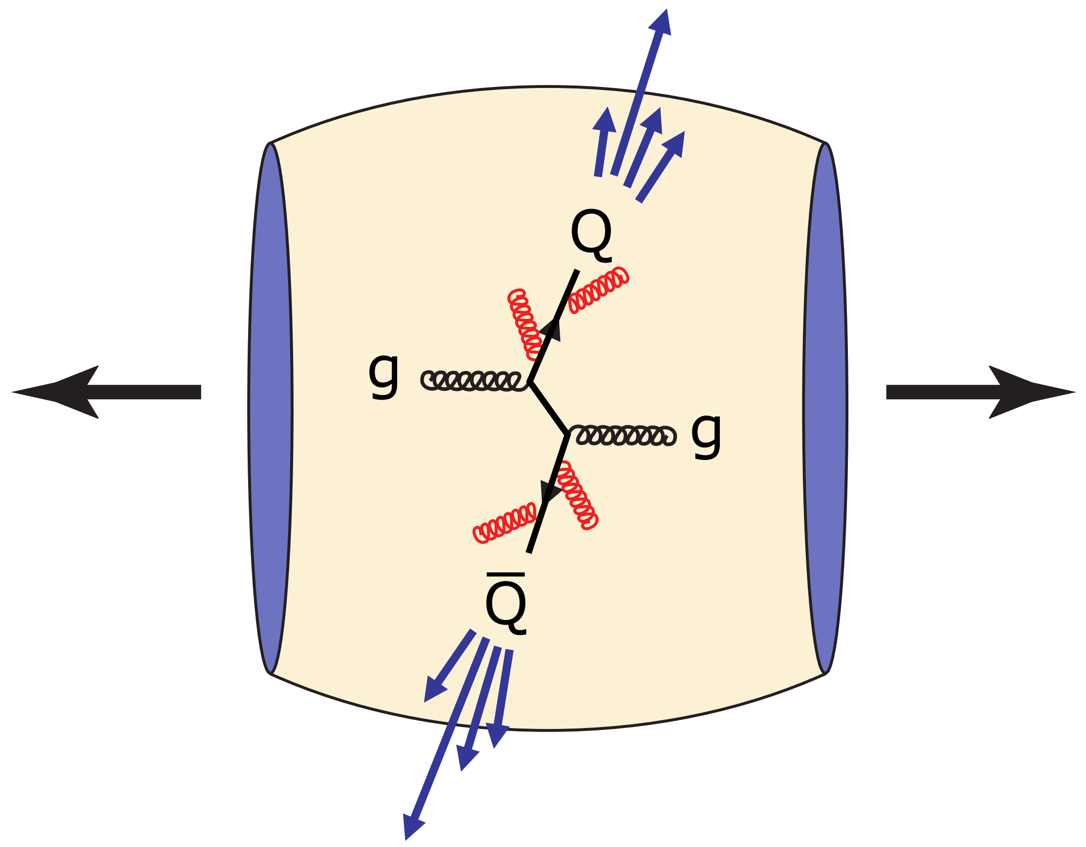

Precision QGP tomography with $c\bar{c} \rightarrow D\bar{D}$ correlations

Nature of quasi-particles in the QGP

Collisional vs. radiative energy loss

Observation of chiral symmetry restoration

Dileptons with $m_{ee} > 1$ GeV with high precision

Discover ρ-a_1 chiral mixing

Hohler, Rapp, Phys. Lett. B731 (2014) 103

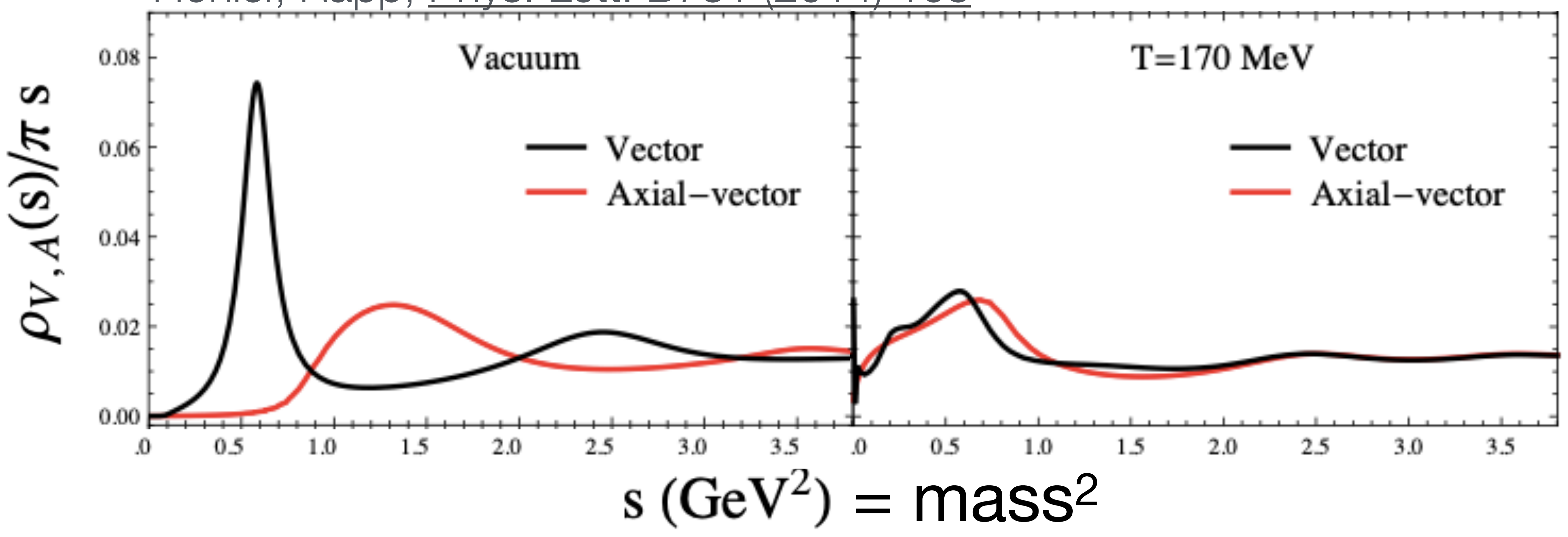

ALICE 3 – A next generation heavy-ion detector

Compact all-silicon tracker with a high-resolution vertex detector and **extremely low material budget**

Superconducting magnet up with B = 2 T

Particle Identification over large acceptance: muons, electrons, hadrons, photons at $|\eta| < 4$

Forward conversion tracker (FCT) : **ultra-soft photons**

Fast read-out and online processing

ALICE 3 letter of intent: arXiv:2211.02491